



About the effects of polarising optics on lidar signals and the $\Delta 90$ -calibration

1 **Volker Freudenthaler¹**

2 ¹Fakultät für Physik, Meteorologisches Institut, Ludwig–Maximilians–Universität, 80333
3 München, Theresienstrasse 37, Germany

4 Correspondence to: V. Freudenthaler (volker.freudenthaler@lmu.de)

5 **Abstract**

6 This paper provides a model for assessing the effects of polarising optics on the signals of
7 typical lidar systems, which is based on the description of the individual optical elements of
8 the lidar and of the state of polarisation of the light by means of the Müller-Stokes formalism.
9 General analytical equations are derived for the dependence of the lidar signals on
10 polarisation parameters, for the linear depolarisation ratio, and for the signals of different
11 polarisation calibration set-ups. The equations can also be used for the calculation of
12 systematic errors caused by non-ideal optical elements, their rotational misalignment, and by
13 non-ideal laser polarisation. We present the description of the lidar signals including the
14 polarisation calibration in a closed form, which can be applied for a large variety of lidar
15 systems.

16 **1 Introduction**

17 The purpose of atmospheric depolarisation measurements with lidar, first described by
18 Schotland et al. (1971), is mainly to discern between more or less depolarising scatterers. The
19 discrimination of ice and water clouds was the main focus in the beginning. Sassen (1991)
20 and Sassen (2005) give an overview about the early work related to that. Aerosol and their
21 interaction with clouds became more important in the last decade because of their
22 insufficiently understood direct and indirect roles in the feedback mechanisms of climate
23 change (Boucher et al., 2013). Multi-wavelength lidar measurements including the
24 depolarisation ratio can be used to discern aerosol types (Sugimoto et al., 2002; Sugimoto and
25 Lee, 2006; Ansmann et al., 2011; Burton et al., 2014; Groß et al., 2014) and to retrieve micro-
26 physical aerosol properties by means of inversion algorithms (Müller et al., 1999; Ansmann



1 and Müller, 2005; Gasteiger et al., 2011; Veselovskii et al., 2013; Böckmann and Osterloh,
2 2014; Müller et al., 2014). Pérez-Ramírez et al. (2013) show the impact of systematic errors
3 of the lidar data on the retrieval of micro-physical particle properties. The additional
4 measurement of the linear (or circular) depolarisation ratio improves the retrievals (Böckmann
5 and Osterloh, 2014; Gasteiger and Freudenthaler, 2014). But the depolarisation ratios are
6 often derived from lidar measurements assuming more or less ideal lidar set-ups neglecting
7 the effects of small system misalignments and of non-ideal optical elements on the
8 polarisation, which can lead to considerable errors in the retrieved depolarisation ratio
9 (Reichardt et al., 2003; Alvarez et al., 2006; Freudenthaler et al., 2009; Mattis et al., 2009).
10 According to Chipman (2009a) Chap. 15.27, one of the primary difficulties in performing
11 accurate polarisation measurements is the systematic error due to non-ideal polarisation
12 elements. Most inclined optical surfaces and optical coatings on beam-splitters are polarising,
13 wherefore all lidars must be considered as “incomplete light-measuring polarimeters”
14 (Chipman, 2009a), even if they are not intended to measure the depolarisation ratio.

15 As model calculations of aerosol scattering properties advance (Nousiainen et al., 2011;
16 Kahnert et al., 2014), the modellers need accurate measurements with small and reliable error
17 bars in order to verify and improve their models. In order to estimate the uncertainties and to
18 improve the measurements, we have to find the error sources. The usual way to do this is to
19 compare the measurements with a model and to investigate the deviations. The only reliable
20 atmospheric model for comparison is the model of the molecular linear depolarisation ratio δ_m
21 (Behrendt and Nakamura, 2002; Freudenthaler et al., 2015). But the measured values δ_m^* of
22 the very small real δ_m (on the order of 0.004) are usually a number of times higher, which
23 makes it difficult to use for calibration with a simple model as $\delta_m^* = A\delta + B$ ((Sassen and
24 Benson, 2001; Reichardt et al., 2003); see also S.9). At present, polarisation calibration
25 techniques of lidars are often not accurate enough to sufficiently determine the two
26 parameters A and B , and actually, as we will show in the following, the model itself is
27 insufficient. But how accurate do we have to be? How accurate can we be? What are the
28 critical parts and adjustments? How can set-ups be improved with minimal costs and
29 complexity, and how can existing lidar systems be checked? To answer these questions, we
30 need a better model for the lidar set-up, which is complete and flexible enough to be applied
31 to a variety of lidar systems and can describe various calibration techniques.



1 Astronomical polarisation measurement set-ups are very similar to lidar set-ups. Elaborate
2 theoretical and experimental investigations of the influence of polarising optics and
3 corresponding corrections for astronomical telescopes and detection optics using the theory of
4 polarimetry and ellipsometry (see Azzam (2009); Chipman (2009a)) can be found quite
5 frequently in the literature (Skumanich et al., 1997; Socas-Navarro et al., 2011; Breckinridge
6 et al., 2015). Although the usefulness of a lidar with polarisation diversity had been realised
7 early (Pal and Carswell, 1973), the need for a complete description with the Müller-Stokes
8 formalism has, to our knowledge, been first expressed by Anderson (1989), but focused only
9 on the atmospheric scattering process. Instrumental aspects including some error calculations
10 have been included by Beyerle (1994), Cairo et al. (1999), Biele et al. (2000), Behrendt and
11 Nakamura (2002), Reichardt et al. (2003), Alvarez et al. (2006), Del Guasta et al. (2006),
12 Hayman and Thayer (2009), Mattis et al. (2009), (Freudenthaler et al., 2009), Hayman (2011),
13 Hayman and Thayer (2012), David et al. (2013), Geier and Arienti (2014), Di et al. (2015),
14 and Volkov et al. (2015). The errors mainly considered are the diattenuation of the receiver
15 optics (see Sect. 2.2), the cross talk of the polarising beam-splitter, non-ideal characteristics of
16 the calibration, and rotational misalignment of polarising components.

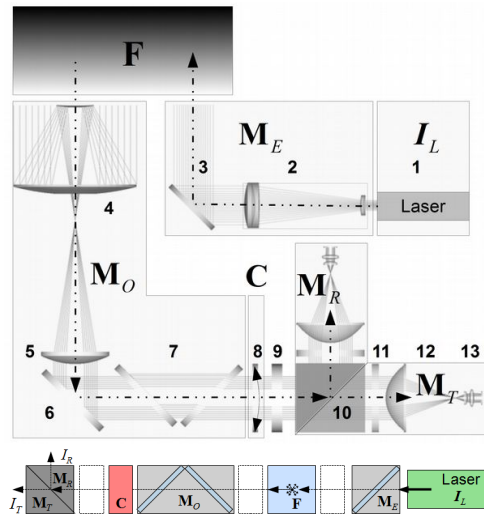
17 In this work we describe lidar set-ups from the laser to the detector by means of the Stokes-
18 Müller formalism (Chipman, 2009b) including the transmitter and receiver optics. The Stokes
19 vector describes the flux and the state of polarisation of the light, and the Müller matrices
20 describe how optical elements change the Stokes vector. We develop equations for the two
21 signals of a polarisation sensitive lidar and for the signals of the polarisation calibration,
22 which are necessary to retrieve the linear depolarisation ratio and the total lidar signal, using
23 different calibration techniques and lidar set-ups. In order to enable the evaluation of the final
24 errors and to analyse their dependencies on certain optical parameters or misalignments of
25 individual optical elements, we will derive first the full equations and then try to find more
26 simple analytical formulations neglecting minor error sources to get an overview of the main
27 critical parameters.

28 For this we neglect the polarisation effects of lenses and of telescope mirrors with small
29 incidence angles of the light beam (Seldomridge et al., 2006) (Clark and Breckinridge, 2011),
30 but 45° folding mirrors as in Newtonian-type telescopes must be considered (Breckinridge et
31 al., 2015; Di et al., 2015), and stress-birefringence in windows and lenses or unfavourable
32 coatings may cause severe polarisation effects. Errors caused by a light beam which is



1 divergent or inclined towards the optical axis are not discussed here; this means the light
 2 beams are assumed to be either perfectly parallel before and after polarisation optics, or that
 3 an optical element is insensitive to the incident angle regarding polarisation.

4 Basic information about the polarisation topics can be found in Goldstein (2003), Clarke
 5 (2009), and in the chapters by Azzam (2009); Bennett (2009a,b); Chipman (2009b,a) of the 3rd
 6 edition of the Handbook of Optics (Bass, 2009). The authors of these chapters follow the
 7 Muller-Nebraska convention Muller (1969) for the definition of signs and directions regarding
 8 e.g. the coordinate system (see S.1), as we do in this work.



9 Figure 1 Top: Exemplary depolarisation lidar set-up with laser 1, beam expander 2, steering
 10 mirror 3, receiving telescope 4, collimator 5, folding mirror 6, dichroic beam-splitters 7, a
 11 rotating element for polarisation calibration 8, interference filter 9, and polarising beam-
 12 splitter cube 10 (PBS, polarising beam-splitter). The neutral density filters and cleaning
 13 polarisers 11, detector optics 12, and the detectors 13. The system can be subdivided in
 14 functional blocks which can be described with the Stokes-Müller formalism: I_L is the Stokes
 15 vector of the laser source, M_E is the Müller matrix of the the laser emitter optics, F of the
 16 atmospheric backscattering volume including depolarisation, M_O includes receiver optics as
 17 beam-splitters, C is the calibrator, and $M_{T,R}$ is the polarising beam-splitter including the
 18 detector optics for the transmitted (T) and reflected (R) optical branches. Bottom: simplified
 19 schematic of the setup.



1 Most of the lidar set-ups for depolarisation measurement reported in the literature are
 2 explicable with the schematic in Fig. (1), in which the individual parts of a lidar system are
 3 grouped in modules, which are in general describable by Müller matrices of combinations of
 4 diattenuators, retarders, and rotators (see Sect.2.2). The set-up in Fig. 1 can be described with
 5 Eq. (1).

$$6 \quad \mathbf{I}_{T,R} = \eta_{T,R} \mathbf{M}_{T,R} \mathbf{C} \mathbf{M}_O \mathbf{F} \mathbf{M}_E \mathbf{I}_L \quad (1)$$

7 Symbols for Müller matrices are bold (\mathbf{M}), vectors are bold-italic (\mathbf{I}), and variables italic (I).
 8 The laser beam with Stokes vector \mathbf{I}_L is expanded and directed towards the atmosphere with
 9 backscatter matrix \mathbf{F} by the emitter module with Müller matrix \mathbf{M}_E . The backscattered photons
 10 are received by the telescope with a subsequent collimation lens and dichroic beam-splitters in
 11 the receiver optics module \mathbf{M}_O . A polarisation calibrator with Müller matrix \mathbf{C} is placed here
 12 before the polarising beam-splitter cube (10) with Müller matrices \mathbf{M}_T for the transmitted and
 13 \mathbf{M}_R for the reflected path, their opto-electronic gains $\eta_{T,R}$, and the final Stokes vectors $\mathbf{I}_{T,R}$ at
 14 the detectors. The opto-electronic gains $\eta_{T,R}$ include the attenuation of all non-polarising
 15 optical elements as neutral density and bandpass filters and, the quantum efficiency of the
 16 detectors, and the amplification of the electronic system. The scattering volume \mathbf{F} can be at
 17 any distance from the lidar (lidar-range), because we assume that the extinction in the range
 18 between the lidar and the scattering volume \mathbf{F} is polarisation independent and that signal
 19 contributions due to forward or multiple scattering in this range can be neglected. Therefore
 20 we neglect all lidar-range dependencies in the following equations. We also do not consider
 21 range dependent effects as the overlap function and the range dependent transmission of
 22 interference filters and dichroic beam-splitters, which are sensitive to the also range
 23 dependent incident angle on the optics.

24 Various lidar systems employ different calibration techniques with calibrating devices with
 25 Müller matrix \mathbf{C} at different places in the optical setup, with the respective equations:

$$26 \quad \text{before the polarising beam-splitter} \quad \mathbf{I}_S = \eta_S \mathbf{M}_S \mathbf{C} \mathbf{M}_O \mathbf{F} \mathbf{M}_E \mathbf{I}_L \quad (2)$$

$$27 \quad \text{before the receiver optics} \quad \mathbf{I}_S = \eta_S \mathbf{M}_S \mathbf{M}_O \mathbf{C} \mathbf{F} \mathbf{M}_E \mathbf{I}_L \quad (3)$$

$$28 \quad \text{behind the laser emitter optics} \quad \mathbf{I}_S = \eta_S \mathbf{M}_S \mathbf{M}_O \mathbf{F} \mathbf{C} \mathbf{M}_E \mathbf{I}_L \quad (4)$$

$$29 \quad \text{before the laser emitter optics} \quad \mathbf{I}_S = \eta_S \mathbf{M}_S \mathbf{M}_O \mathbf{F} \mathbf{M}_E \mathbf{C} \mathbf{I}_L \quad (5)$$



1 In the following we report just a few examples from the literature with sufficient description
2 of their calibration technique. Pal and Carswell (1973) used three telescopes with Glan-
3 Thomson prisms in the receiver optics (Eq. (2)) at 0° , 45° , and 90° orientation with respect to
4 the laser polarisation to determine the first three Stokes parameters of the scattered light, and
5 calibrated them by mechanically switching all polarisers to 0° orientation. Houston and
6 Carswell (1978) extended this set-up by a fourth telescope with a $\lambda/4$ plate to measure all four
7 Stokes parameters, with the same calibration technique as before. The relative polarisation
8 sensitivity of the CALIOP lidar on CALIPSO (Winker et al., 2009) is calibrated with a
9 pseudo-depolariser before the polarising beam-splitter (Hunt et al., 2009), which is described
10 by Eq. (2). Del Guasta et al. (2006) calibrate the gain ratio η_R/η_T of their polarimetric lidar
11 with an unpolarised light source before the polarising beam-splitter (Eq. (2)) and determine
12 the receiving optics Müller matrix \mathbf{M}_O with a linearly polarised light source and rotating the
13 receiving optics, which corresponds to Eq. (3) with a mechanical rotation matrix C . Similar
14 rotation calibration before the polarising beam-splitter is applied with RALI (Nemuc et al.,
15 2013) and the Raymetrics LR331D400 (Bravo-Aranda et al., 2013) with a mechanical
16 rotation $\Delta 90^\circ$ -calibration (see Sect. 5), and with a $\lambda/2$ plate rotation in the MULIS
17 (Freudenthaler et al., 2009) and the Cloud Physics Lidar (McGill et al., 2002; Liu et al.,
18 2004). A sheet polariser at 45° is used before the polarising beam-splitter in the AD-Net lidars
19 (Shimizu et al., 2004). Mechanical rotation before the receiving optics (Eq. (3)) is employed
20 for the DLR HSRL (Esselborn et al., 2008), for POLIS (Freudenthaler et al., 2009), and by
21 Nisantzi et al. (2014). For the McMurdo lidar (Snels et al., 2009) and the PollyXT
22 (Engelmann et al., 2015) a linear polariser is used before the receiving optics. An unpolarised
23 light source before the receiver telescope is used by Mattis et al. (2009). Spinhirne et al.
24 (1982) use a $\lambda/2$ plate for polarisation rotation in the output beam (Eq. (4)). The HSRL-1
25 (Hair et al., 2008) and HSRL-2 (Burton et al., 2015) as well as David et al. (2012) use a $\lambda/2$
26 plate as rotation calibrator before some parts of the emission optics (Eq. (5)). Roy et al. (2011)
27 and Cao et al. (2010) use a $\lambda/2$ plate before the emitter optics (Eq. (5)), but they switch the
28 plane of emitted polarisation continually between horizontal and vertical and calculate the
29 linear depolarisation ratio from the geometric mean of both measurements, which makes a
30 separate calibration unnecessary. However, the equations of this work can still be used for the
31 error analysis. Polarisation switching between laser pulses and with only one detection
32 channel is done by Platt (1977) with mechanical rotation of the receiver optics, by Eloranta
33 and Piironen (1994) with a $\lambda/2$ plate after the emitter optics (Eq. (4)), by Seldomridge et al.



1 (2006) with a nematic liquid crystal before the polarising beam-splitter (Eq. (2)), and by
2 (Flynn et al., 2007) with a $\lambda/2$ plate before the emitter optics (Eq. (5)). Although the explicit
3 equations in this work consider only one variable polarising element (i.e. the calibrator), the
4 equations for more complex lidar setups as with a polarising beam-splitter and a $\lambda/4$ plate in
5 the common emitter/receiver path ((Eloranta, 2005; David et al., 2013) or with different
6 variable polarisation elements in the emitter/receiver path (Kaul et al., 2004; Hayman et al.,
7 2012; Volkov et al., 2015) can be constructed with the equations provided in this work. Snels
8 et al. (2009) present an overview of some potential error sources and other existing
9 polarisation calibration techniques including calibration with assumed known depolarisation
10 from molecules (“clear sky”) or clouds with spherical particles.

11 The equations presented in this work can be used for the design of lidar systems, especially
12 for the determination of the requirements for certain components in order to achieve the
13 desired measurement accuracy, for the analysis of the performance of existing lidar systems
14 by means of different calibration set-ups, and for the final error calculation with respect to the
15 polarisation characteristics.

16 One of the main uncertainties is the orientation of the plane of polarisation of the laser beam
17 (angle α) with respect to the orientation of the polarising beam-splitter (briefly laser rotation),
18 because first, the plane of polarisation of the laser might not only be determined by the
19 orientation of the Pockels cell in the laser cavity, but also by the orientation of the crystals for
20 second and third harmonics generation and by the harmonic separation beam-splitters.
21 Second, the laser and emitter optics are often mounted on a separate optical breadboard,
22 which might be rotated with respect to the receiver breadboard. Furthermore, laser
23 manufacturers usually provide neither an indication of the accuracy of the orientation nor an
24 accurate mechanical reference for it, the orientation cannot be measured easily, and finally, the
25 orientation can change with time and environmental conditions. We take into account that in
26 lidar labs it is usually not possible to perform elaborate and accurate measurements as in an
27 optical lab equipped for ellipsometric measurements. Therefore we want to use simple tools
28 and as few as possible measurements - at best with the tools which we already use for the
29 atmospheric depolarisation measurements.

30 Some optical parts can be made almost ideal and some misalignments can be made very small
31 so that they become negligible. For these cases often much simpler equations can be derived,
32 which show the residual influence of the other non-ideal parts, and which can be used directly



1 in lidar retrieval algorithms. It becomes also clear in which cases corrections are not possible,
2 when additional measurements with simple set-ups can help to retrieve the properties of the
3 disturbing parts, and where one has to be careful in the design of a lidar system to avoid non-
4 correctable errors. We want to find the set-ups and calibrators, with which the calibration can
5 be measured with the least errors, and we want equations to assess the final uncertainties in
6 the retrieved lidar products. Set-ups with 90° separated limit stops can be made very accurate
7 ($< 0.1^\circ$) by means of working machines. Motorised holders with sufficient resolution and
8 accuracy are commercially available. An example for an almost ideal part is the linear
9 polariser. Polarising sheet filters are available with high extinction, well specified by
10 manufacturers. They are relatively insensitive to the incident angle, work over a sufficiently
11 large wavelength range, and are thin, which means that they can be placed even in already
12 existing lidar systems with little space for additional optics. Additionally, they are available in
13 large size at an affordable price - in contrast to crystal polarisers and wave plates, and thus
14 they can also be placed before the telescope. Wave plates and circular polarisers made of
15 plastic sheets are usually not as well specified concerning their phase shift, acceptance angle
16 and wavelength range. For other places, which require only small diameters, true zero-order
17 $\lambda/2$ plates can be used.

18 Since the atmosphere is not stable and the laser power might change between two consecutive
19 measurements, the absolute signals change. But if we use the ratios of the cross and parallel
20 signals, which only change with the atmospheric polarisation parameter a , we can easily find
21 atmospheric situations which introduce negligible errors in the calculations. Therefore we
22 only use signal ratios for the calibrations.

23 Most of the problems can probably be solved with a much smaller theoretical framework. But
24 then often questions arise, how the one or other misalignment, rotation, additional retardance
25 or diattenuation would influence the final results. The impotence of less extended
26 formulations to answer these questions will always leave an uncomfortable uncertainty. This
27 work is an attempt to provide the tools to answer some of these questions, with the
28 disadvantage of being rather extended.

29 Section 2 provides a simplified example as an introduction and preparation for Sect. 3, where
30 we introduce the concepts and parameters which are necessary to formulate the equations in
31 such a general way that they can be applied to a large variety of lidar systems. In order to
32 generalise and to simplify the expressions, several binary parameters are introduced in the



1 equations, which enable us to describe orthogonal orientations of individual elements with
2 just one expression and which reduce the number of equations considerably. In Sect. 4 we
3 develop the general equations for the lidar signals of normal atmospheric measurements
4 (*standard measurements* in the following) and for the linear depolarisation ratio. In Sect. 5 we
5 introduce the general concept of the 45° and $\Delta 90$ calibrations, which is then applied in Sect. 6
6 to 10 for different calibrators and in the subsections for different positions of the calibrators in
7 the emitter-receiver optics. We include the following types of calibrators: unpolarised light
8 (Sect. 6), which has to be inserted by an additional light source or diffuser and has therefore
9 some disadvantages; the mechanical and $\lambda/2$ plate rotator (Sect. 7); the linear polariser (Sect.
10 8), which can be easily included in existing systems; the $\lambda/4$ plate (Sect. 9), which can also be
11 used to determine the amount of circular polarisation (S.14); and the circular polariser (Sect.
12 10). General purpose equations used in several sections are shifted to the appendices, and
13 common equations or concepts, which can also be found in standard text books, are collected
14 in the supplement in order to show their form with the variables used in this work.

15 **2 The basic Müller-Stokes representation of lidar signals with polarisation**

16 In this chapter we use a simple example of Fig.(1), described with Eq. (2), to introduce some
17 basic concepts. It contains a calibrator C before the polarising beam-splitter and neglects the
18 polarising effects of the receiver optics M_o , i.e.

$$19 \quad \mathbf{I}_{T,R} = \eta_{T,R} \mathbf{M}_{T,R} \mathbf{C} \mathbf{F} \mathbf{I}_L \quad (6)$$

20 The total power I_L and the state of polarisation of horizontal-linear polarised laser light are
21 represented by the Stokes vector

$$22 \quad \mathbf{I}_L = I_L \begin{pmatrix} 1 \\ 1 \\ 0 \\ 0 \end{pmatrix} \quad (7)$$

23 The magnitude I_L of the Stokes vector is the total light beam intensity. It is directly
24 measurable with a light detector for the flux of photons. Because a lidar includes optics as
25 telescope and lenses, which change the diameter or focus the light beam, here the colloquial
26 intensity means the radiant flux or radiant energy per unit time. However, the finally
27 measured quantities are the electronic signals I_T and I_R of the detectors in the transmitted and
28 reflected paths. We use flux, intensity and signal alternatively, depending on the context.



1 2.1 Depolarising atmospheric aerosol

2 Müller matrices describe the linear interaction between polarised light and an optical system
 3 (optical elements or medium). For any input, represented as a Stokes vector, the Müller matrix
 4 produces a unique output, in the form of another Stokes vector. For the backscattering of a
 5 volume of randomly oriented, non-spherical particles with rotation and reflection symmetry
 6 the Müller matrix \mathbf{F} can be written as (van de Hulst, 1981; Mishchenko and Hovenier, 1995;
 7 Mishchenko et al., 2002)

$$8 \quad \mathbf{F} = \begin{pmatrix} F_{11} & 0 & 0 & 0 \\ 0 & F_{22} & 0 & 0 \\ 0 & 0 & -F_{22} & 0 \\ 0 & 0 & 0 & F_{44} \end{pmatrix} = F_{11} \begin{pmatrix} 1 & 0 & 0 & 0 \\ 0 & a & 0 & 0 \\ 0 & 0 & -a & 0 \\ 0 & 0 & 0 & 1-2a \end{pmatrix} \quad (8)$$

9 with the polarisation parameter a (Chipman, 2009b; Eq. (93))

$$10 \quad a = \frac{F_{22}}{F_{11}} \quad (9)$$

11 and

$$12 \quad F_{44} = F_{11} - 2F_{22} = F_{11}(1 - 2a) \quad (10)$$

13 Note, that in some literature (Flynn et al., 2007; Gimmestad, 2008; Roy et al., 2011; Gasteiger
 14 and Freudenthaler, 2014) the *de-polarisation parameter* $d = (1 - a)$ is used, and in Borovoi et
 15 al. (2014) d is called *polarisation parameter*. In Volkov et al. (2015) $e = a$ (for randomly
 16 oriented particles) is called *sphericity index*. However, in this work we use the polarisation
 17 parameter a for the reason of brevity, which is the fraction of the backscattered light that
 18 maintains the emitted linear polarisation.

19 The matrix \mathbf{F} in Eq. (8) describes a pure depolariser \mathbf{M}_Δ (Lu and Chipman, 1996), but
 20 including a mirror reflection \mathbf{M}_M for the backscattering direction, with the backscatter
 21 coefficient F_H .

$$22 \quad \mathbf{F} = \mathbf{M}_M \mathbf{M}_\Delta = F_{11} \begin{pmatrix} 1 & 0 & 0 & 0 \\ 0 & 1 & 0 & 0 \\ 0 & 0 & -1 & 0 \\ 0 & 0 & 0 & -1 \end{pmatrix} \begin{pmatrix} 1 & 0 & 0 & 0 \\ 0 & a & 0 & 0 \\ 0 & 0 & a & 0 \\ 0 & 0 & 0 & 2a-1 \end{pmatrix} \quad (11)$$



1 F_{11} and a are the only range dependent parameters in all the following equations. The volume
 2 linear depolarisation ratio δ of the scattering volume, which contains particles and air
 3 molecules, can be written as (Mishchenko and Hovenier, 1995)

$$4 \quad \delta = \frac{F_{11} - F_{22}}{F_{11} + F_{22}} = \frac{1 - a}{1 + a} \Rightarrow a = \frac{1 - \delta}{1 + \delta} \quad (12)$$

5 The Stokes vector \mathbf{I}_{in} of horizontal-linear polarised light \mathbf{I}_L reflected by the atmosphere \mathbf{F} and
 6 incident in the receiving optics is

$$7 \quad \mathbf{I}_{in} = \mathbf{F}\mathbf{I}_L = F_{11} \begin{pmatrix} 1 & 0 & 0 & 0 \\ 0 & a & 0 & 0 \\ 0 & 0 & -a & 0 \\ 0 & 0 & 0 & 1 - 2a \end{pmatrix} \mathbf{I}_L = F_{11} \mathbf{I}_L \begin{pmatrix} 1 \\ a \\ 0 \\ 0 \end{pmatrix} \quad (13)$$

8 2.2 Optical parts: diattenuator with retardation

9 All other optical elements in the lidar receiver can be described as a combination of
 10 diattenuators and retarders (Lu and Chipman, 1996) (retarding diattenuators; Eq. (14)). Often
 11 a polarising beam-splitter cube is used for splitting in transmitted and a reflected components
 12 polarised parallel and perpendicular with respect to the laser polarisation. But also polarising
 13 or even non-polarising beam-splitter plates with subsequent polarisation filters (analysers) can
 14 be used. All of them and combinations of them can be described with the Müller matrix of a
 15 polarising beam-splitter (PBS) (Pezzaniti and Chipman, 1994), considering the remarks in
 16 S.4. The matrix of the transmitting part is

$$17 \quad \mathbf{M}_T = \frac{1}{2} \begin{pmatrix} T_T^p + T_T^s & T_T^p - T_T^s & 0 & 0 \\ T_T^p - T_T^s & T_T^p + T_T^s & 0 & 0 \\ 0 & 0 & 2\sqrt{T_T^p T_T^s} \cos \Delta_T & 2\sqrt{T_T^p T_T^s} \sin \Delta_T \\ 0 & 0 & -2\sqrt{T_T^p T_T^s} \sin \Delta_T & 2\sqrt{T_T^p T_T^s} \cos \Delta_T \end{pmatrix} =$$

$$= T_T \begin{pmatrix} 1 & D_T & 0 & 0 \\ D_T & 1 & 0 & 0 \\ 0 & 0 & Z_T c_T & Z_T s_T \\ 0 & 0 & -Z_T s_T & Z_T c_T \end{pmatrix} \quad (14)$$

18 with the intensity transmission coefficients (transmittance) for light polarised parallel (T^p) and
 19 perpendicular (T^s) to the plane of incidence of the PBS, the diattenuation parameter D_T , and
 20 the average transmittance T_T , i.e. for unpolarised light. Δ_T is the difference of the phase shifts



1 of the parallel and perpendicular polarised electrical fields (retardance) according to the
 2 Muller-Nebraska convention (Muller, 1969).

$$3 \quad T_T = \frac{T_T^p + T_T^s}{2}, \quad D_T = \frac{T_T^p - T_T^s}{T_T^p + T_T^s}, \quad Z_T = \frac{2\sqrt{T_T^p T_T^s}}{T_T^p + T_T^s} = \sqrt{1 - D_T^2}, \quad (15)$$

$$c_T = \cos \Delta_T, \quad s_T = \sin \Delta_T, \quad \Delta_T = \varphi_T^p - \varphi_T^s$$

4 Please note, that this definition differs in two ways from the definition in Chipman (2009b):
 5 the retardance is defined differently there ($\Delta_x = \varphi_x^s - \varphi_x^p$), and we denote with D the
 6 horizontal diattenuation parameter d_h (Chipman, 2009b) and not the diattenuation magnitude
 7 $D_{mag} = |D|$ (see S.4). The Müller matrix for the reflecting part of the PBS Eq. (16) includes a
 8 mirror reflection (S.6) with the corresponding intensity reflection coefficients (reflectance) for
 9 light polarised parallel ($R_p = T_R^p$) and perpendicular ($R_s = T_R^s$) to the plane of incidence (S.1)
 10 of the polarising beam-splitter.

$$11 \quad \mathbf{M}_R = T_R \begin{pmatrix} 1 & D_R & 0 & 0 \\ D_R & 1 & 0 & 0 \\ 0 & 0 & -Z_R c_R & -Z_R s_R \\ 0 & 0 & Z_R s_R & -Z_R c_R \end{pmatrix} = T_R \begin{pmatrix} 1 & 0 & 0 & 0 \\ 0 & 1 & 0 & 0 \\ 0 & 0 & -1 & 0 \\ 0 & 0 & 0 & -1 \end{pmatrix} \begin{pmatrix} 1 & D_R & 0 & 0 \\ D_R & 1 & 0 & 0 \\ 0 & 0 & Z_R c_R & Z_R s_R \\ 0 & 0 & -Z_R s_R & Z_R c_R \end{pmatrix} \quad (16)$$

$$12 \quad T_R = \frac{T_R^p + T_R^s}{2}, \quad D_R = \frac{T_R^p - T_R^s}{T_R^p + T_R^s}, \quad Z_R = \frac{2\sqrt{T_R^p T_R^s}}{T_R^p + T_R^s} = \sqrt{1 - D_R^2}, \quad (17)$$

$$c_R = \cos \Delta_R, \quad s_R = \sin \Delta_R, \quad \Delta_R = \varphi_R^p - \varphi_R^s$$

13 In order to simplify the derivation of the equations, we describe both the reflecting and
 14 transmitting matrices with the matrix \mathbf{M}_S , and replace the subscript s (for splitter) by T
 15 (transmitting) or R (reflecting) where appropriate, which means

$$16 \quad D_S \in \{D_R, D_T\}, \quad \mathbf{M}_S \in \{\mathbf{M}_R, \mathbf{M}_T\}, \quad I_S \in \{I_R, I_T\} \quad (18)$$

17 It has to be emphasised, that for this reason we can't use the diattenuation magnitude D_{mag} ,
 18 which is always positive and almost exclusively used in other publications, but have to use the
 19 diattenuation parameter D , which changes the sign when T_R^s becomes larger than T_R^p (see
 20 S.3). Please keep also in mind that usually $D_R < 0$, that \mathbf{M}_R includes an additional mirror
 21 reflection, and that fluxes measured after the PBS are not influenced by the addition of an
 22 ideal mirror reflection in the optical path.



1 2.3 Calibration, linear depolarisation ratio, and total signal

2 Eq. (6) shows the Stokes vectors of the transmitted (I_T) and reflected (I_R) channels, alias I_S ,
 3 after the polarising beam-splitter \mathbf{M}_S (PBS) without calibrator, i.e. $\mathbf{C} = \mathbf{1}$ = identity matrix. Eq.
 4 (6) represents the standard lidar measurement at the axial rotation of 0° , neglecting for now
 5 additional optics in \mathbf{M}_O .

$$\begin{aligned}
 I_S(0^\circ) &= \eta_S \mathbf{M}_S \mathbf{F} I_L = \eta_S \mathbf{M}_S I_{in} = \\
 6 \quad &= \eta_S T_S \begin{pmatrix} 1 & D_S & 0 & 0 \\ D_S & 1 & 0 & 0 \\ 0 & 0 & Z_S c_S & Z_S s_S \\ 0 & 0 & -Z_S s_S & Z_S c_S \end{pmatrix} F_{11} I_L \begin{pmatrix} 1 \\ a \\ 0 \\ 0 \end{pmatrix} = \eta_S T_S F_{11} I_L \begin{pmatrix} 1 + D_S a \\ D_S + a \\ 0 \\ 0 \end{pmatrix} \quad (19)
 \end{aligned}$$

7 The measured signals I_S are

$$8 \quad I_S(0^\circ) = \eta_S T_S F_{11} I_L (1 + D_S a) \quad (20)$$

9 which correspond to the transmitted and reflected intensities, include the individual channels
 10 gains η_S , i.e. η_T and η_R , which are the product of the electronic amplification of the detectors,
 11 the amplifiers, and of the optical attenuation due to polarisation insensitive attenuation of all
 12 optics including neutral density and interference filters. The latter is in general different in the
 13 two channels. We can solve the equation of the ratio of the measured reflected to the
 14 transmitted signals

$$15 \quad \frac{I_R(0^\circ)}{I_T(0^\circ)} = \frac{\eta_R T_R (1 + D_R a)}{\eta_T T_T (1 + D_T a)} = \frac{\eta_R (T_R^p + T_R^s \delta)}{\eta_T (T_T^p + T_T^s \delta)} \quad (21)$$

16 for the linear depolarisation ratio δ if we know the calibration factor

$$17 \quad \eta \equiv \frac{\eta_R T_R}{\eta_T T_T} \quad (22)$$

18 (with reflectance T_R and transmittance T_T for unpolarised light) and the transmission
 19 parameters of the polarising beam-splitter T_T^p , T_T^s , T_R^p , and T_R^s for the correction of its cross
 20 talk. We could get the calibration factor η already with the measurements in Eq. (21) if the
 21 light incident on the analyser was unpolarised, i.e. $a = 0$. Else, η can be determined by means
 22 of calibration measurements, e.g. by rotating the the PBS including the detectors by $+45^\circ$ or
 23 -45° about the optical axis (Eq. (23)).



$$\begin{aligned}
 I_s(\pm 45^\circ) &= \eta_s \mathbf{M}_s \mathbf{R}(\pm 45^\circ) \mathbf{F} I_m = \\
 &= \eta_s \mathbf{M}_s \begin{pmatrix} 1 & 0 & 0 & 0 \\ 0 & 0 & \mp 1 & 0 \\ 0 & \pm 1 & 0 & 0 \\ 0 & 0 & 0 & 1 \end{pmatrix} F_{11} I_L \begin{pmatrix} 1 \\ a \\ 0 \\ 0 \end{pmatrix} = \eta_s T_s \begin{pmatrix} 1 & D_s & 0 & 0 \\ D_s & 1 & 0 & 0 \\ 0 & 0 & Z_s c_s & Z_s s_s \\ 0 & 0 & -Z_s s_s & Z_s c_s \end{pmatrix} F_{11} I_L \begin{pmatrix} 1 \\ 0 \\ \pm a \\ 0 \end{pmatrix} = \\
 &= \eta_s T_s F_{11} I_L \begin{pmatrix} 1 \\ D_s \\ \pm a Z_s c_s \\ \mp a Z_s s_s \end{pmatrix}
 \end{aligned} \tag{23}$$

2 With the rotations $\mathbf{R}(\pm 45^\circ)$ it is intended to produce at the entrance of the PBS equal light
 3 intensities in the transmitted and reflected paths, independent of the atmospheric
 4 depolarisation. The error from an inaccurate $\pm 45^\circ$ alignment can be reduced by the $\Delta 90^\circ$
 5 calibration explained in Sect. 5. From Eq. (23) we get the signal intensities

$$6 \quad I_s(\pm 45^\circ) = \eta_s T_s F_{11} I_L \tag{24}$$

7 and the calibration factor η from the signal ratio

$$8 \quad \frac{I_R(\pm 45^\circ)}{I_T(\pm 45^\circ)} = \frac{\eta_R T_R}{\eta_T T_T} = \eta \tag{25}$$

9 With known η we can express the measured signal ratio δ^* in Eq. (21) as

$$10 \quad \delta^* \equiv \frac{1}{\eta} \frac{I_R(0^\circ)}{I_T(0^\circ)} = \frac{I_R(\pm 45^\circ)}{I_R(0^\circ)} \frac{I_R(0^\circ)}{I_T(0^\circ)} = \frac{T_T T_R^p + T_R^s \delta}{T_R T_T^p + T_T^s \delta} \tag{26}$$

11 which is almost equal to the linear depolarisation ratio δ , but still includes the diattenuation
 12 and cross talk of the imperfect polarising beam-splitter. From δ^* we retrieve the linear
 13 depolarisation ratio δ

$$14 \quad \delta = \frac{\delta^* T_R T_T^p - T_T T_R^p}{T_T T_R^s - \delta^* T_R T_T^s} \tag{27}$$

15 With the assumption for good PBSs

$$16 \quad T_T^s \ll 1 \Rightarrow \left\{ T_R^s \approx 1, T_T \approx 0.5 T_T^p, T_R \approx 0.5 (1 + T_R^p) \right\} \tag{28}$$

17 we get an approximation

$$18 \quad \delta \approx \delta^* - T_R^p (1 - \delta^*) \tag{29}$$



1 Next we will determine the total lidar backscatter signal from the two signals I_T and I_R
 2 measured at 0° . This is the range dependent signal, which we use for the inversion of the
 3 backscatter coefficient F_{11} with the lidar inversion methods. From Eq. (20) we can get F_{11}
 4 either from the transmitted or from the reflected signal

$$5 \quad F_{11} = \frac{I_S(0^\circ)}{\eta_S T_S I_L (1 + D_S a)} \quad (30)$$

6 The polarisation parameter a can be extracted from the signal ratio in Eq. (21)

$$7 \quad a = \frac{\eta I_T - I_R}{I_R D_T - \eta I_T D_R}, \quad (31)$$

8 and substituted in Eq. (30) to yield

$$9 \quad I_L F_{11} = \frac{\eta_T T_T D_T I_R - \eta_R T_R D_R I_T}{\eta_T T_T \eta_R T_R (D_T - D_R)} = \frac{1}{D_T - D_R} \left(\frac{D_T I_R}{\eta_R T_R} - \frac{D_R I_T}{\eta_T T_T} \right). \quad (32)$$

10 Equation (32) shows that we cannot determine an absolute F_{11} without an absolute calibration
 11 of the individual channel gains η_R and η_T and knowledge of the laser intensity I_L . However, for
 12 the lidar signal inversions, which use a reference value at a certain range or similar, we only
 13 need a relative, range dependent F_{11} . Hence we can choose any of the range independent
 14 parameters in Eq. (32), in which only I_T and I_R are range dependent, which we cancel and get

$$15 \quad F_{11} \propto D_T I_R - \eta D_R I_T = \frac{T_T^p - T_T^s}{T_T^p + T_T^s} I_R - \eta \frac{T_R^p - T_R^s}{T_R^p + T_R^s} I_T. \quad (33)$$

16 In case the polarising beam-splitter is ideal, i.e. $T_T^p = T_R^s = 1$ and $T_T^s = T_R^p = 0$, and hence $D_R =$
 17 -1 and $D_T = +1$, Eq. (33) becomes as expected

$$18 \quad F_{11} \propto I_R + \eta I_T, \quad (34)$$

19 Please bear in mind that in general $T_R^s > T_R^p$, and therefore $(T_R^p - T_R^s) < 0$ and $D_R < 0$
 20 according to our definition in Eq. (17).

21 Summarising: we have to find the calibration factor η and correct the cross talk. δ is retrieved
 22 from two signals at 0° represented by δ^* , Eq. (26), plus two signals for the calibration factor at
 23 $\pm 45^\circ$, Eq. (25), and the knowledge of the PBS parameters T_T^p , T_T^s , T_R^p , and T_R^s for the
 24 correction of the cross talk.



1 3 Complete Müller-Stokes lidar setup with rotation of optical elements

2 In the previous section, a basic lidar setup is described with the Müller-Stokes formalism as
 3 an introduction, which includes only a horizontal-linear polarised laser, the matrices for the
 4 atmospheric aerosol backscattering and depolarisation, and the polarising beam-splitter. In
 5 order to expand this setup to a realistic but still manageable model for a large variety of lidar
 6 systems and calibration techniques, we introduce in this section some concepts and variables,
 7 which will enable us to describe the variety of setups with as few as possible equations.

8 The Stokes-Müller formalism (Chipman, 2009b) represents four linear equations (Eq. (35)),
 9 which relate the four output with the four input Stokes parameters.

$$\begin{aligned}
 \mathbf{I}_{out} &= \begin{pmatrix} I_{out} \\ Q_{out} \\ U_{out} \\ V_{out} \end{pmatrix} = \mathbf{M} \mathbf{I}_{in} = \begin{pmatrix} M_{11} & M_{12} & M_{13} & M_{14} \\ M_{21} & M_{22} & M_{23} & M_{24} \\ M_{31} & M_{32} & M_{33} & M_{34} \\ M_{41} & M_{42} & M_{43} & M_{44} \end{pmatrix} \begin{pmatrix} I_{in} \\ Q_{in} \\ U_{in} \\ V_{in} \end{pmatrix} = \\
 10 & \\
 &= M_{11} \mathbf{I}_{in} \begin{pmatrix} 1 & m_{12} & m_{13} & m_{14} \\ m_{21} & m_{22} & m_{23} & m_{24} \\ m_{31} & m_{32} & m_{33} & m_{34} \\ m_{41} & m_{42} & m_{43} & m_{44} \end{pmatrix} \begin{pmatrix} i_{in} \\ q_{in} \\ u_{in} \\ v_{in} \end{pmatrix} \quad (35)
 \end{aligned}$$

11 The small letter matrix (m_{ij}) and vector components at the right of Eq. (35) are normalised by
 12 their first element, i.e. M_{11} and I_{in} ; hence $m_{11} = i_{in} = 1$. However, in the following we usually
 13 keep the variable i_{in} in order to allow for later expansions of the equations. While the first
 14 Stokes vector parameter I_{out} can be directly detected with a photon detector, the other output
 15 Stokes parameters can each be determined with two measurements of output intensities using
 16 additional polarisation elements (Chipman, 2009a) (see Eq. S.2.2). We derive the backscatter
 17 coefficient F_{11} and the linear polarisation parameter a of the Müller matrix \mathbf{F} of the
 18 atmosphere (see Sect. 2.1) from the first two equations of I_{out} and Q_{out} in Eq. (35), which in
 19 turn are determined from the two measurements of I_R and I_T using the two orthogonal linear
 20 analysers of the polarising beam-splitter. For the determination of each additional unknown
 21 parameter we need additional measurements. For the relative calibration factor η of the two
 22 polarisation signals I_R and I_T we use an additional calibrator element with Müller matrix \mathbf{C} .
 23 The lidar setup shown in Fig (1) is described by Eq. (6), i.e. $\mathbf{I}_S = \eta_S \mathbf{M}_S \mathbf{C} \mathbf{M}_O \mathbf{F} \mathbf{M}_E \mathbf{I}_L$, where
 24 the matrices $\mathbf{M}_{T,R}$ (alias \mathbf{M}_S) represent the two paths of the polarising beam-splitter, i.e.
 25 subscripts T for transmission and R for reflection. Since the laser in our model can be



1 arbitrarily polarised and because "parallel" and "perpendicular" are defined relative to the
 2 incident plane of a beam-splitter (superscripts p and s , respectively; see S.1) and don't
 3 necessarily describe the polarisation behind it with respect to the laser polarisation, we can't
 4 use these terms here for the two branches behind the polarising beam-splitter. $C(\Psi)$ describes
 5 the calibrator matrix, which can be a mechanical rotation of the detection optics by Ψ or an
 6 optical device as a polarising sheet filter rotated by angle Ψ , for example. The purpose of the
 7 calibrator device is to produce equal intensities for both polarisation channels, independent of
 8 the laser light polarisation and independent of backscattering characteristics of the
 9 atmosphere. This is e.g. achieved with an ideal polarising sheet filter oriented at 45° with
 10 respect to the incident plane of the PBS. The calibration factor η of the relative sensitivity of
 11 both polarisation channels can be retrieved from the ratio of the measured intensities. The
 12 calibration factor includes electronic gains and the polarisation transmission of optical
 13 elements behind the calibrator. In our model the calibrator can be at three different positions
 14 in the optical chain, which are indicated by the red blocks in Fig. (2). The calibrator positions
 15 and the respective equations are these:

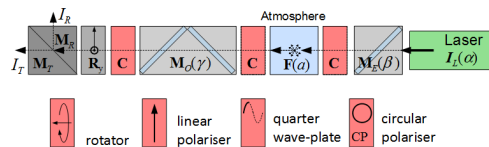
16 behind the laser emitter optics \mathbf{M}_E
$$I_s = \eta_s \mathbf{M}_s \mathbf{M}_O \mathbf{F} \mathbf{C} \mathbf{M}_E I_L = \eta_s \mathbf{M}_s \mathbf{M}_O \mathbf{F} \mathbf{C} I_{in} \quad (36)$$

17 before the telescope / receiver optics \mathbf{M}_O
$$I_s = \eta_s \mathbf{M}_s \mathbf{M}_O \mathbf{C} \mathbf{F} \mathbf{M}_E I_L = \eta_s \mathbf{M}_s \mathbf{M}_O \mathbf{C} I_{in} \quad (37)$$

18 before the polarising beam-splitter \mathbf{M}_S
$$I_s = \eta_s \mathbf{M}_s \mathbf{C} \mathbf{M}_O \mathbf{F} \mathbf{M}_E I_L = \eta_s \mathbf{M}_s \mathbf{C} I_{in} \quad (38)$$

19 In case the telescope and/or the collimating lens don't change the state of polarisation of the
 20 incoming light, the placement of the calibrator after those elements is equivalent to the
 21 position before the telescope.

22 We develop the equations for all three positions of the calibrator, and additionally for the
 23 calibration with an unpolarised light source before the receiving optics (Sect. 6). In the
 24 equations we use as calibrator elements the Müller matrix \mathbf{C} as a place holder for any sort of
 25 calibrator, which are \mathbf{M}_{rot} for mechanical rotation or by means of a $\lambda/2$ plate, \mathbf{M}_P for a linear
 26 polariser, \mathbf{M}_{QW} for a $\lambda/4$ plate, and \mathbf{M}_{CP} for a circular polariser.





1 Figure 2: Schematic of a 2-channel, polarisation sensitive lidar setup (compare Fig. 1) with
 2 Müller matrix block elements and different calibrator (red block) positions (top), and three
 3 options for the calibrator \mathbf{C} (bottom). \mathbf{I}_L : laser Stokes vector, \mathbf{M}_E : emitter optics; \mathbf{F} :
 4 atmospheric backscatter matrix with polarisation parameter a ; \mathbf{M}_O : receiver optics; \mathbf{R}_y :
 5 rotation matrix for the 0° ($y=+1$) and 90° ($y=-1$) detection setup (see text); $\mathbf{M}_{T,R}$: transmitted
 6 and reflected part of the polarising beam-splitter; $\mathbf{I}_{T,R}$: transmitted and reflected detection
 7 signals. Angles α , β , and γ are rotations around the optical axis.

8 3.1 The analyser $\langle \text{bra} |$ and input $| \text{ket} \rangle$ vectors

9 The general structure of all the considered lidar setups can be described with three groups of
 10 optical elements: elements before the calibrator, the calibrator, and elements behind the
 11 calibrator. To simplify the equations, we combine the matrices after the calibrator to an
 12 analyser matrix \mathbf{A}_S , and the matrices before the calibrator together with the Stokes vector of
 13 the laser beam \mathbf{I}_L to an input Stokes vector \mathbf{I}_{in} . Since \mathbf{A}_S and \mathbf{I}_{in} are the same for all calibrator
 14 types, they have to be derived only once and can then be used for the different setups. "After"
 15 and "before" denote the order with respect to the light direction, i.e. from right to left in the
 16 Müller-Stokes equations.

17 Since photo detectors are, in general, insensitive to the polarisation, we measure the intensity
 18 I_S at the detector, which is the first parameter of the output Stokes vector. I_S is determined by
 19 the top row of a matrix \mathbf{A}_S and an input vector \mathbf{I}_{in} .

$$20 \begin{pmatrix} I_S \\ - \\ - \\ - \end{pmatrix} = \eta_S \mathbf{A}_S \mathbf{I}_{in} = \eta_S \begin{pmatrix} A_{11} & A_{12} & A_{13} & A_{14} \\ - & - & - & - \\ - & - & - & - \\ - & - & - & - \end{pmatrix} \begin{pmatrix} I_{in} \\ Q_{in} \\ U_{in} \\ V_{in} \end{pmatrix} = \eta_S \begin{pmatrix} A_{11}I_{in} + A_{12}Q_{in} + A_{13}U_{in} + A_{14}V_{in} \\ - \\ - \\ - \end{pmatrix} \quad (39)$$

21 Using the $\langle \text{bra} | \text{ket} \rangle$ matrix-vector notation (see App. B and App. D), we define for this work
 22 the row vector $\langle \mathbf{A}_S |$ as the top row of a matrix \mathbf{A}_S ,

$$23 \langle \mathbf{A}_S | = \langle A_{11} \quad A_{12} \quad A_{13} \quad A_{14} | \quad (40)$$

24 and use analogously the column vector $| \mathbf{I}_{in} \rangle$. With this notation the equation for the intensity
 25 I_S can be written as

$$26 \begin{aligned} I_S &= \eta_S \langle \mathbf{A}_S | \mathbf{I}_{in} \rangle = \eta_S I_{in} \langle A_{11} \quad A_{12} \quad A_{13} \quad A_{14} | I_{in} \quad Q_{in} \quad U_{in} \quad V_{in} \rangle = \\ &= \eta_S I_{in} (A_{11}I_{in} + A_{12}Q_{in} + A_{13}U_{in} + A_{14}V_{in}) \end{aligned} \quad (41)$$



1 For example, the equation for signal I_S of a calibration measurement with the calibrator before
 2 the PBS (see Eq. (38)) can be expressed as

$$3 \quad I_S(y, x, \varepsilon) = \eta_S \langle \mathbf{M}_S \mathbf{R}_y | \mathbf{C}(x45^\circ + \varepsilon) | \mathbf{M}_O \mathbf{F} \mathbf{M}_E \mathbf{I}_L \rangle = \eta_S \langle \mathbf{A}_S | \mathbf{C} | \mathbf{I}_{in} \rangle \quad (42)$$

4 and the respective standard atmospheric measurement signals without the calibrator can be
 5 expressed with the same vectors $\langle \mathbf{A}_S |$ and $|\mathbf{I}_{in} \rangle$ as

$$6 \quad I_S(y) = \eta_S \langle \mathbf{M}_S \mathbf{R}_y | \mathbf{M}_O \mathbf{F} \mathbf{M}_E \mathbf{I}_L \rangle = \eta_S \langle \mathbf{A}_S | \mathbf{I}_{in} \rangle \quad (43)$$

7 In Eqs. (42) and (43) we already used the binary operators y , x , and the variable ε for different
 8 rotation angles, and the rotation matrix \mathbf{R}_y , which will be explained in detail in Sect. 3.3.

9 **3.2 Laser polarisation and atmospheric depolarisation**

10 The light leaving commercial Nd:YAG lasers is usually linearly polarised. Manufacturers
 11 often specify a polarisation "purity" $> 95\%$ or similar, which is not very accurate. Actually,
 12 the laser light is often much better polarised, but the measurement of the polarisation of
 13 individual lasers in a series is expensive and it can change during the operation and with
 14 ageing of the laser. Probably for that reason the manufacturers seem to specify a lower limit
 15 which they can assure under all circumstances. A secure method to ensure a high degree of
 16 linear polarisation is to use a polariser as the last element at the laser output. Often the
 17 orientation of the laser polarisation relative to the orientation of the polarising beam-splitter in
 18 the receiving optics is not well known, first, because the state of polarisation of short laser
 19 pulses with high power is difficult to measure accurately, and second, the state of polarisation
 20 of the laser can change during the operation of the laser over periods with changing
 21 environmental conditions. Hence we consider a possible rotation α of the plane of horizontal-
 22 linear polarisation of the laser (laser rotation). Furthermore, beam expanders and especially
 23 steering mirrors after the laser can degrade the degree of linear polarisation considerably
 24 producing elliptical polarised light. Hence we start with an emitter Stokes vector with
 25 arbitrary state of polarisation leaving the laser, which includes all effects of cleaning, shaping
 26 and steering optics

$$27 \quad \mathbf{I}_E = \mathbf{M}_E \mathbf{I}_L = T_E \mathbf{I}_L | i_E \quad q_E \quad u_E \quad v_E \rangle \quad (44)$$

28 We will develop all equations first for a general emitter beam polarisation as in Eq. (44), and
 29 then as an explicit example for a linearly polarised laser with intensity I_L and laser rotation α



1 (see App. D) to elaborate the errors due to misalignments of the calibration and measurement
 2 optics.

$$3 \quad \mathbf{I}_L(\alpha) = I_L |1 \quad c_{2\alpha} \quad s_{2\alpha} \quad 0\rangle \quad (45)$$

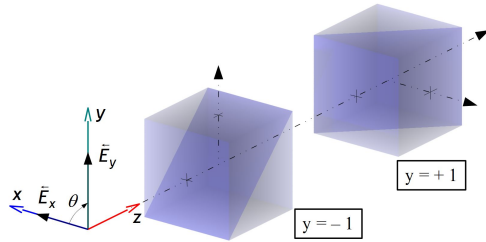
4 Depolarisation of the laser (with linear polarisation parameter a_L), caused by volume or
 5 surface scattering in or on optical elements, is hardly probable, and the scattered radiation
 6 reaching the lidar telescope would be negligible. However, it is briefly treated in S.3. The
 7 Stokes vector \mathbf{I}_F , which is reflected by the atmosphere with scattering matrix $\mathbf{F}(a)$ with linear
 8 polarisation parameter a from a generally polarised emitter \mathbf{I}_E , is (see S.3)

$$9 \quad \frac{\mathbf{I}_F(a)}{F_{11}T_E I_L} = \frac{\mathbf{F}(a)|\mathbf{M}_E \mathbf{I}_L\rangle}{F_{11}T_E I_L} = |i_E \quad aq_E \quad -au_E \quad (1-2a)v_E\rangle \quad (46)$$

10 3.3 Receiver optics and calibrator

11 In order to investigate the effect of misalignments of the optical elements on the final
 12 measurement and the calibration results, i.e. the total signal and the linear depolarisation ratio,
 13 we apply to each optical element in Eqs. (36) to (38) an additional rotation error about the
 14 optical axis (see Fig. (2)). The reference coordinate system is in general defined by the
 15 incident plane of the polarising beam-splitter (Fig. (3)), wherefore no rotation error is
 16 considered in \mathbf{M}_S . Nevertheless, the polarising beam-splitter can be mechanically rotated by
 17 90° in some existing lidar systems without changing the rest of the setup. We include this
 18 additional fixed rotation by introducing the rotation matrix \mathbf{R}_y with the polarising beam-
 19 splitter orientation parameter y (Fig. (3)). For $y = +1$ the parallel laser polarisation is detected
 20 in the transmitted channel and for $y = -1$ in the reflected channel. This seems a bit confusing,
 21 but it is necessary to get control of all the actually existing lidar set-ups. The rotation matrix
 22 \mathbf{R}_y is shown in Eq. (47).

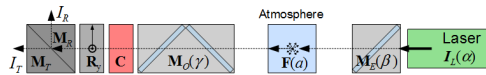
$$23 \quad \mathbf{R}_y = \mathbf{R}(y) = \begin{pmatrix} 1 & 0 & 0 & 0 \\ 0 & y & 0 & 0 \\ 0 & 0 & y & 0 \\ 0 & 0 & 0 & 1 \end{pmatrix} \Rightarrow \begin{matrix} \mathbf{R}(y = -1) = \mathbf{R}(90^\circ) \\ \mathbf{R}(y = +1) = \mathbf{R}(0^\circ) \end{matrix} \quad (47)$$



1 Figure 3: Definition of the global coordinate reference system and the binary operator y with respect to the
 2 incident plane of the polarising beam-splitter. If the polarising beam-splitter orientation parameter $y = +1$, the
 3 vibration of the horizontal-linear polarisation with vector E_x is parallel to the plane of incidence, while for $y = -$
 4 1 it is perpendicular.

5 The whole lidar system shown in Fig.(2) is then described by Eq. (48) with rotation angles α ,
 6 β , γ , and Ψ around the optical axis.

$$7 \quad I_S(y, \Psi, \gamma, a, \beta, \alpha) = \eta_S \mathbf{M}_S \mathbf{R}(y) \mathbf{C}(\Psi) \mathbf{M}_O(\gamma) \mathbf{F}(a) \mathbf{M}_E(\beta) I_L(\alpha) \quad (48)$$



8 It would be possible to include the \mathbf{R}_y rotation by changing the laser angle α in Eq. (48), but
 9 we choose to do it before the polarising beam-splitter for two reasons: first we want to use the
 10 angle α only for rotation errors, and second, in some lidar systems a rotation of the receiving
 11 optics is used for the calibration, and with these setups a change between the two \mathbf{R}_y versions
 12 of a lidar is easily accomplished and can be used for certain test measurements without
 13 changing the rest of the equations. On the other hand, an arbitrary rotation of the laser
 14 polarisation is usually not possible. A rotation γ of a retarding diattenuator \mathbf{M}_O can complicate
 15 the equations considerably, as it converts linearly polarised light into elliptically polarised,
 16 which cannot be analysed by a simple polarising beam-splitter. Therefore, diattenuating and
 17 retarding optics before the polarising beam-splitter should be carefully oriented with their
 18 eigen axes parallel to the ones of the polarising beam-splitter to avoid the resulting
 19 uncertainties. Such an element can e.g. be a dichroic beam-splitter, which does not reflect
 20 exactly to 0° or 90° . For what we call $\Delta 90^\circ$ -calibration, we use two calibrator orientations
 21 $\mathbf{C}(\Psi)$ with

$$22 \quad \begin{aligned} \Psi^+ &= +45^\circ + \varepsilon \\ \Psi^- &= -45^\circ + \varepsilon \end{aligned} \quad (49)$$



1 so that

$$2 \quad \Psi^+ - \Psi^- = 90^\circ \quad (50)$$

3 We choose these special angles, because in the geometric mean of two calibrations at
 4 orientations exactly 90° apart the error terms sometimes compensate very well. Note, that the
 5 $\Delta 90$ error angle ε describes the rotational misalignment of the whole $\Delta 90$ -calibrator setup
 6 with respect to the polarising beam-splitter, not the error in the 90° difference. So, $\pm 45^\circ$
 7 means either $+45^\circ$ or -45° , and $\Delta 90$ means the combination of measurements at $+45^\circ + \varepsilon$ and
 8 $-45^\circ - \varepsilon$. To obtain general equations, we combine these angles using the binary operator x for
 9 calibrations

$$10 \quad x = \pm 1: \Psi(x, \varepsilon) = x45^\circ + \varepsilon \quad (51)$$

11 We use this definition in a setup with a rotation calibrator \mathbf{M}_{rot} (Sect. 7)

$$12 \quad \mathbf{C}(\Psi, h) = \mathbf{M}_{rot}(x45^\circ + \varepsilon, h) = \mathbf{M}_{rot}(x, \varepsilon, h) \quad (52)$$

13 with the binary operator h to discern between a mechanical ($h = +1$) and a $\lambda/2$ plate rotation
 14 (S.10.15), and can express the four equations for the reflected and transmitted signals I_R and I_T
 15 of the two calibration measurements at $\Psi = \pm 45^\circ + \varepsilon$ with the one formula Eq. (53)

$$16 \quad I_S(y, x, \varepsilon, h, \gamma, a, \beta, \alpha) = \eta_S \langle \mathbf{M}_S \mathbf{R}_y | \mathbf{M}_{rot}(x, \varepsilon, h) | \mathbf{M}_O(\gamma) \mathbf{F}(a) \mathbf{M}_E(\beta) \mathbf{I}_L(\alpha) \rangle \quad (53)$$

17 and the four equations for the standard measurements at $\Psi = 0^\circ$ ($y = +1$) and $\Psi = 90^\circ$ ($y = -1$)
 18 using the same analyser and input Stokes vectors with just another formula Eq. (54)

$$19 \quad I_S(y, \varepsilon, h, \gamma, a, \beta, \alpha) = \eta_S \langle \mathbf{M}_S \mathbf{R}_y | \mathbf{R}(\varepsilon) \mathbf{M}_h | \mathbf{M}_O(\gamma) \mathbf{F}(a) \mathbf{M}_E(\beta) \mathbf{I}_L(\alpha) \rangle \quad (54)$$

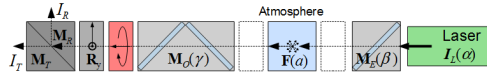
20 Using the rotation calibrator we have to consider the same alignment error ε for the standard
 21 measurements at 0° and 90° as for the calibration at the $\pm 45^\circ$, because this calibrator is not
 22 removed from the lidar setup after the calibration measurements. Hence we have to differ, if
 23 necessary, between ε for the standard measurements and $\varepsilon_{P, QW, CP}$, with P for the polariser, QW
 24 for the $\lambda/4$ plate, and CP for the circular polariser. Please note that $\varepsilon = 0$ for all other
 25 calibrators.

26 **4 Retrieval of the total signal and of the linear depolarisation ratio**

27 The final goal of this work is to investigate how the polarisation calibration factor, the linear
 28 depolarisation ratio, and the total lidar signal can be retrieved from the measurements I_T and



1 I_R , how much the various rotational misalignments and the crosstalk of the calibrator influence
 2 them, and how the deviations can possibly be corrected. The standard atmospheric
 3 measurement signals I_S in Eq. (54) include a rotational error ε before the polarising beam-
 4 splitter.

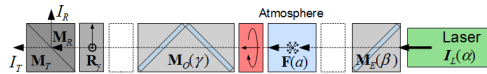


5 We get Eq. (55) for the analyser part with Eqs. (D.5), (S.5.1.6), and (S.10.15.2), and with the
 6 most general input I_E from Eq. (E.31) with atmospheric polarisation parameter a we get the
 7 signal I_S from Eq. (S.7.1.2)

$$8 \quad \langle \mathbf{A}_S(y) | \mathbf{R}(\varepsilon, h) \rangle = \langle \mathbf{M}_S \mathbf{R}_y | \mathbf{R}(\varepsilon) \mathbf{M}_h \rangle = T_S \langle 1 \quad y c_{2\varepsilon} D_S \quad -y h s_{2\varepsilon} D_S \quad 0 \rangle \quad (55)$$

$$\begin{aligned} \frac{I_S}{\eta_S T_S T_{rot} T_O F_{11} T_E I_L} &= \frac{\langle \mathbf{A}_S(y) | \mathbf{R}(\varepsilon) \mathbf{M}_h | I_{in}(\gamma, a) \rangle}{T_S T_{rot} T_O F_{11} T_E I_L} = \frac{\langle \mathbf{M}_S \mathbf{R}_y | \mathbf{R}(\varepsilon) \mathbf{M}_h | \mathbf{M}_O(\gamma) \mathbf{F}(a) I_E \rangle}{T_S T_{rot} T_O F_{11} T_E I_L} = \\ &= (1 + y D_S D_O c_{2\gamma + h 2\varepsilon}) i_E - y D_S Z_O S_O s_{2\gamma + h 2\varepsilon} v_E + \\ &+ a \left\{ D_O (c_{2\gamma} q_E - s_{2\gamma} u_E) + y D_S \left[(c_{2\varepsilon} q_E + s_{h 2\varepsilon} u_E) - s_{2\gamma + h 2\varepsilon} (W_O (s_{2\gamma} q_E + c_{2\gamma} u_E) - 2 Z_O S_O v_E) \right] \right\} \end{aligned}$$

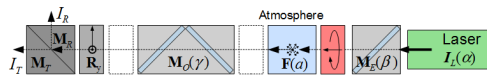
9 (56)



10 In case the rotational error is before the receiving optics, the equation becomes more complex.

11 With Eq. (D.7) for the analyser part and (E.26) for the input vector we get from Eq. (S.7.2.1)

$$\begin{aligned} \frac{I_S}{\eta_S T_S T_O T_{rot} F_{11} T_E I_L} &= \frac{\langle \mathbf{A}_S(y, \gamma) | I_{in, \varepsilon}(\varepsilon, h, a) \rangle}{T_S T_O T_{rot} F_{11} T_E I_L} = \frac{\langle \mathbf{M}_S \mathbf{R}_y \mathbf{M}_O(\gamma) | \mathbf{R}(\varepsilon) \mathbf{M}_h \mathbf{F}(a) I_E \rangle}{T_S T_O T_{rot} F_{11} T_E I_L} = \\ 12 \quad &= (1 + y D_O D_S c_{2\gamma}) i_E - y D_S Z_O S_O s_{2\gamma} h v_E + \\ &+ a \left\{ D_O [c_{2\gamma - 2\varepsilon} q_E - s_{2\gamma - 2\varepsilon} h u_E] - y D_S W_O s_{2\gamma} [s_{2\gamma - 2\varepsilon} q_E + c_{2\gamma - 2\varepsilon} h u_E] + \right. \\ &\left. + y D_S [q_E c_{2\varepsilon} + h u_E s_{2\varepsilon} + 2 s_{2\gamma} Z_O S_O h v_E] \right\} \end{aligned} \quad (57)$$





1 The case of rotational error behind the emitter optics can be retrieved from Eq. (57) by simply
 2 replacing ε with $-\varepsilon$ according to S.7.3. Special cases of I_E for Eqs. (56) and (57) can be found
 3 in Sect. E.2.

4 4.1 General formulations for the total signal and the linear depolarisation ratio

5 From Eqs. (56) and (57) we see that all standard signals I_S can be expressed by introducing
 6 two variables G_S and H_S for the terms without and with atmospheric polarisation, respectively,

$$7 \quad I_S = \eta_S T_S T_O T_{rot} F_{11} T_E I_L (G_S + aH_S) \quad (58)$$

8 Using Eq. (56) as an example, the two variables are

$$9 \quad \begin{aligned} G_S(y, \varepsilon, h, \gamma) &= (1 + yD_S D_O c_{2\gamma+h2\varepsilon}) i_E - yD_S Z_O s_{2\gamma+h2\varepsilon} v_E \\ H_S(y, \varepsilon, h, \gamma, \beta, \alpha) &= \\ &= D_O (c_{2\gamma} q_E - s_{2\gamma} u_E) + yD_S \left[(c_{2\varepsilon} q_E + s_{h2\varepsilon} u_E) - s_{2\gamma+h2\varepsilon} (W_O (s_{2\gamma} q_E + c_{2\gamma} u_E) - 2Z_O s_O v_E) \right] \end{aligned} \quad (59)$$

10 With Eq. (58) the measured signal ratio becomes

$$11 \quad \delta^* = \frac{1}{\eta} \frac{I_R}{I_T} = \frac{G_R + aH_R}{G_T + aH_T} \quad (60)$$

12 with the calibration factor $\eta = \frac{\eta_R T_R}{\eta_T T_T}$, which has to be determined with one of the methods in
 13 the following chapters. G_S and H_S describe the polarisation cross-talk terms of the lidar setup
 14 depending on the diattenuation parameters D and the retardation (described by s_O and c_O) of
 15 the individual optical elements, depending on the relative rotation of the elements and on the
 16 polarisation parameter of the atmosphere a . From Eq. (60) we retrieve the general equations
 17 for the polarisation parameter a in Eq. (61) and for the linear depolarisation ratio δ in Eq. (62)
 18 (compare Eq. (12)).

$$19 \quad a = \frac{\delta^* G_T - G_R}{H_R - \delta^* H_T} \quad (61)$$

$$20 \quad \delta = \frac{1-a}{1+a} = \frac{\delta^* (G_T + H_T) - (G_R + H_R)}{(G_R - H_R) - \delta^* (G_T - H_T)} \quad (62)$$

21 Remind that δ^* and hence a and δ are range dependent. For the retrieval of the total lidar
 22 signal, which is equivalent to F_{11} , we substitute Eq. (61) in Eq. (58) in the transmitted or the



1 reflected version of $I_S \in \{I_T, I_R\}$ and replace δ^* by Eq. (60). Using the transmitted signal I_T
 2 from Eq. (58) we get Eq. (63), and after some restructuring (see Eqs.(S.8.1) and (S.8.2)) we
 3 get the attenuated backscatter coefficient Eq. (64).

$$4 \quad \eta_T T_T T_O F_{11} T_E I_L = \frac{I_T}{G_T + a H_T} \quad (63)$$

$$5 \quad F_{11} = \frac{1}{T_O T_E I_L} \frac{H_R \frac{I_T}{\eta_T T_T} - H_T \frac{I_R}{\eta_R T_R}}{H_R G_T - H_T G_R} \quad (64)$$

6 For the inversion of the lidar signal we only need the relative attenuated backscatter
 7 coefficient, for which we can get a much simpler formula by removing all factors in Eq. (64)
 8 which are not range dependent (compare Eq. 32 ff), which yields Eq.(65)

$$9 \quad F_{11} \propto \eta H_R I_T - H_T I_R \quad (65)$$

10 The individual calibration methods can add errors and uncertainties due to additional optics
 11 with unknown diattenuation and retardation and due to rotation errors. The possible
 12 uncertainties of the calibration factor η can be assessed from the analytical expressions of the
 13 gain ratio η^* (see Sect.(5)).

14 For systems without a polarising beam-splitter, i.e. pure backscatter lidars with one channel
 15 for each wavelength, the total signal is I_T from the transmitted signal, but with $D_S = D_T = 0$,
 16 and without calibrator ($\Rightarrow h = 1$) and without calibrator rotation error angle ε . Hence, we get
 17 from both Eqs. (56) and (57) the transmitted signal with Eq. (66)

$$18 \quad \begin{aligned} D_T = 0, T_T = 1, \varepsilon = 0, y = 1 \Rightarrow \\ I_T = \eta_T T_T T_O F_{11} T_E I_L \left[i_E + a D_O (c_{2\gamma} q_E - s_{2\gamma} u_E) \right] \end{aligned} \quad (66)$$

19 which shows that there is a distortion of the total signal due to the receiver optics
 20 diattenuation and depending on the atmospheric depolarisation, even if the laser beam behind
 21 the emitter optics is perfectly horizontal-linearly polarised and without receiver optics
 22 rotation. i.e. Eq. (66) with

$$23 \quad \begin{aligned} \gamma = 0, T_E = 1, i_E = q_E = 1, u_E = 0 \Rightarrow \\ I_T = \eta_T T_O F_{11} I_L [1 + a D_O] \end{aligned} \quad (67)$$



4.2 Simplifications for standard measurements

For the case of Eq.(56), i.e. rotational error ε before the polarising beam-splitter, and with a general emitter Stokes vector $\mathbf{I}_E = T_E \mathbf{I}_L |i_E \ q_E \ u_E \ v_E\rangle$ (see Sect. App. E.2) we get from Eq. (59) the variables in Eq. (58), i.e. $\mathbf{I}_S = \eta_S T_S T_O T_{rot} F_{\parallel} T_E \mathbf{I}_L (G_S + aH_S)$:

$$\begin{array}{l} \mathbf{G}_S \\ \mathbf{H}_S \end{array} \quad \begin{array}{l} (1 + yD_S D_O c_{2\gamma+h2\varepsilon}) i_E - yD_S Z_O S_O S_{2\gamma+h2\varepsilon} v_E \\ D_O (c_{2\gamma} q_E - s_{2\gamma} u_E) + yD_S [(c_{2\varepsilon} q_E + s_{h2\varepsilon} u_E) - s_{2\gamma+h2\varepsilon} \{W_O (s_{2\gamma} q_E + c_{2\gamma} u_E) - 2Z_O s_O v_E\}] \end{array} \quad \begin{array}{l} (68) \\ (69) \end{array}$$

$$\varepsilon = 0 \quad D_O (c_{2\gamma} q_E - s_{2\gamma} u_E) + yD_S [q_E - s_{2\gamma} \{W_O (s_{2\gamma} q_E + c_{2\gamma} u_E) - 2Z_O s_O v_E\}] \quad (70)$$

$$\gamma = 0 \quad D_O q_E + yD_S [c_{2\varepsilon} q_E + s_{h2\varepsilon} Z_O (c_O u_E + 2s_O v_E)] \quad (71)$$

$$\gamma = \varepsilon = 0 \quad (D_O + yD_S) q_E \quad (72)$$

$$D_O = W_O = s_O = 0 \quad 1 \quad yD_S (c_{2\varepsilon} q_E + s_{h2\varepsilon} u_E) \quad (73)$$

The same as above, but with a rotated, linearly polarised emitter Stokes vector $\mathbf{I}_E = |i_E \ q_E \ u_E \ v_E\rangle = T_E \mathbf{I}_L |1 \ c_{2\alpha} \ s_{2\alpha} \ 0\rangle \Rightarrow$

$$\begin{array}{l} \mathbf{G}_S \\ \mathbf{H}_S \end{array} \quad \begin{array}{l} 1 + yD_S D_O c_{2\gamma+h2\varepsilon} \\ D_O c_{2\alpha+2\gamma} + yD_S (c_{2\alpha-2\varepsilon} - s_{2\gamma+h2\varepsilon} s_{2\alpha+2\gamma} W_O) \end{array} \quad \begin{array}{l} (74) \\ (75) \end{array}$$

$$\alpha = \varepsilon = 0 \quad 1 + yD_S D_O c_{2\gamma} \quad D_O c_{2\gamma} + yD_S (1 - s_{2\gamma}^2 W_O) \quad (76)$$

$$\gamma = 0 \quad 1 + yD_S D_O c_{h2\varepsilon} \quad D_O c_{2\alpha} + yD_S (c_{2\alpha-2\varepsilon} - s_{2\alpha} s_{h2\varepsilon} W_O) \quad (77)$$

$$\alpha = \gamma = 0 \quad 1 + yD_S D_O c_{h2\varepsilon} \quad D_O + yD_S c_{2\varepsilon} \quad (78)$$

$$\gamma = \varepsilon = 0 \quad 1 + yD_S D_O \quad (D_O + yD_S) c_{2\alpha} \quad (79)$$

$$\alpha = \gamma = \varepsilon = 0 \quad 1 + yD_S D_O \quad D_O + yD_S \quad (80)$$

$$D_O = W_O = 0 \quad 1 \quad + yD_S c_{2\alpha-2\varepsilon} \quad (81)$$



1 5 The 45° and Δ90 calibration, the gain ratios and calibration factor

2 The measured, apparent calibration factor η^* of the polarisation channels, which we call in the
 3 following gain ratio in contrast to the calibration factor η , can be determined from the two
 4 calibration signals I_S , i.e. I_T and I_R , with a calibrator at +45° or -45°, which we call 45°-
 5 calibration (Eq. (80)). The calibration factor η is not directly measurable. Hence we need
 6 equations to retrieve η from the measured η^* .

$$7 \left. \begin{aligned} \eta^*(+45^\circ) &= \frac{I_R(+45^\circ)}{I_T(+45^\circ)} \\ \eta^*(-45^\circ) &= \frac{I_R(-45^\circ)}{I_T(-45^\circ)} \end{aligned} \right\} \rightarrow \eta^* = \frac{I_R}{I_T}(x45^\circ) \quad (80)$$

8 η^* includes alignment errors and cross talks. The theoretical dependence of these errors and
 9 cross-talks on the known parameters of our lidar model (Fig. 1) can be determined using the
 10 analytical expressions of Eqs. (81) and (82).

$$11 I_S(y, x45^\circ + \varepsilon) = \eta_S \langle \mathbf{A}_S(y) | \mathbf{C}(x45^\circ + \varepsilon) | \mathbf{I}_{in} \rangle \quad (81)$$

$$12 \eta^* = \frac{I_R(y, x45^\circ + \varepsilon)}{I_T(y, x45^\circ + \varepsilon)} = \frac{\eta_R \langle \mathbf{A}_R(y) | \mathbf{C}(x45^\circ + \varepsilon) | \mathbf{I}_{in} \rangle}{\eta_T \langle \mathbf{A}_T(y) | \mathbf{C}(x45^\circ + \varepsilon) | \mathbf{I}_{in} \rangle} \quad (82)$$

13 The theoretical correction K of the gain ratio to get the calibrator factor can be retrieved from
 14 the analytical expression Eq. (83), which is then used to correct the measurement Eq. (84).

$$15 K = \frac{\eta^*}{\eta} = \eta^* \frac{\eta_T T_T}{\eta_R T_R} = \frac{T_T \langle \mathbf{A}_R(y) | \mathbf{C}(x45^\circ + \varepsilon) | \mathbf{I}_{in} \rangle}{T_R \langle \mathbf{A}_T(y) | \mathbf{C}(x45^\circ + \varepsilon) | \mathbf{I}_{in} \rangle} \quad (83)$$

$$16 \eta = \frac{1}{K} \eta^* = \frac{1}{K} \frac{I_R}{I_T}(x45^\circ) \quad (84)$$

17 Furthermore, additional equations for the estimation of the uncertainty of η can be derived
 18 from Eq. (83). Since the errors due to ε cancel very well at orientations of the calibrator
 19 exactly Δ90 apart (i.e. $x = \pm 1$), as we will see in the following sections, a better estimation of
 20 the gain ratio can be retrieved from the geometric mean of the two gain ratios at ±45°, which
 21 we call Δ90-calibration.



$$1 \quad \eta_{\Delta 90}^* \equiv \sqrt{\eta^*(+45^\circ + \varepsilon)\eta^*(-45^\circ + \varepsilon)} = \sqrt{\frac{I_R(+45^\circ + \varepsilon)}{I_T(+45^\circ + \varepsilon)} \cdot \frac{I_R(-45^\circ + \varepsilon)}{I_T(-45^\circ + \varepsilon)}} \quad (85)$$

2 While the two calibration signals I_T and I_R are taken at the same time, the two measurements
 3 for the $\Delta 90$ -calibration at $\pm 45^\circ + \varepsilon$ are done subsequently, and the atmosphere can change in
 4 between. If the gain ratio η^* in Eq. (82) depends on the atmospheric polarisation parameter a ,
 5 the $\Delta 90$ gain ratio $\eta_{\Delta 90}^*$ in Eq. (85) depends also on the temporal change of a . In order to
 6 avoid this dependency, we either have to choose an appropriate setup and adjust it so that η^*
 7 doesn't depend on a , or we have to choose a calibration range in which a doesn't change with
 8 time. In the following we assume the latter, i.e. that the atmospheric polarisation parameter a
 9 does not change in the calibration range between the two calibration measurements at $\pm 45^\circ + \varepsilon$.
 10 This does not mean that the backscatter coefficient, an extrinsic parameter, must not change,
 11 but only that the aerosol composition with its intrinsic parameter a stays the same and that the
 12 contribution of the air molecules to a is negligible. Nevertheless, in Sect. 11 we describe a
 13 method to determine and consequently correct for ε , which is one of the major factors in the
 14 a -dependency of η^* . By the way, the method of 90° different polariser angles to reduce errors
 15 in polarimetric measurements seems to be common in ellipsometry (Nee, 2006).

16 In the following sections we derive \mathbf{A}_S and \mathbf{I}_m for several positions of the calibrator \mathbf{C} , and
 17 with that we will analyse special cases of the measurements I_S and the retrieved calibration
 18 factor η . The most general equation Eq. (86) for our lidar model, with e.g. a calibrator before
 19 the PBS, contains eight optical parameters of the four optical elements and the atmosphere,
 20 and four variables, i.e. the rotation angles of the optical elements and of the laser polarisation.
 21 Note, because detectors only detect the flux of light, the retardation of the polarising beam-
 22 splitter Δ_S is irrelevant. For each setup we firstly derive the general formulations (Eq. (86)).
 23 Then, in order to reduce the complexity of the equations and to carve out the most important
 24 and useful relations, we neglect certain parameters and variables in the detailed equations of
 25 special cases. We often omit the explicit description of the laser emitter optics \mathbf{M}_E (Eq. (87)),
 26 which means that we assume the light emitted to the atmosphere as arbitrarily polarised (see
 27 App. E.2) $\mathbf{I}_E = \mathbf{M}_E \mathbf{I}_L = T_E I_L |i_E \quad q_E \quad u_E \quad v_E\rangle$. If necessary \mathbf{I}_E can be expanded in the final
 28 equations by the appropriate ones in App. E. But we also consider the more simple case of a
 29 rotated linearly polarised laser $\mathbf{I}_E = \mathbf{I}_L = I_L |1 \quad c_{2\alpha} \quad s_{2\alpha} \quad 0\rangle$. Furthermore, it is quite easy to
 30 remove the cross talk of the polarising beam-splitter \mathbf{M}_S by means of additional polarisation



1 filters behind it, which removes many terms in the equation (Eq. (88)). We call such an
 2 analyser “cleaned”. The rotation γ of the receiving optics \mathbf{M}_o is very disturbing, which can be
 3 avoided in the very beginning of the lidar design (Eq. (89)). And at last, this paper provides
 4 the tools to determine how good a calibrator must be to be considered as ideal. With such a
 5 calibrator the equations become less complex (Eq.(90)).

$$6 \quad I_S = \eta_S \mathbf{M}_S(D_S) \mathbf{R}_y \mathbf{C}(D_C, \Delta_C, \varepsilon) \mathbf{M}_o(D_O, \Delta_O, \gamma) \mathbf{F}(a) \mathbf{M}_E(D_E, \Delta_E, \beta) I_L(\alpha) \quad (86)$$

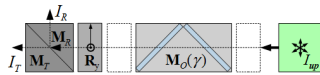
$$7 \quad I_S = \eta_S \mathbf{M}_S(D_S) \mathbf{R}_y \mathbf{C}(D_C, \Delta_C, \varepsilon) \mathbf{M}_o(D_O, \Delta_O, \gamma) \mathbf{F}(a) \quad I_E \quad (87)$$

$$8 \quad I_S = \eta_S \mathbf{M}_{S_{clean}} \mathbf{R}_y \mathbf{C}(D_C, \Delta_C, \varepsilon) \mathbf{M}_o(D_O, \Delta_O, \gamma) \mathbf{F}(a) \quad I_E \quad (88)$$

$$9 \quad I_S = \eta_S \mathbf{M}_S(D_S) \mathbf{R}_y \mathbf{C}(D_C, \Delta_C, \varepsilon) \mathbf{M}_o(D_O, \Delta_O, 0) \mathbf{F}(a) \quad I_E \quad (89)$$

$$10 \quad I_S = \eta_S \mathbf{M}_S(D_S) \mathbf{R}_y \quad \mathbf{C}_{ideal} \quad \mathbf{M}_o(D_O, \Delta_O, \gamma) \mathbf{F}(a) \quad I_E \quad (90)$$

11 6 Calibration with unpolarised input before the receiving optics



12 In principle, an additional light source with a known state of polarisation, which is placed
 13 before the telescope, can be used for the calibration. For other states of polarisation of the
 14 calibration light source the equations in Sect. (7.2) can be used together with the appropriate
 15 description of the input Stokes vector. But the beam from an additional light source has some
 16 disadvantages, because it fills the apertures of the individual optical elements differently than
 17 the backscattered light from the lidar laser, and also the distribution of the incident angles on
 18 elements with limited acceptance angles, as dichroic beams splitters and interference filters, is
 19 different. Furthermore, the wavelength band of the light source is usually different from that
 20 of the lidar laser, which introduces wavelength dependent transmission, diattenuation, and
 21 retardation effects. This can lead to errors in the calibration factor, which can additionally be
 22 range dependent. Such errors are very difficult to assess. We therefore prefer to use the
 23 atmospheric backscatter of the lidar laser for the calibration, which provides the same spatial
 24 and angular characteristics and the same wavelengths for the calibration as for the
 25 measurements. Nevertheless, the output Stokes vector I_S of an unpolarised light source before
 26 the receiving optics is given by Eq. (91).



1 $I_S = \eta_S \mathbf{M}_S \mathbf{R}_y \mathbf{M}_O \mathbf{I}_{up} \Rightarrow \mathbf{A}_S = \mathbf{M}_S \mathbf{R}_y \mathbf{M}_O$ and $\mathbf{I}_{in} = \mathbf{I}_{up}$ (91)

2 With the analyser vector from Eq. (D.7) and the unpolarised input Stokes vector \mathbf{I}_{in} before the
 3 lidar optics from Eq. (92) we get the calibration signals in Eq. (93).

4 $\mathbf{I}_{in} = \mathbf{I}_{up} = I_{up} |1 \ 0 \ 0 \ 0\rangle$ (92)

5 $I_S = \eta_S \langle \mathbf{M}_S \mathbf{R}_y \mathbf{M}_O(\gamma) | \mathbf{I}_{up} = \eta_S T_S T_O I_{up} (1 + y D_S c_{2\gamma} D_O)$ (93)

6 The gain ratio can be retrieved directly with Eq. (93)

7 $\eta^* = \frac{I_R}{I_T} = \frac{\eta_R T_R}{\eta_T T_T} \frac{1 + y D_R D_O c_{2\gamma}}{1 + y D_T D_O c_{2\gamma}} = \eta \frac{1 + y D_R D_O c_{2\gamma}}{1 + y D_T D_O c_{2\gamma}}$ (94)

8 Error sources are the unknown receiver optics rotation γ and the diattenuation D_O . With a
 9 cleaned analyser \mathbf{M}_S (see S.10.10) and $\gamma = 0$ we get from Eq. (94)

10 $\frac{\eta^*}{\eta} = \frac{1 - y D_O}{1 + y D_O}$ (95)

11 With $D_O = \frac{T_O^p - T_O^s}{T_O^p + T_O^s}$ we get the gain ratios for the two setups $y = \pm 1$ from

12 $\frac{\eta^*(y=+1)}{\eta} = \frac{T_O^s}{T_O^p}, \quad \frac{\eta^*(y=-1)}{\eta} = \frac{T_O^p}{T_O^s}$ (96)

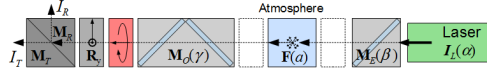
13 As there are no calibrator induced rotational errors ε , all equations for the standard
 14 measurements of Sect. 4 are with $\varepsilon = 0^\circ$.

15 **7 Calibration with a rotator - mechanical or by $\lambda/2$ plate (HWP)**

16 With an ideal HWP rotator the input Stokes vector is rotated with respect to the coordinate
 17 system, while with the mechanical rotator the polarising beam-splitter and, if so, the receiving
 18 optics are rotated in the opposite direction to achieve the same effect. Mathematically the
 19 latter means a rotation of the coordinate system (see S.5). Furthermore, the rotation with a
 20 HWP includes a retardance of 180° and hence a mirroring of the input Stokes vector (see
 21 S.10.13, Eq. (S.10.13.2)). We combine the two methods in the rotator matrix \mathbf{M}_{rot} (S.10.15) by
 22 introducing the rotator operator h (Eq. (S.10.15.1)), which is $h = +1$ for the mechanical rotator
 23 and $h = -1$ for the HWP rotator.



1 7.1 Calibration with a rotator before the polarising beam-splitter



2 The general formula for the output Stokes vector I_S with a rotation calibrator \mathbf{M}_{rot} before the
 3 polarising beam-splitter is Eq. (97).

$$4 \quad \begin{aligned} I_S &= \eta_S \mathbf{M}_S \mathbf{R}_y \mathbf{M}_{rot} (x45^\circ + \varepsilon, h) \mathbf{M}_O(\gamma) \mathbf{F}(a) \mathbf{M}_E(\beta) I_L(\alpha) = \\ &= \eta_S \mathbf{A}_S(y) \mathbf{M}_{rot} (x45^\circ + \varepsilon, h) I_{in}(\gamma, a, \beta, \alpha) \end{aligned} \quad (97)$$

5 With the analyser part \mathbf{A}_S from Eq. (D.5), \mathbf{M}_{rot} from Eq. (S.10.15.1), and the input Stokes
 6 vector I_{in} from App. E.4 we get Eq. (98) for the calibration signals, and with the expanded
 7 input Stokes vector Eq. (E.31) we get from Eq. (98) the general calibration signals Eq. (99).

$$8 \quad \begin{aligned} \frac{I_S}{\eta_S T_S T_{rot} I_{in}} &= \frac{\langle \mathbf{M}_S \mathbf{R}_y | \mathbf{M}_{rot} (x45^\circ + \varepsilon, h) | I_{in} \rangle}{T_S T_{rot} I_{in}} = \\ &= \left\langle \begin{array}{c} 1 \\ yD_S \\ 0 \\ 0 \end{array} \left| \begin{array}{cccc} 1 & 0 & 0 & 0 \\ 0 & -xs_{2\varepsilon} & -xhc_{2\varepsilon} & 0 \\ 0 & xc_{2\varepsilon} & -xhs_{2\varepsilon} & 0 \\ 0 & 0 & 0 & h \end{array} \right| \begin{array}{c} i_{in} \\ q_{in} \\ u_{in} \\ v_{in} \end{array} \right\rangle = \left\langle \begin{array}{c} 1 \\ -xys_{2\varepsilon}D_S \\ -xyhc_{2\varepsilon}D_S \\ 0 \end{array} \left| \begin{array}{c} i_{in} \\ q_{in} \\ u_{in} \\ v_{in} \end{array} \right\rangle = \\ &= i_{in} - xyD_S (s_{2\varepsilon}q_{in} + hc_{2\varepsilon}u_{in}) \end{aligned} \quad (98)$$

$$9 \quad \begin{aligned} \frac{I_S}{\eta_S T_S T_{rot} T_O F_{11} T_E I_L} &= \frac{\langle \mathbf{M}_S \mathbf{R}_y | \mathbf{M}_{rot} (x45^\circ + \varepsilon, h) | \mathbf{F}(a) I_E \rangle}{T_S T_{rot} T_O F_{11} T_E I_L} = \\ &= i_E + aD_O (c_{2\gamma}q_E - s_{2\gamma}u_E) - xyD_S \left\{ \begin{array}{l} s_{2\varepsilon+h2\gamma}D_O i_E + a(s_{2\varepsilon}q_E - hc_{2\varepsilon}u_E) + \\ + hc_{2\varepsilon+h2\gamma} [W_O a (s_{2\gamma}q_E + c_{2\gamma}u_E) + Z_O s_O (1-2a)v_E] \end{array} \right\} \end{aligned} \quad (99)$$

10 Since i_{in} in Eq. (98) is independent of ε , x , and y , we can define the function E in Eq. (100)
 11 and get for the calibration signals Eq. (101) and for the gain ratios η^* (Sect. 5) Eq. (102).

$$12 \quad \begin{aligned} E(\varepsilon, h, \gamma, a, \beta, \alpha) &\equiv \frac{s_{2\varepsilon}q_{in} + hc_{2\varepsilon}u_{in}}{i_{in}} = \\ &= \frac{s_{2\varepsilon+h2\gamma}D_O i_E + a(s_{2\varepsilon}q_E - hc_{2\varepsilon}u_E) + hc_{2\varepsilon+h2\gamma} [W_O a (s_{2\gamma}q_E + c_{2\gamma}u_E) + Z_O s_O (1-2a)v_E]}{i_E + aD_O (c_{2\gamma}q_E - s_{2\gamma}u_E)} \end{aligned} \quad \#(100)$$

$$13 \quad I_S = \eta_S T_S T_{rot} I_{in} [1 - xyD_S E] i_{in} \quad (101)$$



$$1 \quad \eta^* = \frac{I_R}{I_T} = \frac{\eta_R T_R}{\eta_T T_T} \frac{1 - xy D_R E}{1 - xy D_T E} = \eta \frac{1 - xy D_R E}{1 - xy D_T E} \quad (102)$$

2 Eq. (103) shows the gain ratio from the $\Delta 90$ -calibration, assuming that the polarisation
 3 parameter a doesn't change in the calibration range between the two calibration
 4 measurements, i.e. $E_+ = E_-$ (see Sect. 5).

$$5 \quad \frac{\eta_{\Delta 90}^*}{\eta} = \sqrt{\frac{1 - y D_R E_+}{1 - y D_T E_+} \frac{1 + y D_R E_-}{1 + y D_T E_-}} = \sqrt{\frac{1 - D_R^2 E^2}{1 - D_T^2 E^2}} \quad (103)$$

6 • Special cases: We immediately see that it is advantageous to use a cleaned analyser (see
 7 S.10.10), because with $D_T = 1, D_R = -1$ Eq. (102) becomes Eq. (104) and all possible errors in
 8 the $\Delta 90$ -calibration from Eq. (103) are removed in Eq. (105), besides the problem of temporal
 9 change of a .

$$10 \quad D_T = +1, D_R = -1 \Rightarrow \frac{\eta^*}{\eta} = \frac{1 + xyE}{1 - xyE} \quad (104)$$

$$11 \quad \frac{\eta_{\Delta 90}^*}{\eta} = \sqrt{\frac{1 - E^2}{1 - E^2}} = 1 \Rightarrow \eta = \eta_{\Delta 90}^* \quad (105)$$

12 • From Eq. (100) we get Eq. (106) without emitter and receiver optics rotation, without laser
 13 rotation, but with calibrator rotation ε and with a horizontal-linearly polarised laser I_L (Eq.
 14 (E.5)).

$$15 \quad \gamma = \beta = \alpha = 0 \wedge I_E = I_L = I_L |1 \ 1 \ 0 \ 0\rangle \Rightarrow E(\varepsilon, h, 0, a, 0, 0) = s_{2\varepsilon} \frac{D_O + a}{1 + a D_O} \quad (106)$$

16 • If additionally without calibrator rotation error ε , Eq. (106) becomes Eq. (107) and thus η^*
 17 and $\eta_{\Delta 90}^*$ are independent of the atmospheric polarisation parameter a and any atmospheric
 18 changes (see Eqs. (102) and (103)).

$$19 \quad \varepsilon = 0 \Rightarrow E(0, h, 0, a, 0, 0) = 0 \quad (107)$$

20 • A more general case without receiver optics rotation γ and without calibrator rotation ε , but
 21 with unknown laser and emitter optics rotation, Eq (100) becomes Eq. (108).



1 with $\gamma = \varepsilon = 0 \Rightarrow E(0, h, 0, a, \beta, \alpha) = \frac{u_{in}}{i_{in}} = \frac{hZ_o [s_o(1-2a)v_E - c_o a u_E] + (h-1) a u_E}{i_E + a D_o q_E}$ (108)

2 Eq. (108) stays quite complex if we use I_E with rotated emitter optics (Eq. (E.12)), and even if
 3 we assume a linearly polarised laser (Eq. (E.9)).

4 • With a horizontal-linearly polarised laser (Eq. (E.13)) aligned with the rotated emitter optics
 5 ($\alpha = \beta$) we get from Eq. (100)

6 with $\alpha = \beta \wedge I_E = T_E I_L (1 + D_E) |1 \ c_{2\alpha} \ s_{2\alpha} \ 0\rangle \Rightarrow$

$$E(\varepsilon, h, \gamma, a, \alpha, \alpha) = \frac{s_{2\varepsilon+h2\gamma} D_o + a \left[(s_{2\varepsilon} c_{2\alpha} - h c_{2\varepsilon} s_{2\alpha}) + h c_{2\varepsilon+h2\gamma} W_o (s_{2\gamma} c_{2\alpha} + c_{2\gamma} s_{2\alpha}) \right]}{1 + a D_o (c_{2\gamma} c_{2\alpha} - s_{2\gamma} s_{2\alpha})} =$$

$$= \frac{s_{2\varepsilon+h2\gamma} D_o + a (h c_{2\varepsilon+h2\gamma} s_{2\gamma+2\alpha} W_o + s_{2\varepsilon-h2\alpha})}{1 + a D_o c_{2\gamma+2\alpha}}$$
 (109)

7 Note: $D_E = 0$ means without emitter optics, and $W_o = (1 - Z_o c_o)$.

8 • Eq. (109) with laser, emitter and receiver optics aligned with each other becomes

9 with $\alpha = \beta = -\gamma \wedge I_E = T_E I_L (1 + D_E) |1 \ c_{2\alpha} \ s_{2\alpha} \ 0\rangle \Rightarrow$

$$E(\varepsilon, h, \gamma, a, -\gamma, -\gamma) = s_{2\varepsilon+h2\gamma} \frac{D_o + h a}{1 + a D_o}$$
 (110)

10 • Eq. (109) with receiver optics and calibrator aligned =>

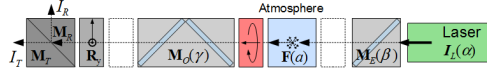
11 with $\alpha = \beta, \varepsilon = -h\gamma \wedge I_E = T_E I_L (1 + D_E) |1 \ c_{2\alpha} \ s_{2\alpha} \ 0\rangle \Rightarrow$

$$E(-\gamma, h, \gamma, a, \alpha, \alpha) = \frac{h s_{2\gamma+2\alpha} a (1 - Z_o c_o - h)}{1 + a D_o c_{2\gamma+2\alpha}}$$
 (111)

12 In summary: the $\Delta 90$ -calibration with a cleaned analyser results in a calibration factor η
 13 independent of I_{in} , i.e independent of any optics before the calibrator and independent of the
 14 rotation error ε of the calibrator. Calibrations without a cleaned analyser include error terms
 15 which increase rapidly with increasing ε and α for the individual $\pm 45^\circ$ calibrations (Bravo-
 16 Aranda et al., 2016), because D_T and D_R in the numerator and denominator have opposite
 17 signs in Eq. (102). The geometric mean of the two $\pm 45^\circ$ calibrations in Eq. (103) removes the
 18 opposite signs and the increasing error with increasing ε and α is reduced by orders of
 19 magnitude compared to the individual $\pm 45^\circ$ calibrations (Freudenthaler et al., 2009).



1 7.2 Calibration with a rotator before the receiving optics



2 The general formula for the output Stokes vector I_S with rotation calibrator before the
 3 receiving optics M_O and the polarising beam-splitter M_S is given in Eq. (112).

$$4 \quad \begin{aligned} I_S &= \eta_S \mathbf{M}_S \mathbf{R}_y \mathbf{M}_O(\gamma) \mathbf{M}_{rot}(x45^\circ + \varepsilon, h) \mathbf{F}(a) \mathbf{M}_E(\beta) I_L(\alpha) = \\ &= \eta_S \mathbf{A}_S(y, \gamma) \mathbf{M}_{rot}(x45^\circ + \varepsilon, h) I_{in}(a, \beta, \alpha) \end{aligned} \quad (112)$$

5 With \mathbf{A}_S from Eq. (D.7), \mathbf{M}_{rot} from Eq. (S.10.15.1), and I_{in} from App. E.3, i.e. Eq. (E.19), we
 6 get Eq. (113) for the calibration signals using the trigonometric relations in S.12.

$$7 \quad \begin{aligned} \frac{I_S}{\eta_S T_S T_O T_{rot} F_{11} T_E I_L} &= \frac{\langle \mathbf{M}_S \mathbf{R}_y \mathbf{M}_O(\gamma) | \mathbf{M}_{rot}(x45^\circ + \varepsilon, h) | \mathbf{F}(a) I_E \rangle}{T_S T_O T_{rot} F_{11} T_E I_L} = \\ &= \left\langle \begin{array}{l} 1 + y c_{2\gamma} D_O D_S \\ c_{2\gamma} D_O + y D_S (1 - s_{2\gamma}^2 W_O) \\ s_{2\gamma} (D_O + y c_{2\gamma} D_S W_O) \\ -y s_{2\gamma} D_S Z_O S_O \end{array} \left| \begin{array}{cccc} 1 & 0 & 0 & 0 \\ 0 & -x s_{2\varepsilon} & -x h c_{2\varepsilon} & 0 \\ 0 & x c_{2\varepsilon} & -x h s_{2\varepsilon} & 0 \\ 0 & 0 & 0 & h \end{array} \right| \begin{array}{l} i_E \\ a q_E \\ -a u_E \\ (1 - 2a) v_E \end{array} \right\rangle = \\ &= (1 + y c_{2\gamma} D_O D_S) i_E - y h s_{2\gamma} D_S Z_O S_O (1 - 2a) v_E + \\ &\quad -x a \left\{ D_O (q_E s_{2\varepsilon - 2\gamma} - h u_E c_{2\varepsilon - 2\gamma}) - y D_S [s_{2\gamma} W_O (q_E c_{2\varepsilon - 2\gamma} + h u_E s_{2\varepsilon - 2\gamma}) - (q_E s_{2\varepsilon} - h u_E c_{2\varepsilon})] \right\} \end{aligned} \quad (113)$$

8 Special cases: Without receiver optics rotation, i.e. $\gamma = 0$, Eq. (113) becomes Eq. (114), which
 9 is less complex and independent of retardation terms $Z_O S_O$ and W_O , and the gain ratios η^*
 10 (Sect. 5) can be written as Eqs. (115) and (116).

$$11 \quad \gamma = 0 \Rightarrow I_S / (\eta_S T_S T_O T_{rot} F_{11} T_E I_L) = (1 + y D_O D_S) i_E - x a (D_O + y D_S) (q_E s_{2\varepsilon} - h u_E c_{2\varepsilon}) \quad (114)$$

$$12 \quad \frac{\eta^*}{\eta} = \frac{(1 + y D_O D_R) i_E - x a (D_O + y D_R) (q_E s_{2\varepsilon} - h u_E c_{2\varepsilon})}{(1 + y D_O D_T) i_E - x a (D_O + y D_T) (q_E s_{2\varepsilon} - h u_E c_{2\varepsilon})} \quad (115)$$

$$13 \quad \frac{\eta_{A90}^*}{\eta} = \sqrt{\frac{(1 + y D_O D_R)^2 i_E^2 - (D_O + y D_R)^2 (q_E s_{2\varepsilon} - h u_E c_{2\varepsilon})^2}{(1 + y D_O D_T)^2 i_E^2 - (D_O + y D_T)^2 (q_E s_{2\varepsilon} - h u_E c_{2\varepsilon})^2}} \quad (116)$$

14 • With a cleaned analyser (see S.10.10) Eqs. (115) and (116) become Eqs. (117) and (118).



$$1 \quad \gamma = 0^\circ, D_T = +1, D_R = -1 \Rightarrow \quad (117)$$

$$\frac{\eta^*}{\eta} = \frac{1 - yD_O i_E + xy a (q_E s_{2\varepsilon} - hu_E c_{2\varepsilon})}{1 + yD_O i_E - xy a (q_E s_{2\varepsilon} - hu_E c_{2\varepsilon})}$$

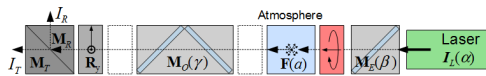
$$2 \quad \frac{\eta_{\Delta 90}^*}{\eta} = \frac{1 - yD_O}{1 + yD_O} \quad (118)$$

3 The gain ratio $\eta_{\Delta 90}^*$ in Eq. (118) is independent of the input Stokes vector, i.e. the laser
 4 polarisation, independent of the calibrator type (mechanical or $\lambda/2$ plate rotation) and of the
 5 calibrator rotation ε . Using the two calibration setups Eqs. (118) and (105) it is possible to
 6 retrieve the receiver optics diattenuation parameter D_O (Belegante et al., 2016). Furthermore,
 7 with this setup and the measured gain ratio $\eta_{\Delta 90}^*$ from Eq. (118) we get the polarisation
 8 parameter a (Eq.(119)) and the backscatter coefficient F_{11} (Eq.(120)) with Eq. (78) directly
 9 from the measurement signals I_R and I_T according to Eqs. (61) and (65) without the explicit
 10 knowledge of D_O or any other correction.

$$11 \quad a = y \frac{\eta_{\Delta 90}^* I_T - I_R}{\eta_{\Delta 90}^* I_T + I_R} \quad (119)$$

$$12 \quad F_{11} \propto \eta_{\Delta 90}^* I_T + I_R \quad (120)$$

13 7.3 Calibration with a rotator behind the emitter optics



14 The general formula for the output Stokes vector I_S with rotation calibrator \mathbf{M}_{rot} (Eq.
 15 (S.10.15.2)) behind the emitter optic \mathbf{M}_E and all derivations therefrom can be derived from the
 16 previous Sect. 7.2 using Eq. (121) and considering the mirror effect of \mathbf{F} and the associated
 17 sign changes in the rotation angle (S.6.3) when mathematically moving the calibrator \mathbf{M}_{rot}
 18 from behind the emitter optics \mathbf{M}_E to before the receiving optics \mathbf{M}_O . Regarding the rotation
 19 and mirror relations see S.5 and S.6.

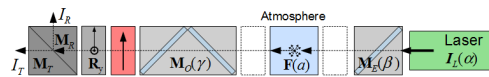
$$20 \quad \begin{aligned} I_S &= \eta_S \mathbf{M}_S \mathbf{R}_y \mathbf{M}_O(\gamma) \mathbf{F}(a) \mathbf{M}_{rot}(x45^\circ + \varepsilon, h) \mathbf{M}_E(\beta) I_L(\alpha) = \\ &= \eta_S \mathbf{M}_S \mathbf{R}_y \mathbf{M}_O(\gamma) \mathbf{F}(a) \mathbf{R}(x45^\circ) \mathbf{R}(\varepsilon) \mathbf{M}_h \mathbf{M}_E(\beta) I_L(\alpha) = \\ &= \eta_S \mathbf{M}_S \mathbf{R}_y \mathbf{M}_O(\gamma) \mathbf{R}(-x45^\circ) \mathbf{R}(-\varepsilon) \mathbf{M}_h \mathbf{F}(a) \mathbf{M}_E(\beta) I_L(\alpha) \\ &= \eta_S \mathbf{M}_S \mathbf{R}_y \mathbf{M}_O(\gamma) \mathbf{M}_{rot}(-x45^\circ - \varepsilon, h) \mathbf{F}(a) \mathbf{M}_E(\beta) I_L(\alpha) \end{aligned} \quad (121)$$



1 8 Calibration with a linear polariser (P)

2 A linear polariser is a retarding linear diattenuator (Sect. S.10.3). The output of an ideal linear
 3 polariser is linearly polarised light independent of the state of polarisation of the input, which
 4 seems to be ideal for our purpose. Polarising sheet filters are thin and have large acceptance
 5 angles. Hence they can be easily included in existing lidar systems, even in diverging or
 6 converging light paths as close to the telescope focus. However, to achieve an acceptable
 7 uncertainty of the calibration factor, a rather good extinction ratio of the linear polariser of
 8 order 10^{-4} and better is necessary. Crystal polarisers exhibit such high extinction ratios, but the
 9 available diameters are limited, they are bulky and have smaller acceptance angles. Wire grid
 10 and liquid crystal polarisers usually don't show high enough extinction ratios. A linear
 11 polariser is described in the same way as a polarising beam-splitter, which is a retarding
 12 diattenuator (S.4 and S.10.3 ff), with high diattenuation ($\mathbf{D}_p \approx 1$). Since the standard
 13 atmospheric measurements have to be performed without the linearly polarising calibrator,
 14 there is no rotational misalignment ε for the standard measurement signals of Sect. 4. As the
 15 equations become too complex with a real linear polariser with diattenuation and retardation,
 16 we use a real linear polariser only in Sect. 8.1 to show as an example how the uncertainty of
 17 the extinction ratio influences the accuracy of the calibration factor, and else we use an ideal
 18 linear polariser. The general formula with a real linear polariser can be found in App. C.2.

19 8.1 Calibration with a linear polariser before the polarising beam-splitter



$$\begin{aligned}
 I_S &= \eta_S \mathbf{M}_S \mathbf{R}(y) \mathbf{M}_p(x45^\circ + \varepsilon) \mathbf{M}_O(\gamma) \mathbf{F}(a) \mathbf{M}_E(\beta) I_L(\alpha) = \\
 20 \quad &= \eta_S \mathbf{A}_S(y) \mathbf{M}_p(x45^\circ + \varepsilon) I_{in}(\gamma, a, \beta, \alpha)
 \end{aligned}
 \tag{122}$$

21 With Eq. (D.5) for the analyser part \mathbf{A}_S , Eq. (S.10.6.1) for the rotated linear polariser, and I_{in}
 22 from App. E.4 we get the general calibration signals Eq. (123).



$$\begin{aligned}
 \frac{I_S}{\eta_S T_S T_P I_{in}} &= \frac{\langle \mathbf{M}_S \mathbf{R}_y | \mathbf{M}_P (x45^\circ + \varepsilon) | \mathbf{I}_{in} \rangle}{T_S T_P I_{in}} = \\
 1 \quad &= \left\langle \begin{array}{c} 1 - xys_{2\varepsilon} D_P D_S \\ -xs_{2\varepsilon} D_P + yD_S (1 - c_{2\varepsilon}^2 W_P) \\ xc_{2\varepsilon} D_P - ys_{2\varepsilon} c_{2\varepsilon} W_P D_S \\ -xy c_{2\varepsilon} Z_P S_P D_S \end{array} \middle| \begin{array}{c} i_{in} \\ q_{in} \\ u_{in} \\ v_{in} \end{array} \right\rangle = \\
 &= i_{in} + yD_S [q_{in} - c_{2\varepsilon} W_P (c_{2\varepsilon} q_{in} + s_{2\varepsilon} u_{in})] - \\
 &\quad -x [D_P (s_{2\varepsilon} q_{in} - c_{2\varepsilon} u_{in}) + yD_S (s_{2\varepsilon} D_P i_{in} + c_{2\varepsilon} Z_P S_P v_{in})]
 \end{aligned} \tag{123}$$

- 2 • Special cases: Without calibrator rotation error ε Eq.(123) becomes Eq. (124).

$$\varepsilon = 0 \Rightarrow$$

$$\begin{aligned}
 3 \quad \frac{I_S}{\eta_S T_S T_P I_{in}} &= i_{in} + yD_S [1 - W_P] q_{in} + x [u_{in} D_P - yD_S Z_P S_P v_{in}] = \\
 &= i_{in} + xD_P u_{in} + yD_S Z_P (c_P q_{in} - s_P v_{in})
 \end{aligned} \tag{124}$$

- 4 • We get with a cleaned analyser and horizontal-linearly polarised input \mathbf{I}_{in} , with Eq. (124) the
 5 gain ratios (Sect. 5) in Eq. (125).

$$\varepsilon = 0, D_T = +1, D_R = -1, \mathbf{I}_{in} = |1 \ 1 \ 0 \ 0\rangle \Rightarrow$$

$$6 \quad \frac{\eta^*}{\eta} = \frac{1 - yZ_P}{1 + yZ_P} \tag{125}$$

- 7 • Using Eq. (S.10.10.8) for the extinction ratio ρ of the real linear polariser, we get the
 8 approximation Eq. (126) for the gain ratios depending on ρ , with which we can estimate the
 9 error of the gain ratio if we use a real polariser with extinction ratio ρ for the measurements
 10 but assume an ideal polariser as calibrator in the correction equations. Eq. (126) with $\rho = 10^{-5}$
 11 and $\rho = 10^{-4}$, e.g., gives relative errors of the gain ratios of about 1.3% and 8%, respectively.

$$\text{with } \rho = k_2/k_1 \text{ and } k_2 \ll k_1 \Rightarrow$$

$$12 \quad \frac{\eta^*}{\eta} \approx \frac{1 - 2y\sqrt{\rho}}{1 + 2y\sqrt{\rho}} \approx 1 - 4y\sqrt{\rho} \tag{126}$$

- 13 • With an ideal linear polariser Eq.(123) becomes Eq. (127), and the gain ratios Eq. (128) are
 14 independent of \mathbf{I}_{in} , i.e. independent of the laser polarisation, of the atmospheric depolarisation,
 15 and of any optics before the calibrator. The error due to the calibrator rotation ε is largely
 16 reduced with the $\Delta 90$ -calibration in Eq. (129) compared to the $\pm 45^\circ$ -calibration in Eq. (128).



$$D_p = 1 \Rightarrow W_p = 1, Z_p = 0 \Rightarrow$$

$$1 \quad \frac{I_S}{\eta_S T_S T_P I_{in}} = (1 - x y s_{2\varepsilon} D_S) \begin{pmatrix} 1 & -x s_{2\varepsilon} & x c_{2\varepsilon} & 0 \\ i_{in} & q_{in} & u_{in} & v_{in} \end{pmatrix} =$$

$$= (1 - x y s_{2\varepsilon} D_S) \left[i_{in} - x (s_{2\varepsilon} q_{in} - c_{2\varepsilon} u_{in}) \right] \quad (127)$$

$$2 \quad \frac{\eta^*}{\eta} = \frac{1 - x y s_{2\varepsilon} D_R}{1 - x y s_{2\varepsilon} D_T} \quad (128)$$

$$3 \quad \frac{\eta_{\Delta 90}^*}{\eta} = \sqrt{\frac{1 - s_{2\varepsilon}^2 D_R^2}{1 - s_{2\varepsilon}^2 D_T^2}} \quad (129)$$

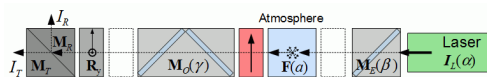
4 • If additionally a cleaned analyser is used (see S.10.10), Eqs. (128) and (129) become Eqs.
 5 (130) and (131). Eq. (130) is of the form of Eq. (193) and can be used to determine ε (see
 6 Sect. 11). Eq. (131) shows that the $\Delta 90$ -calibration with a cleaned analyser is free of ε error.

$$7 \quad \text{with } D_p = 1, W_p = 1, Z_p = 0, D_T = +1, D_R = -1 \Rightarrow$$

$$\frac{\eta^*}{\eta} = \frac{1 + x y s_{2\varepsilon}}{1 - x y s_{2\varepsilon}} \quad (130)$$

$$8 \quad \eta_{\Delta 90}^* = \eta = \frac{\eta_R T_R^s}{\eta_T T_T^p} \quad (131)$$

9 8.2 Calibration with an ideal linear polariser before the receiving optics



$$10 \quad I_S = \eta_S \mathbf{M}_S \mathbf{R}(y) \mathbf{M}_O(\gamma) \mathbf{M}_P(x45^\circ + \varepsilon) \mathbf{F}(a) \mathbf{M}_E(\beta) I_L(\alpha) =$$

$$= \eta_S \mathbf{A}_S(y, \gamma) \mathbf{M}_P(x45^\circ + \varepsilon) I_{in}(a, \beta, \alpha) \quad (132)$$

11 With Eq. (D.7) for the analyser part \mathbf{A}_S , Eq. (S.10.8.6) for the ideal linear polariser \mathbf{M}_P , and
 12 any of the input Stokes vectors I_{in} of App. E.3 we get Eq. (133) for the calibration signals I_S .
 13 Since the last term of Eq. (133) is independent of the analyser diattenuation parameters D_S ,
 14 this term cancels in the ratio of the gain ratios (Sect. 5) in Eq. (134), which are therefore
 15 independent of the input Stokes vector.



with $D_p = 1 \Rightarrow$

$$1 \quad \frac{I_S}{\eta_S T_S T_O T_P F_{11} T_E I_L} = \frac{\langle \mathbf{M}_S \mathbf{R}_y \mathbf{M}_O(\gamma) | \mathbf{M}_P(x45^\circ + \varepsilon) | \mathbf{F}(a) \mathbf{I}_E \rangle}{T_S T_O T_P F_{11} T_E I_L} =$$

$$= \left\langle \begin{array}{c} 1 + yc_{2\gamma} D_S D_O \\ c_{2\gamma} D_O + yD_S (1 - s_{2\gamma}^2 W_O) \\ s_{2\gamma} (D_O + yc_{2\gamma} D_S W_O) \\ -ys_{2\gamma} D_S Z_O S_O \end{array} \left\| \begin{array}{c} 1 \\ -xs_{2\varepsilon} \\ xc_{2\varepsilon} \\ 0 \end{array} \right\rangle \left\langle \begin{array}{c} 1 \\ -xs_{2\varepsilon} \\ xc_{2\varepsilon} \\ 0 \end{array} \left\| \begin{array}{c} i_E \\ aq_E \\ -au_E \\ (1-2a)v_E \end{array} \right\rangle \right\rangle = \quad (133)$$

$$= \left[(1 + yc_{2\gamma} D_S D_O) - x \left\{ s_{2\varepsilon-2\gamma} D_O + yD_S [s_{2\varepsilon} - s_{2\gamma} c_{2\varepsilon-2\gamma} W_O] \right\} \right] [i_E - xa(s_{2\varepsilon} q_E + c_{2\varepsilon} u_E)]$$

$$2 \quad \frac{\eta^*}{\eta} = \frac{(1 + yc_{2\gamma} D_O D_R) - x \left[s_{2\varepsilon-2\gamma} D_O + yD_R (s_{2\varepsilon} - s_{2\gamma} c_{2\varepsilon-2\gamma} W_O) \right]}{(1 + yc_{2\gamma} D_O D_T) - x \left[s_{2\varepsilon-2\gamma} D_O + yD_T (s_{2\varepsilon} - s_{2\gamma} c_{2\varepsilon-2\gamma} W_O) \right]} \quad (134)$$

3 • **Special cases:** Eq. (134) gets neither • with a cleaned analyser alone (Eq. (135)) nor • without
 4 receiver optics rotation γ alone (Eq. (136)) very simple, but • with both conditions Eq. (137) is
 5 of the form of Eq. (193) and can be used to estimate the calibrator rotation ε (see Sect. 11).
 6 The corresponding $\Delta 90$ -calibration in Eq. (138) can be used together with the calibration
 7 measurements which directly yield η (see Eqs. (131) or (105), for example) to determine the
 8 diattenuation parameter D_O of the receiving optics.

with $D_p = 1, D_T = +1, D_R = -1 \Rightarrow$

$$9 \quad \frac{\eta^*}{\eta} = \frac{(1 - yc_{2\gamma} D_O) - x \left[s_{2\varepsilon-2\gamma} D_O - y (s_{2\varepsilon} - s_{2\gamma} c_{2\varepsilon-2\gamma} W_O) \right]}{(1 + yc_{2\gamma} D_O) - x \left[s_{2\varepsilon-2\gamma} D_O + y (s_{2\varepsilon} - s_{2\gamma} c_{2\varepsilon-2\gamma} W_O) \right]} \quad (135)$$

with $D_p = 1, \gamma = 0 \Rightarrow$

$$10 \quad \frac{\eta^*}{\eta} = \frac{(1 + yD_O D_R) - xs_{2\varepsilon} [D_O + yD_R]}{(1 + yD_O D_T) - xs_{2\varepsilon} [D_O + yD_T]} \quad (136)$$

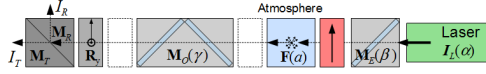
with $D_p = 1, D_T = +1, D_R = -1, \gamma = 0 \Rightarrow$

$$11 \quad \frac{\eta^*}{\eta} = \frac{(1 - yD_O) - xs_{2\varepsilon} (D_O - y)}{(1 + yD_O) - xs_{2\varepsilon} (D_O + y)} = \frac{1 - yD_O}{1 + yD_O} \frac{1 + xys_{2\varepsilon}}{1 - xys_{2\varepsilon}} \quad (137)$$

$$12 \quad \frac{\eta_{\Delta 90}^*}{\eta} = \frac{1 - yD_O}{1 + yD_O} \quad (138)$$



1 8.3 Calibration with an ideal linear polariser behind the emitter optics



$$2 \quad \begin{aligned} \mathbf{I}_S &= \eta_S \mathbf{M}_S \mathbf{R}_y \mathbf{M}_O(\gamma) \mathbf{F}(a) \mathbf{M}_P(x45^\circ + \varepsilon) \mathbf{M}_E(\beta) \mathbf{I}_L(\alpha) = \\ &= \eta_S \mathbf{A}_S(y, \gamma, a) \mathbf{M}_P(x45^\circ + \varepsilon) \mathbf{I}_{in}(\beta, \alpha) \end{aligned} \quad (139)$$

3 With Eq. (D.13) for the analyser part \mathbf{A}_S , Eq. (S.10.8.6) for the ideal linear polariser \mathbf{M}_P , and
 4 any of the emitter Stokes vectors \mathbf{I}_E of App. E.2 we get the calibration signals I_S in Eq. (140).
 5 Since the the last term of Eq. (140) is independent of analyser diattenuation parameters D_S , it
 6 cancels in the ratio of the gain ratios (Sect. 5), and the gain ratios in Eq. (141) are independent
 7 of the input Stokes vector.

$$8 \quad \begin{aligned} \text{with } D_p = 1 \Rightarrow \\ \frac{I_S}{\eta_S T_S T_O F_{11} T_P I_{in}} &= \frac{\langle \mathbf{M}_S \mathbf{R}_y \mathbf{M}_O(\gamma) | \mathbf{F}(a) \mathbf{M}_P(x45^\circ + \varepsilon) | \mathbf{I}_E \rangle}{T_S T_O F_{11} T_P I_E} \\ &= \left\langle \begin{array}{c} 1 + y c_{2\gamma} D_S D_O \\ a [c_{2\gamma} D_O + y D_S (1 - s_{2\gamma}^2 W_O)] \\ -a s_{2\gamma} (D_O + y c_{2\gamma} D_S W_O) \\ -(1 - 2a) y s_{2\gamma} D_S Z_O S_O \end{array} \right| \left| \begin{array}{c} 1 \\ -x s_{2\varepsilon} \\ x c_{2\varepsilon} \\ 0 \end{array} \right\rangle \left\langle \begin{array}{c} 1 \\ -x s_{2\varepsilon} \\ x c_{2\varepsilon} \\ 0 \end{array} \right| \left| \begin{array}{c} i_E \\ q_E \\ u_E \\ v_E \end{array} \right\rangle = \\ &= \left[(1 + y c_{2\gamma} D_S D_O) - a x \left\{ s_{2\varepsilon+2\gamma} D_O + y D_S [s_{2\varepsilon} + s_{2\gamma} c_{2\varepsilon+2\gamma} W_O] \right\} \right] \left[i_E - x (s_{2\varepsilon} q_E - c_{2\varepsilon} u_E) \right] \end{aligned} \quad (140)$$

$$9 \quad \frac{\eta^*}{\eta} = \frac{(1 + y c_{2\gamma} D_O D_R) - x a [s_{2\varepsilon+2\gamma} D_O + y D_R (s_{2\varepsilon} + s_{2\gamma} c_{2\varepsilon+2\gamma} W_O)]}{(1 + y c_{2\gamma} D_O D_T) - x a [s_{2\varepsilon+2\gamma} D_O + y D_T (s_{2\varepsilon} + s_{2\gamma} c_{2\varepsilon+2\gamma} W_O)]} \quad (141)$$

10 • Special cases: Eq.(141) with a cleaned analyser becomes Eq. (142), without receiver optics
 11 rotation Eq. (143), and with both conditions Eq. (144). Eq. (144) is of the form of Eq. (199)
 12 and can be used to determine ε (see Sect. 11). As before in Eq.(138) the corresponding $\Delta 90$ -
 13 calibration becomes Eq. (145),

$$14 \quad \begin{aligned} \text{with } D_p = 1, D_T = +1, D_R = -1 \Rightarrow \\ \frac{\eta^*}{\eta} &= \frac{(1 - y c_{2\gamma} D_O) - x a [s_{2\varepsilon+2\gamma} D_O - y (s_{2\varepsilon} + s_{2\gamma} c_{2\varepsilon+2\gamma} W_O)]}{(1 + y c_{2\gamma} D_O) - x a [s_{2\varepsilon+2\gamma} D_O + y (s_{2\varepsilon} + s_{2\gamma} c_{2\varepsilon+2\gamma} W_O)]} \end{aligned} \quad (142)$$

$$15 \quad \begin{aligned} \text{with } D_p = 1, \gamma = 0 \Rightarrow \\ \frac{\eta^*}{\eta} &= \frac{(1 + y D_O D_R) - x a s_{2\varepsilon} [D_O + y D_R]}{(1 + y D_O D_T) - x a s_{2\varepsilon} [D_O + y D_T]} \end{aligned} \quad (143)$$



with $D_p = 1, D_T = +1, D_R = -1, \gamma = 0 \Rightarrow$

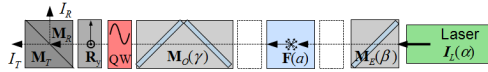
$$1 \quad \frac{\eta^*}{\eta} = \frac{(1 - yD_O) - xas_{2\varepsilon}(D_O - y)}{(1 + yD_O) - xas_{2\varepsilon}(D_O + y)} = \frac{(1 - yD_O)(1 + xyas_{2\varepsilon})}{(1 + yD_O)(1 - xyas_{2\varepsilon})} \quad (144)$$

$$2 \quad \frac{\eta_{\Delta 90}^*}{\eta} = \frac{1 - yD_O}{1 + yD_O} \quad (145)$$

3 9 Calibration with a $\lambda/4$ plate (QWP)

4 A $\lambda/4$ -plate (QWP) is a retarding linear diattenuator (S.4) with 90° phase shift between the
 5 polarisation parallel and perpendicular to the fast axis and without diattenuation (S.10.16 ff).
 6 Further details can be found in Bennett (2009a), Bennett (2009b), and Chipman (2009b).
 7 Oriented at $\pm 45^\circ$ relative to incident linear polarisation, its output is circularly polarised. Since
 8 the equations with a real QWP with retardation error ω (S.10.16) are too complex, we
 9 consider ω only in Sect. 9.1 to show with an example how this uncertainty influences the
 10 accuracy of the calibration factor. The general formula with a real QWP can be found in App.
 11 C.3.

12 9.1 Calibration with a $\lambda/4$ plate before the the polarising beam-splitter



$$13 \quad \mathbf{I}_S = \eta_S \mathbf{M}_S \mathbf{R}_y \mathbf{M}_{QW} (x45^\circ + \varepsilon, \omega) \mathbf{M}_O(\gamma) \mathbf{F}(a) \mathbf{I}_E = \eta_S \mathbf{A}_S(y) \mathbf{M}_{QW}(x45^\circ + \varepsilon, \omega) \mathbf{I}_{in}(\gamma, a, \beta, \alpha) \quad (146)$$

14 With Eq. (D.5) for the analyser part \mathbf{A}_S , Eq. (S.10.16.3) for the $\lambda/4$ plate \mathbf{M}_{QW} with phase shift
 15 error ω , and with the input Stokes vector \mathbf{I}_{in} from App. E.4 we get the calibration signals I_S in
 16 Eq. (147).

$$17 \quad \begin{aligned} \Delta_{QW} = 90^\circ + \omega \Rightarrow \\ \frac{I_S}{\eta_S T_S T_{QW} I_{in}} &= \frac{\langle \mathbf{M}_S \mathbf{R}_y | \mathbf{M}_{QW}(x45^\circ + \varepsilon, \omega) | \mathbf{I}_{in} \rangle}{\eta_S T_S T_{QW} I_{in}} = \\ &= \left\langle \begin{matrix} 1 \\ yD_S \\ 0 \\ 0 \end{matrix} \left| \begin{pmatrix} 1 & 0 & 0 & 0 \\ 0 & s_{2\varepsilon}^2 - c_{2\varepsilon}^2 s_\omega & -s_{2\varepsilon} c_{2\varepsilon} (1 + s_\omega) & -x c_{2\varepsilon} c_\omega \\ 0 & -s_{2\varepsilon} c_{2\varepsilon} (1 + s_\omega) & c_{2\varepsilon}^2 - s_{2\varepsilon}^2 s_\omega & -x s_{2\varepsilon} c_\omega \\ 0 & x c_{2\varepsilon} c_\omega & x s_{2\varepsilon} c_\omega & -s_\omega \end{pmatrix} \right| \begin{matrix} i_{in} \\ q_{in} \\ u_{in} \\ v_{in} \end{matrix} \right\rangle = \\ &= i_{in} + yD_S [s_{2\varepsilon} (s_{2\varepsilon} q_{in} - c_{2\varepsilon} u_{in}) - c_{2\varepsilon} s_\omega (c_{2\varepsilon} q_{in} + s_{2\varepsilon} u_{in}) - x c_{2\varepsilon} c_\omega v_{in}] \end{aligned} \quad (147)$$



- 1 • Special cases: For the investigation of the effect of the phase shift error ω we neglect the
 2 rotation error ε in Eq. (147) and get the calibration signals Eq. (148) and the gain ratios Eq.
 3 (149).

$$4 \quad \varepsilon = 0 \Rightarrow$$

$$4 \quad I_S = \eta_S T_S T_{QW} I_{in} [i_{in} - y D_S (s_{\omega} q_{in} + x c_{\omega} v_{in})] \quad (148)$$

$$5 \quad \frac{\eta^*}{\eta} = \frac{i_{in} - y D_R s_{\omega} q_{in} - x y D_R c_{\omega} v_{in}}{i_{in} - y D_T s_{\omega} q_{in} - x y D_T c_{\omega} v_{in}} \quad (149)$$

- 6 • With a cleaned analyser, the gain ratios from Eq. (149) become Eq. (150) and for the $\Delta 90$ -
 7 calibration Eq. (151), from which we can estimate the influence of a phase shift error ω .

with $\varepsilon = 0, D_T = +1, D_R = -1 \Rightarrow$

$$8 \quad \frac{\eta^*}{\eta} = \frac{i_{in} + y s_{\omega} q_{in} + x y c_{\omega} v_{in}}{i_{in} - y s_{\omega} q_{in} - x y c_{\omega} v_{in}} \quad (150)$$

$$9 \quad \frac{\eta_{\Delta 90}^*}{\eta} = \sqrt{\frac{(i_{in} + y s_{\omega} q_{in})^2 - c_{\omega}^2 v_{in}^2}{(i_{in} - y s_{\omega} q_{in})^2 - c_{\omega}^2 v_{in}^2}} \quad (151)$$

- 10 • Without phase shift error ω in Eq. (147) but with calibrator rotation error ε we get the
 11 calibration signals Eq. (152) and the gain ratios Eq. (153).

$$12 \quad \omega = 0 \Rightarrow$$

$$12 \quad I_S = \eta_S T_S T_{QW} I_{in} \left\{ i_{in} + y D_S [s_{2\varepsilon} (s_{2\varepsilon} q_{in} - c_{2\varepsilon} u_{in}) - x c_{2\varepsilon} v_{in}] \right\} \quad (152)$$

$$13 \quad \frac{\eta^*}{\eta} = \frac{i_{in} + y D_R s_{2\varepsilon} (s_{2\varepsilon} q_{in} - c_{2\varepsilon} u_{in}) - x y D_R c_{2\varepsilon} v_{in}}{i_{in} + y D_T s_{2\varepsilon} (s_{2\varepsilon} q_{in} - c_{2\varepsilon} u_{in}) - x y D_T c_{2\varepsilon} v_{in}} \quad (153)$$

$\omega = 0, D_T = +1, D_R = -1 \Rightarrow$

$$14 \quad \frac{\eta_{\Delta 90}^*}{\eta} = \sqrt{\frac{(i_{in} - y s_{2\varepsilon} (s_{2\varepsilon} q_{in} - c_{2\varepsilon} u_{in}))^2 - c_{2\varepsilon}^2 v_{in}^2}{(i_{in} + y s_{2\varepsilon} (s_{2\varepsilon} q_{in} - c_{2\varepsilon} u_{in}))^2 - c_{2\varepsilon}^2 v_{in}^2}} \quad (154)$$

- 15 The terms without the x-factor in Eq. (150) containing ω and in Eq. (153) containing ε are not
 16 compensated with the $\Delta 90$ -calibration in Eq. (151) and Eq. (154), even if a cleaned analyser is
 17 used. This is a disadvantage of the QWP compared to the linear polariser (see Eq. (129)).

- 18 • From Eq.(153) without calibrator rotation ε we get the gain ratios Eqs. (155) and (156).



$$\omega = \varepsilon = 0 \Rightarrow$$

$$1 \quad \frac{\eta^*}{\eta} = \frac{i_{in} - xyD_R v_{in}}{i_{in} - xyD_T v_{in}} \quad (155)$$

$$2 \quad \frac{\eta_{\Delta 90}^*}{\eta} = \sqrt{\frac{i_{in}^2 - D_R^2 v_{in}^2}{i_{in}^2 - D_T^2 v_{in}^2}} \quad (156)$$

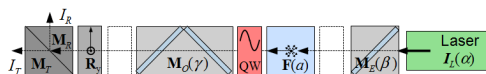
3 • With a cleaned analyser Eq. (156) becomes Eq. (157).

$$4 \quad \begin{aligned} \omega = \varepsilon = 0, D_T = +1, D_R = -1 \Rightarrow \\ \eta_{\Delta 90}^* = \eta \end{aligned} \quad (157)$$

5 • The advantage of the QWP calibrator is that we can retrieve from Eqs. (157) and (155) with
 6 a cleaned analyser the degree of circular polarisation v_{in}/i_{in} of the light before the polarising
 7 beam-splitter according to Eq. (158). Bear in mind that η^* and $\eta_{\Delta 90}^*$ in Eq. (158) are values
 8 directly derived from measured signals. The errors due to uncertainties in ε or ω can be
 9 estimated by means of equations earlier in this section.

$$10 \quad \frac{v_{in}}{i_{in}} = \frac{1}{xy} \frac{\eta^* - \eta_{\Delta 90}^*}{\eta^* + \eta_{\Delta 90}^*} \quad (158)$$

11 9.2 Calibration with an ideal $\lambda/4$ plate before the receiving optics



$$12 \quad \begin{aligned} \mathbf{I}_S &= \eta_S \mathbf{M}_S \mathbf{R}(y) \mathbf{M}_O(\gamma) \mathbf{M}_{QW}(x45^\circ + \varepsilon) \mathbf{F}(a) \mathbf{I}_E(\beta, \alpha) = \\ &= \eta_S \mathbf{A}_S(y, \gamma) \mathbf{M}_{QW}(x45^\circ + \varepsilon) \mathbf{I}_{in}(a, \beta, \alpha) \end{aligned} \quad (159)$$

13 With Eq. (D.7) for the analyser part \mathbf{A}_S , an ideal $\lambda/4$ plate \mathbf{M}_{QW} Eq. (S.10.17.2), and with an
 14 input Stokes vector \mathbf{I}_{in} from App. E.3 we get the general calibration signals \mathbf{I}_S in Eq. (160).



$$\begin{aligned}
 \frac{I_S}{\eta_S T_S T_O T_{QW} F_{11} T_E I_L} &= \frac{\langle \mathbf{M}_S \mathbf{R}_y \mathbf{M}_O(\gamma) | \mathbf{M}_{QW}(x45^\circ + \varepsilon) | \mathbf{F}(a) \mathbf{M}_E \mathbf{I}_L \rangle}{T_S T_O T_{QW} F_{11} T_E I_L} = \\
 1 \quad &= \left\langle \begin{array}{c} 1 + y c_{2\gamma} D_S D_O \\ c_{2\gamma} D_O + y D_S (1 - s_{2\gamma}^2 W_O) \\ s_{2\gamma} (D_O + y c_{2\gamma} D_S W_O) \\ -y s_{2\gamma} D_S Z_O S_O \end{array} \left| \begin{array}{cccc} 1 & 0 & 0 & 0 \\ 0 & s_{2\varepsilon}^2 & -s_{2\varepsilon} c_{2\varepsilon} & -x c_{2\varepsilon} \\ 0 & -s_{2\varepsilon} c_{2\varepsilon} & c_{2\varepsilon}^2 & -x s_{2\varepsilon} \\ 0 & x c_{2\varepsilon} & x s_{2\varepsilon} & 0 \end{array} \right. \begin{array}{c} i_E \\ a q_E \\ -a u_E \\ (1-2a)v_E \end{array} \right\rangle = \\
 &= \left\langle \begin{array}{c} 1 + y c_{2\gamma} D_S D_O \\ s_{2\varepsilon} D_O s_{2\varepsilon-2\gamma} + y D_S [s_{2\varepsilon}^2 - s_{2\varepsilon} s_{2\gamma} W_O c_{2\varepsilon-2\gamma} - x c_{2\varepsilon} s_{2\gamma} Z_O S_O] \\ -c_{2\varepsilon} D_O s_{2\varepsilon-2\gamma} - y D_S [s_{2\varepsilon} c_{2\varepsilon} - c_{2\varepsilon} s_{2\gamma} W_O c_{2\varepsilon-2\gamma} + x s_{2\varepsilon} s_{2\gamma} Z_O S_O] \\ -x \{ D_O c_{2\varepsilon-2\gamma} + y D_S [c_{2\varepsilon} + s_{2\gamma} W_O s_{2\varepsilon-2\gamma}] \} \end{array} \left| \begin{array}{c} i_E \\ a q_E \\ -a u_E \\ (1-2a)v_E \end{array} \right. \right\rangle
 \end{aligned} \quad (160)$$

- 2 • Special cases: Without receiver optics rotation γ we get from Eq. (E.19) and Eq.(160) the
 3 calibration signals Eq. (161) and the gain ratios Eq. (162).

$$\begin{aligned}
 \gamma = 0 \Rightarrow \\
 \frac{I_S}{\eta_S T_S T_O T_{QW} F_{11} T_E I_L} &= \frac{\langle \mathbf{A}_S(y, 0) | \mathbf{M}_{QW}(x45^\circ + \varepsilon) | \mathbf{F}(a) \mathbf{M}_E \mathbf{I}_L \rangle}{T_S T_O T_{QW} F_{11} T_E I_L} = \\
 4 \quad &= \left\langle \begin{array}{c} 1 + y D_S D_O \\ s_{2\varepsilon}^2 (D_O + y D_S) \\ -c_{2\varepsilon} s_{2\varepsilon} (D_O + y D_S) \\ -x c_{2\varepsilon} (D_O + y D_S) \end{array} \left| \begin{array}{c} i_E \\ a q_E \\ -a u_E \\ (1-2a)v_E \end{array} \right. \right\rangle = \\
 &= (1 + y D_S D_O) i_E + (D_O + y D_S) [s_{2\varepsilon} a (s_{2\varepsilon} q_E + c_{2\varepsilon} u_E) - x c_{2\varepsilon} (1-2a)v_E]
 \end{aligned} \quad (161)$$

$$\begin{aligned}
 \gamma = 0 \Rightarrow \\
 5 \quad \frac{\eta^*}{\eta} &= \frac{(1 + y D_R D_O) i_E + (D_O + y D_R) [s_{2\varepsilon} a (s_{2\varepsilon} q_E + c_{2\varepsilon} u_E) - x c_{2\varepsilon} (1-2a)v_E]}{(1 + y D_T D_O) i_E + (D_O + y D_T) [s_{2\varepsilon} a (s_{2\varepsilon} q_E + c_{2\varepsilon} u_E) - x c_{2\varepsilon} (1-2a)v_E]}
 \end{aligned} \quad (162)$$

- 6 • Eq.(162) with a cleaned PBS (S.10.10) becomes Eq. (163), and without calibrator rotation ε
 7 Eq.(162) becomes Eq. (164).

$$\begin{aligned}
 \gamma = 0, D_T = +1, D_R = -1 \Rightarrow \\
 8 \quad \frac{\eta^*}{\eta} &= \frac{1 - y D_O i_E - y [s_{2\varepsilon} a (s_{2\varepsilon} q_E + c_{2\varepsilon} u_E) - x c_{2\varepsilon} (1-2a)v_E]}{1 + y D_O i_E + y [s_{2\varepsilon} a (s_{2\varepsilon} q_E + c_{2\varepsilon} u_E) - x c_{2\varepsilon} (1-2a)v_E]}
 \end{aligned} \quad (163)$$

$$\begin{aligned}
 \gamma = \varepsilon = 0 \Rightarrow \\
 9 \quad \frac{\eta^*}{\eta} &= \frac{(1 + y D_R D_O) i_E - x (D_O + y D_R) (1-2a)v_E}{(1 + y D_T D_O) i_E - x (D_O + y D_T) (1-2a)v_E}
 \end{aligned} \quad (164)$$



- 1 • With a cleaned analyser and without calibrator rotation ε the gain ratios in Eq.(162) become
 2 Eq. (165) and for the $\Delta 90$ -calibration Eq. (166).

$$3 \quad \gamma = \varepsilon = 0, D_T = +1, D_R = -1 \Rightarrow$$

$$4 \quad \frac{\eta^*}{\eta} = \frac{1 - yD_O i_E + xy(1 - 2a)v_E}{1 + yD_O i_E - xy(1 - 2a)v_E} \quad (165)$$

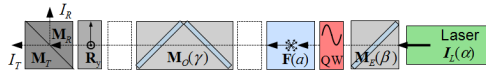
$$5 \quad \frac{\eta_{\Delta 90}^*}{\eta} = \frac{1 - yD_O}{1 + yD_O} \quad (166)$$

- 6 • Eq. (165) can be rearranged with Eq. (166) to Eq. (167), from which we get the degree of
 7 circular polarisation v_E/i_E of the beam behind the emitter optics in Eq. (168). The atmospheric
 8 polarisation parameter a must be estimated from a standard measurement, and if we use an
 9 atmospheric range without aerosols it becomes $a \approx 1$. While v_{in} in Eq. (158) includes the
 10 mostly unknown retardation terms of the receiving optics, v_E in Eq. (168) is free of them and
 hence a better estimation for the elliptical polarisation of the laser.

$$11 \quad \frac{\eta^*}{\eta_{\Delta 90}^*} = \frac{i_E + xy(1 - 2a)v_E}{i_E - xy(1 - 2a)v_E} \Rightarrow \quad (167)$$

$$12 \quad \frac{v_E}{i_E} = \frac{1}{xy(1 - 2a)} \frac{\eta^* - \eta_{\Delta 90}^*}{\eta^* + \eta_{\Delta 90}^*} \quad (168)$$

13 9.3 Calibration with an ideal $\lambda/4$ plate behind the emitter optics



$$14 \quad \begin{aligned} \mathbf{I}_S &= \eta_S \mathbf{M}_S \mathbf{R}(y) \mathbf{M}_O(\gamma) \mathbf{F}(a) \mathbf{M}_{QW}(x45^\circ + \varepsilon) \mathbf{M}_E(\beta) \mathbf{I}_L(\alpha) = \\ &= \eta_S \mathbf{A}_S(y, \gamma, a) \mathbf{M}_{QW}(x45^\circ + \varepsilon) \mathbf{I}_{in}(\beta, \alpha) \end{aligned} \quad (169)$$

- 15 With Eq. (D.13) for the analyser part \mathbf{A}_S , an ideal $\lambda/4$ plate \mathbf{M}_{QW} Eq. (S.10.17.2), and with an
 16 input Stokes vector \mathbf{I}_{in} from Eq.(E.8) we get the general calibration signals I_S in Eq. (170).



$$\begin{aligned}
 & \frac{I_S}{\eta_S T_S T_O F_{11} T_{QW} T_E I_L} = \frac{\langle \mathbf{M}_S \mathbf{R}_y \mathbf{M}_O(\gamma) \mathbf{F}(a) | \mathbf{M}_{QW}(x45^\circ + \varepsilon) | \mathbf{M}_E \mathbf{I}_L \rangle}{T_S T_O F_{11} T_{QW} T_E I_L} = \\
 1 & \quad = \left\langle \begin{array}{c} 1 + y c_{2\gamma} D_S D_O c \\ a [c_{2\gamma} D_O + y D_S (1 - s_{2\gamma}^2 W_O)] \\ -a s_{2\gamma} (D_O + y c_{2\gamma} D_S W_O) \\ -(1 - 2a) y s_{2\gamma} D_S Z_O S_O \end{array} \left| \begin{array}{cccc} 1 & 0 & 0 & 0 \\ 0 & s_{2\varepsilon}^2 & -s_{2\varepsilon} c_{2\varepsilon} & -x c_{2\varepsilon} \\ 0 & -s_{2\varepsilon} c_{2\varepsilon} & c_{2\varepsilon}^2 & -x s_{2\varepsilon} \\ 0 & x c_{2\varepsilon} & x s_{2\varepsilon} & 0 \end{array} \right| \begin{array}{c} i_E \\ q_E \\ u_E \\ v_E \end{array} \right\rangle \quad (170)
 \end{aligned}$$

- 2 • **Special cases:** Equivalent to Sect.9.2 we get from Eq. (170) without receiver optics rotation
 3 γ the calibration signals in Eq. (171).

with $\gamma = 0 \Rightarrow$

$$4 \quad \frac{I_S}{\eta_S T_S T_O T_{QW} F_{11} T_E I_L} = \frac{\langle \mathbf{A}_S(y, 0, a) | \mathbf{M}_{QW}(x45^\circ + \varepsilon) | \mathbf{M}_E \mathbf{I}_L \rangle}{T_S T_O T_{QW} F_{11} T_E I_L} = \left\langle \begin{array}{c} 1 + y D_S D_O \\ s_{2\varepsilon}^2 a (D_O + y D_S) \\ -c_{2\varepsilon} s_{2\varepsilon} a (D_O + y D_S) \\ -x c_{2\varepsilon} a (D_O + y D_S) \end{array} \left| \begin{array}{c} i_E \\ q_E \\ u_E \\ v_E \end{array} \right. \right\rangle \quad (171)$$

- 5 • From Eq. (171) without calibrator rotation ε we get the gain ratios Eq. (172), • with
 6 additionally a cleaned analyser we get Eq. (173), and with the corresponding $\Delta 90$ -calibration
 7 Eq. (174).

with $\gamma = \varepsilon = 0 \Rightarrow$

$$8 \quad \frac{\eta^*}{\eta} = \frac{(1 + y D_R D_O) i_E - x a (D_O + y D_R) v_E}{(1 + y D_T D_O) i_E - x a (D_O + y D_T) v_E} \quad (172)$$

with $\gamma = \varepsilon = 0, D_T = +1, D_R = -1 \Rightarrow$

$$9 \quad \frac{\eta^*}{\eta} = \frac{1 - y D_O i_E + x y a v_E}{1 + y D_O i_E - x y a v_E} \quad (173)$$

$$10 \quad \frac{\eta_{\Delta 90}^*}{\eta} = \frac{1 - y D_O}{1 + y D_O} \quad (174)$$

- 11 • Eq. (173) can be rearranged with Eq. (174) to Eq. (175) from which we get the degree of
 12 circular polarisation v_E/i_E of the beam behind the emitter optics if the atmospheric polarisation
 13 parameter a is known, as e.g. when we use the lidar signals from an atmospheric range
 14 without aerosols where $a \approx 1$.

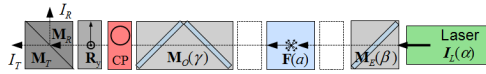
$$15 \quad \frac{\eta^*}{\eta_{\Delta 90}^*} = \frac{i_E + x y a v_E}{i_E - x y a v_E} \Rightarrow \frac{v_E}{i_E} = \frac{1}{x y a} \frac{\eta^* - \eta_{\Delta 90}^*}{\eta^* + \eta_{\Delta 90}^*} \quad (175)$$



1 10 Calibration with a circular polariser (CP)

2 The use of a circular polariser seems to be ideal for the calibration, but the uncertainties of a
 3 real circular polariser are usually not provided by manufacturers and might be difficult to
 4 determine. A real CP is mostly a combination of a linear polariser followed by a QWP at $z45^\circ$
 5 ($z = \pm 1$) (see S.10.18), and therefore it combines the uncertainties of both (see Sects. 8 and 9).
 6 Before the results of a circularly polarising calibrator can be trusted, the diattenuation of the
 7 linear polariser and the phase shift uncertainties should be determined and the error
 8 assessment performed using the general Eq. (C.10) for the calibration signals. If we consider
 9 all possible error terms, the Müller matrix for a real CP becomes too complex for this
 10 investigation, wherefore we assume a circular polariser with phase shift error ω but with an
 11 ideal linear polariser from Eq. (S.10.18.4) in the following in order to show the possibilities of
 12 this calibrator.

13 10.1 Calibration with a circular polariser before the polarising beam-splitter



$$14 \quad \begin{aligned} \mathbf{I}_S &= \eta_S \mathbf{M}_S \mathbf{R}_y \mathbf{M}_{CP}(z, x45^\circ + \varepsilon, \omega) \mathbf{M}_O(\gamma) \mathbf{F}(\alpha) \mathbf{M}_E(\beta) \mathbf{I}_L(\alpha) = \\ &= \eta_S \mathbf{A}_S(y) \mathbf{M}_{CP}(z, x45^\circ + \varepsilon, \omega) \mathbf{I}_{in}(\gamma, \alpha, \beta, \alpha) \end{aligned} \quad (176)$$

15 With \mathbf{A}_S from Eq. (D.5), the circularly polarising calibrator \mathbf{M}_{CP} with retardation error ω from
 16 Eq. (S.10.18.4), and the input Stokes vectors \mathbf{I}_{in} from App. E.4 we get Eq. (177) for the
 17 calibration signals \mathbf{I}_S . As the last term of Eq. (177) is independent of D_S , it cancels out in the
 18 gain ratios Eq. (178), which is therefore independent of the input Stokes vector, but still
 19 includes ε and ω terms.

$$20 \quad \begin{aligned} \frac{I_S}{\eta_S T_S T_{CP} I_{in}} &= \frac{\langle \mathbf{M}_S \mathbf{R}_y | \mathbf{M}_{CP}(z, x45^\circ + \varepsilon, \omega) | \mathbf{I}_{in} \rangle}{T_S T_{CP} I_{in}} = \\ &= \left\langle \begin{array}{c} 1 \\ yD_S \\ 0 \\ 0 \end{array} \middle| \begin{array}{c} 1 \\ xS_{2\varepsilon}S_\omega \\ -xC_{2\varepsilon}S_\omega \\ zC_\omega \end{array} \right\rangle \left\langle \begin{array}{c} 1 \\ -xS_{2\varepsilon} \\ xC_{2\varepsilon} \\ 0 \end{array} \middle| \begin{array}{c} i_{in} \\ q_{in} \\ u_{in} \\ v_{in} \end{array} \right\rangle = [1 + xyD_S S_{2\varepsilon} S_\omega] \left\langle \begin{array}{c} 1 \\ -xS_{2\varepsilon} \\ xC_{2\varepsilon} \\ 0 \end{array} \middle| \begin{array}{c} i_{in} \\ q_{in} \\ u_{in} \\ v_{in} \end{array} \right\rangle = \\ &= (1 + xyD_S S_{2\varepsilon} S_\omega) [i_{in} - x(s_{2\varepsilon} q_{in} - c_{2\varepsilon} u_{in})] \end{aligned} \quad (177)$$



$$1 \quad \frac{\eta^*}{\eta} = \frac{1 + xyD_R S_{2\varepsilon} S_\omega}{1 + xyD_T S_{2\varepsilon} S_\omega} \quad (178)$$

- 2 • If ω is zero, we have an ideal circular polariser with which we get the gain ratio
 3 independently of ε , and if ε is zero ω doesn't matter (Eq. (179)).

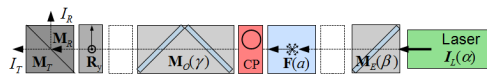
$$4 \quad \omega = 0 \vee \varepsilon = 0 \Rightarrow \frac{\eta^*}{\eta} = 1 \quad (179)$$

- 5 • With a cleaned analyser we get from Eq. (178) Eqs. (180) and (181), which show that the
 6 deviations of the gain ratios are fully compensated by the $\Delta 90$ -calibration. ω can be
 7 determined by means of the successive approximation in Sect. 11, Eqs. (198) ff.

$$8 \quad D_T = +1, D_R = -1 \Rightarrow \frac{\eta^*}{\eta} = \frac{1 - xyS_{2\varepsilon} S_\omega}{1 + xyS_{2\varepsilon} S_\omega} \quad (180)$$

$$9 \quad \frac{\eta_{\Delta 90}^*}{\eta} = 1 \quad (181)$$

10 10.2 Calibration with a circular polariser before the receiving optics



$$11 \quad \begin{aligned} I_S &= \eta_S \mathbf{M}_S \mathbf{R}_y \mathbf{M}_O(\gamma) \mathbf{M}_{CP}(z, x45^\circ + \varepsilon, \omega) \mathbf{F}(a) \mathbf{M}_E(\beta) I_L(\alpha) = \\ &= \eta_S \mathbf{A}_S(y, \gamma) \mathbf{M}_{CP}(z, x45^\circ + \varepsilon, \omega) I_{in}(a, \beta, \alpha) \end{aligned} \quad (182)$$

- 12 With \mathbf{A}_S from App. D.2, \mathbf{M}_{CP} with retardation error ω from Eq. (S.10.18.4), and I_{in} from App.
 13 E.3 we get Eq. (183) for the calibration signals I_S .



$$\begin{aligned}
 \frac{I_S}{\eta_S T_S T_{CP} T_O F_{11} T_E I_L} &= \frac{\langle \mathbf{M}_S \mathbf{R}_y \mathbf{M}_O(\gamma) | \mathbf{M}_{CP}(z, x45^\circ + \varepsilon, \omega) | \mathbf{F}(a) \mathbf{M}_E I_L \rangle}{T_S T_O T_{CP} F_{11} T_E I_L} = \\
 1 \quad &= \left\langle \begin{pmatrix} 1 + y c_{2\gamma} D_S D_O \\ c_{2\gamma} D_O + y D_S (1 - s_{2\gamma}^2 W_O) \\ s_{2\gamma} (D_O + y c_{2\gamma} D_S W_O) \\ -y s_{2\gamma} D_S Z_O S_O \end{pmatrix} \begin{pmatrix} 1 \\ x s_{2\varepsilon} S_\omega \\ -x c_{2\varepsilon} S_\omega \\ z c_\omega \end{pmatrix} \begin{pmatrix} 1 \\ -x s_{2\varepsilon} \\ x c_{2\varepsilon} \\ 0 \end{pmatrix} \begin{pmatrix} i_E \\ a q_E \\ -a u_E \\ (1 - 2a) v_E \end{pmatrix} \right\rangle = \\
 &= \left\{ 1 + y D_S (c_{2\gamma} D_O - s_{2\gamma} Z_O S_O z c_\omega) + \right. \\
 &\quad \left. + x s_\omega [D_O s_{2\varepsilon - 2\gamma} + y D_S (s_{2\varepsilon} - s_{2\gamma} W_O c_{2\varepsilon - 2\gamma})] \right\} [i_E - x a (s_{2\varepsilon} q_E + c_{2\varepsilon} u_E)]
 \end{aligned} \tag{183}$$

2 As the last term of Eq. (183) is independent of D_S , it cancels out in the gain ratio. However,
 3 as long as the receiver optics rotation γ doesn't vanish, the gain ratios include deviations
 4 which don't cancel with the $\Delta 90$ -calibration, even if we • use a cleaned analyser (Eq. (184))
 5 and • additionally an ideal circular polariser (Eq. (185)) or • without calibrator error ε (Eq.
 6 (186)).

$$\begin{aligned}
 D_T = +1, D_R = -1 &\Rightarrow \\
 7 \quad \frac{\eta^*}{\eta} &= \frac{1 - y (c_{2\gamma} D_O - s_{2\gamma} Z_O S_O z c_\omega) + x s_\omega [D_O s_{2\varepsilon - 2\gamma} - y (s_{2\varepsilon} - s_{2\gamma} W_O c_{2\varepsilon - 2\gamma})]}{1 + y (c_{2\gamma} D_O - s_{2\gamma} Z_O S_O z c_\omega) + x s_\omega [D_O s_{2\varepsilon - 2\gamma} + y (s_{2\varepsilon} - s_{2\gamma} W_O c_{2\varepsilon - 2\gamma})]}
 \end{aligned} \tag{184}$$

$$\begin{aligned}
 D_T = +1, D_R = -1, \omega = 0 &\Rightarrow \\
 8 \quad \frac{\eta^*}{\eta} &= \frac{1 - y (c_{2\gamma} D_O - s_{2\gamma} Z_O S_O)}{1 + y (c_{2\gamma} D_O - s_{2\gamma} Z_O S_O)}
 \end{aligned} \tag{185}$$

$$\begin{aligned}
 D_T = +1, D_R = -1, \varepsilon = 0 &\Rightarrow \\
 9 \quad \frac{\eta^*}{\eta} &= \frac{1 - y (c_{2\gamma} D_O - s_{2\gamma} Z_O S_O z c_\omega) - x s_\omega s_{2\gamma} [D_O - y W_O c_{2\gamma}]}{1 + y (c_{2\gamma} D_O - s_{2\gamma} Z_O S_O z c_\omega) - x s_\omega s_{2\gamma} [D_O + y W_O c_{2\gamma}]}
 \end{aligned} \tag{186}$$

10 • From Eq. (183) without receiver optics rotation γ we get Eq. (187), and
 11 • with additionally a cleaned analyser the Eqs. (188) and (189) are the same as in the previous
 12 sections but with the prefactor of Eq. (189).

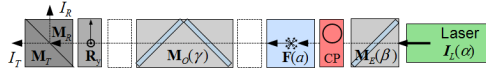
$$13 \quad \gamma = 0 \Rightarrow \quad \frac{\eta^*}{\eta} = \frac{1 + y D_R D_O + x s_\omega s_{2\varepsilon} (D_O + y D_R)}{1 + y D_T D_O + x s_\omega s_{2\varepsilon} (D_O + y D_T)} \tag{187}$$

$$14 \quad \gamma = 0, D_T = +1, D_R = -1 \Rightarrow \quad \frac{\eta^*}{\eta} = \frac{1 - y D_O}{1 + y D_O} \frac{1 - x y s_\omega s_{2\varepsilon}}{1 + x y s_\omega s_{2\varepsilon}} \tag{188}$$



$$1 \quad [\gamma = 0, D_T = +1, D_R = -1] \wedge [\omega = 0 \vee \varepsilon = 0] \Rightarrow \frac{\eta^*}{\eta} = \frac{1 - yD_O}{1 + yD_O} \quad (189)$$

2 10.3 Calibration with a circular polariser behind the emitter optics



$$3 \quad \begin{aligned} I_S &= \eta_S \mathbf{M}_S \mathbf{R}_y \mathbf{M}_O(\gamma) \mathbf{F}(a) \mathbf{M}_{CP}(z, x45^\circ + \varepsilon) \mathbf{M}_E(\beta) I_L(\alpha) = \\ &= \eta_S \mathbf{A}_S(y, \gamma, a) \mathbf{M}_{CP}(z, x45^\circ + \varepsilon) I_E(\beta, \alpha) \end{aligned} \quad (190)$$

4 With \mathbf{A}_S from App. D.3, \mathbf{M}_{CP} with retardation error ω from Eq. (S.10.18.4), and I_m from App.
 5 E.2 we get Eq. (191) for the calibration signals I_S , which differs from Eq. (183) in the last
 6 section just by the prefactors depending on the atmospheric polarisation parameter a . The
 7 same holds for the gain ratios derived with a • cleaned analyser in Eqs. (192) compared to Eq.
 8 (184) and all the subsequent derivations there.

$$9 \quad \begin{aligned} \frac{I_S}{\eta_S T_S T_O F_{11} T_{CP} T_E I_L} &= \frac{\langle \mathbf{M}_S \mathbf{R}_y \mathbf{M}_O(\gamma) \mathbf{F}(a) | \mathbf{M}_{CP}(z, x45^\circ + \varepsilon, \omega) | \mathbf{M}_E I_L \rangle}{T_S T_O F_{11} T_{CP} T_E I_L} = \\ &= \left\langle \begin{array}{l} 1 + yc_{2\gamma} D_S D_O c \\ a [c_{2\gamma} D_O + yD_S (1 - s_{2\gamma}^2 W_O)] \\ -as_{2\gamma} (D_O + yc_{2\gamma} D_S W_O) \\ -(1 - 2a) ys_{2\gamma} D_S Z_O s_O \end{array} \right| \left\langle \begin{array}{l} 1 \\ xs_{2\varepsilon} s_\omega \\ -xc_{2\varepsilon} s_\omega \\ zc_\omega \end{array} \right\rangle \left\langle \begin{array}{l} 1 \\ -xs_{2\varepsilon} \\ xc_{2\varepsilon} \\ 0 \end{array} \right| \left\langle \begin{array}{l} i_E \\ q_E \\ u_E \\ v_E \end{array} \right\rangle = \\ &= \left\{ \begin{array}{l} 1 + yD_S (c_{2\gamma} D_O - (1 - 2a) s_{2\gamma} Z_O s_O zc_\omega) + \\ + xas_\omega [D_O s_{2\varepsilon - 2\gamma} + yD_S (s_{2\varepsilon} - s_{2\gamma} W_O c_{2\varepsilon - 2\gamma})] \end{array} \right\} \left[i_E - x(s_{2\varepsilon} q_E + c_{2\varepsilon} u_E) \right] \end{aligned} \quad (191)$$

$$10 \quad \begin{aligned} D_T = +1, D_R = -1 \Rightarrow \\ \frac{\eta^*}{\eta} &= \frac{1 - y(c_{2\gamma} D_O - s_{2\gamma} (1 - 2a) Z_O s_O zc_\omega) + xas_\omega [D_O s_{2\varepsilon - 2\gamma} - y(s_{2\varepsilon} - s_{2\gamma} W_O c_{2\varepsilon - 2\gamma})]}{1 + y(c_{2\gamma} D_O - s_{2\gamma} (1 - 2a) Z_O s_O zc_\omega) + xas_\omega [D_O s_{2\varepsilon - 2\gamma} + y(s_{2\varepsilon} - s_{2\gamma} W_O c_{2\varepsilon - 2\gamma})]} \end{aligned} \quad (192)$$

11 11 Determination of the calibrator rotation ε

12 The calibration measurements can be used to determine and consequentially correct the
 13 calibrator rotation ε , which is especially important for the rotation calibrator (Sect. 7), because
 14 here the rotation error ε is also present in the standard atmospheric measurements and has to
 15 be corrected, either mechanically before the measurements or analytically after the



1 measurements. If the $\pm 45^\circ$ calibration measurements can be described or approximated by Eq.
 2 (193) with $f(y, \dots)$ being a function of any parameter but not of x and ε , it is possible to
 3 estimate the calibrator rotation ε by means of the relative difference of the $\pm 45^\circ$ gain ratios as
 4 in Eq. (194) and using the tangent half-angle substitution (S.12.1) to achieve ε from Eq. (195).
 5 Note: η is assumed to be unknown.

$$6 \quad \frac{\eta^*}{\eta} = f(y, \dots) \frac{1 + x s_{2\varepsilon}}{1 - x s_{2\varepsilon}} \quad (193)$$

$$7 \quad Y(\varepsilon) \equiv \frac{\eta^*(y, +45^\circ + \varepsilon) - \eta^*(y, -45^\circ + \varepsilon)}{\eta^*(y, +45^\circ + \varepsilon) + \eta^*(y, -45^\circ + \varepsilon)} = \frac{\frac{1 + s_{2\varepsilon}}{1 - s_{2\varepsilon}} - \frac{1 - s_{2\varepsilon}}{1 + s_{2\varepsilon}}}{\frac{1 + s_{2\varepsilon}}{1 - s_{2\varepsilon}} + \frac{1 - s_{2\varepsilon}}{1 + s_{2\varepsilon}}} = \frac{2s_{2\varepsilon}}{1 + s_{2\varepsilon}^2} \quad (194)$$

$$8 \quad \varepsilon(Y) = 0.5 * \arcsin \left[\tan \left(0.5 * \arcsin [Y] \right) \right] \quad (195)$$

9 With the assumption $\sin(2\varepsilon) \ll 1$ we get a good approximation for ε in the simple Eq. (196),
 10 which deviates by about 5% at $\varepsilon \approx 6^\circ$ and $Y(\varepsilon) \approx 0.4$.

$$11 \quad s_{2\varepsilon} \ll 1 \Rightarrow Y(\varepsilon) \approx 2s_{2\varepsilon} \Rightarrow \varepsilon \approx 0.25 * Y \quad (196)$$

12 Eq. (193) is applicable in Eqs. (130) and (137) for the linear polariser calibrator, and it is a
 13 good approximation for Eq (144) if the atmospheric polarisation parameter $a \approx 1$. For the
 14 rotation calibration before the receiving optics (Sect. 7.2, Eq.(117)) we have to assume that a
 15 ≈ 1 and additionally that the laser beam behind the emitter optics is horizontal-linearly
 16 polarised. Eq.(117) can then be approximated by Eq. (197).

$$17 \quad \frac{\eta^*}{\eta} \approx \frac{1 - y D_O}{1 + y D_O} \frac{1 + x s_{2\varepsilon}}{1 - x s_{2\varepsilon}} \quad (197)$$

with $\gamma = 0, D_T = +1, D_R = -1, i_E = q_E = 1, u_E = v_E = 0, a \approx 1 \Rightarrow$

18 If instead of Eq.(193) we have a form as Eq. (198) (see Sect. S.12.1), we get Eqs. (199) and
 19 (200). If ε is known, Eq.(200) can be solved for K , which yields Eq. (201).

$$20 \quad \frac{\eta^*}{\eta} = f(y, \dots) \frac{1 + K x s_{2\varepsilon}}{1 - K x s_{2\varepsilon}} \quad \text{with } K \leq 1 \quad (198)$$

$$21 \quad Y(\varepsilon, K) \equiv \frac{\eta^*(y, +45^\circ + \varepsilon, K) - \eta^*(y, -45^\circ + \varepsilon, K)}{\eta^*(y, +45^\circ + \varepsilon, K) + \eta^*(y, -45^\circ + \varepsilon, K)} = \frac{2K s_{2\varepsilon}}{1 + K^2 s_{2\varepsilon}^2} \quad (199)$$



$$1 \quad \varepsilon = \frac{1}{2} \arcsin \left[\frac{1}{K} \tan \left(\frac{\arcsin [Y(\varepsilon, K)]}{2} \right) \right] \quad (200)$$

$$2 \quad K = \left[\frac{1}{\sin 2\varepsilon} \tan \left(\frac{\arcsin [Y(\varepsilon, K)]}{2} \right) \right] \quad (201)$$

3 If the true ε and K are unknown, we can retrieve them by successive approximation. With $K <$
 4 1 we find as a first approximation ε_1 from Eq. (202) and make the next calibration
 5 measurement after adjusting the calibrator rotation by $-\varepsilon_1$, which results in the actual position
 6 $(\varepsilon - \varepsilon_1)$ and the corresponding Eq. (203).

$$7 \quad \varepsilon_1 = \frac{1}{2} \arcsin \left[\tan \left(\frac{\arcsin [Y(\varepsilon, K)]}{2} \right) \right] < \varepsilon \quad (202)$$

$$8 \quad Y(\varepsilon - \varepsilon_1, K) = \frac{2Ks_{2(\varepsilon - \varepsilon_1)}}{1 + K^2s_{2(\varepsilon - \varepsilon_1)}^2} \quad (203)$$

9 Using the calibration measurements at the two positions ε and $(\varepsilon - \varepsilon_1)$ with Eqs.(199) and
 10 (203), we get an estimation of the true ε with Eq. (205) derived from the ratio in Eq. (204).

$$11 \quad \frac{Y(\varepsilon - \varepsilon_1, K)}{Y(\varepsilon, K)} = \frac{(1 + K^2s_{2\varepsilon}^2)2Ks_{2(\varepsilon - \varepsilon_1)}}{(1 + K^2s_{2(\varepsilon - \varepsilon_1)}^2)2Ks_{2\varepsilon}} \approx \frac{s_{2(\varepsilon - \varepsilon_1)}}{s_{2\varepsilon}} \approx \frac{(\varepsilon - \varepsilon_1)}{\varepsilon} = 1 - \frac{\varepsilon_1}{\varepsilon} \quad (204)$$

$$12 \quad \varepsilon \approx \frac{Y(\varepsilon, K)}{Y(\varepsilon, K) - Y(\varepsilon - \varepsilon_1, K)} \varepsilon_1 \quad (205)$$

13 Finally, with known ε , we can use Eq. (201) to estimate K .

14 **12 Determination of the rotation α of the plane of polarisation of the emitted** 15 **laser beam.**

16 The orientation of the plane of polarisation of the laser beam is in general specified by
 17 manufacturers just as *vertical* or *horizontal*, without specifying the reference and the
 18 accuracy. Furthermore, the assembly of the laser with the telescope and the receiver optics in
 19 a lidar system can often not be done with similar accuracy as the assembly of the optical
 20 elements in the receiver optics, and the necessary alignment mechanisms for the tilt between
 21 the laser and telescope axes additionally introduces variability and uncertainty. On top of that,



- 1 the adjustments may change after every laser maintenance. Therefore it is desirable to
- 2 determine the laser rotation once in a while.
- 3 Using the calibrator equations for the calibrator before the receiver optics from App. C with
- 4 an analyser without receiver optics rotation ($\gamma = 0$; Eq. (D.8)), i.e.

$$\begin{aligned} \gamma = 0^\circ &\Rightarrow \langle \mathbf{A}_S | (y, 0^\circ) \rangle = \langle \mathbf{M}_S \mathbf{R}_y | \mathbf{M}_O(0^\circ) = T_O T_S \langle 1 + yD_S D_O \quad D_O + yD_S \quad 0 \quad 0 \rangle = \\ &= \langle \mathbf{M}_{SyO}(0^\circ) | = T_{SyO} \langle 1 \quad D_{SyO} \quad 0 \quad 0 \rangle, \\ &\Rightarrow A_S^3 = A_S^4 = 0 \end{aligned}$$

- 6 with elliptically polarised emitted laser light as Eq. (E.25),

$$7 \quad \frac{I_{in}(a, b, \alpha)}{I_{in}} = \frac{\mathbf{F}(a) \mathbf{I}_E}{F_{11} T_E I_L} = \left| 1 \quad abc_{2\alpha} \quad -abs_{2\alpha} \quad (1-2a)\sqrt{1-b^2} \right|,$$

- 8 and with ideal calibrators, we get the signals for the four ideal calibrator types in Eqs. (206)
- 9 to (209).

$$\begin{aligned} 10 \quad \frac{I_S}{\eta_S I_{in}} &= \frac{\langle \mathbf{A}_S | \mathbf{M}_{rot}(x45^\circ + \varepsilon, h) | \mathbf{I}_{in} \rangle}{I_{in}} = \\ &= A_S^1 i_{in} + A_S^4 h v_{in} - x \left[(s_{2\varepsilon} A_S^2 - c_{2\varepsilon} A_S^3) q_{in} + (c_{2\varepsilon} A_S^2 + s_{2\varepsilon} A_S^3) h u_{in} \right] = \\ &= T_{SyO} (1 - xabD_{SyO} s_{2\varepsilon - h2\alpha}) \end{aligned} \quad (206)$$

$$\begin{aligned} D_p = 1 &\Rightarrow \\ 11 \quad \frac{I_S}{\eta_S T_p I_{in}} &= \frac{\langle \mathbf{A}_S | \mathbf{M}_p(x45^\circ + \varepsilon) | \mathbf{I}_{in} \rangle}{T_p I_{in}} = \left[A_S^1 + x(c_{2\varepsilon} A_S^3 - s_{2\varepsilon} A_S^2) \right] \left[i_{in} + x(c_{2\varepsilon} u_{in} - s_{2\varepsilon} q_{in}) \right] = \\ &= T_{SyO} (1 - x s_{2\varepsilon} D_{SyO}) (1 - xabs_{2\alpha+2\varepsilon}) = T_{SyO} \left[1 + abD_{SyO} s_{2\varepsilon} s_{2\alpha+2\varepsilon} - x(s_{2\varepsilon} D_{SyO} + abs_{2\alpha+2\varepsilon}) \right] \end{aligned} \quad (207)$$

$$\begin{aligned} \omega = 0 &\Rightarrow \\ 12 \quad \frac{I_S}{\eta_S T_{QW} I_{in}} &= \frac{\langle \mathbf{A}_S | \mathbf{M}_{QW}(x45^\circ + \varepsilon, 0) | \mathbf{I}_{in} \rangle}{T_{QW} I_{in}} = \\ &= A_S^1 i_{in} - (s_{2\varepsilon} A_S^2 - c_{2\varepsilon} A_S^3) (s_{2\varepsilon} q_{in} - c_{2\varepsilon} u_{in}) - x \left[A_S^4 (c_{2\varepsilon} q_{in} + s_{2\varepsilon} u_{in}) + (c_{2\varepsilon} A_S^2 + s_{2\varepsilon} A_S^3) v_{in} \right] = \\ &= T_{SyO} \left[1 - abD_{SyO} s_{2\varepsilon} s_{2\varepsilon+2\alpha} + xD_{SyO} c_{2\varepsilon} (1-2a)\sqrt{1-b^2} \right] \end{aligned} \quad (208)$$

$$\begin{aligned} \omega = 0, D_p = 1 &\Rightarrow \\ 13 \quad \frac{I_S}{\eta_S T_{CP} I_{in}} &= \frac{\langle \mathbf{A}_S | \mathbf{M}_{CP}(z, x45^\circ + \varepsilon) | \mathbf{I}_{in} \rangle}{T_{CP} I_{in}} = (A_S^1 + zA_S^4) (i_{in} - x(c_{2\varepsilon} u_{in} - s_{2\varepsilon} q_{in})) = \\ &= T_{SyO} (1 + xabs_{2\alpha+2\varepsilon}) \end{aligned} \quad (209)$$



1 Eqs. (206) and (209) are of the type of Eq. (193), wherefore the solutions described in Sect.
 2 11 can be applied, but only to determine $\varepsilon \pm \alpha$. In order to determine α alone, ε must be
 3 known, or a series of measurements with variable ε are fitted to the gain ratios η^* formulated
 4 with one of the Eqs. (206) to (209), as explained by Alvarez et al. (2006).

5 Furthermore, for the case of the linear polariser calibrator (Eq. (207)), an unpolarised light
 6 source (i.e. $i_{in} = 1$ and $q_{in} = u_{in} = v_{in} = 0$) before the receiver optics / telescope gives Eq. (210)
 7 from Eq. (207), which is of the type of Eq. (193), and with a cleaned analyser $D_{SyO} = \pm 1$.

$$8 \quad D_p = 1, \quad i_{in} = 1, \quad q_{in} = u_{in} = v_{in} = 0 \Rightarrow \quad \frac{I_s}{\eta_s T_p I_{in}} = \frac{\langle \mathbf{A}_s | \mathbf{M}_p(x45^\circ + \varepsilon) | \mathbf{I}_{in} \rangle}{T_p I_{in}} = T_{SyO} (1 - xS_{2\varepsilon} D_{SyO}) \quad (210)$$

9 13 Summary and conclusions

10 The presented equations can be used to analyse the effects of polarising optics of a variety of
 11 lidar systems and to assess the accuracy and error of several calibration techniques. Major
 12 findings are, that a cleaned analyser and no rotation of the receiving optics with respect to the
 13 laser polarisation avoid many error terms and allow to determine and correct other
 14 misalignments and the optics diattenuation, and that the $\Delta 90^\circ$ -calibration can decrease the error
 15 of a single $\pm 45^\circ$ calibration into insignificance.

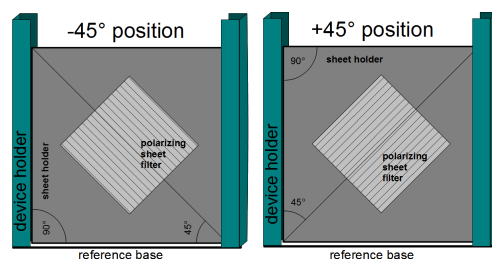
16 We showed that a linear polariser as calibrator should have a very good extinction ratio in
 17 order to avoid large calibration errors (Eq. (126)). The advantage of a sheet polariser (and $\lambda/4$
 18 sheet filters) is its tenuity, wherefore it can be included in many existing lidar systems with
 19 minimal space requirement, for example with a sheet holder as shown in Fig. 4. Such a sheet
 20 holder guarantees an accurate $\Delta 90^\circ$ rotation of the sheet, wherefore the absolute accuracy of
 21 the 45° orientation is not important. Together with an existing calibration technique or
 22 inserted at different positions, the filter holder can be used to determine the diattenuation of
 23 the optics between the two positions (see Eqs. (131) and (138) / (145)). Furthermore, the
 24 determination of the calibration factor with an ideal linear polariser calibrator is always
 25 independent of changes of the input light and hence independent of the atmospheric
 26 depolarisation, in contrast to the other calibrators. Plastic sheet filters can easily be cut to be
 27 used in a rotation holder as in Fig. 5, so that the filter can be automatically rotated to $\Delta 90^\circ$
 28 positions and out of the optical path for standard measurements. Large acceptance angles of
 29 linearly polarising sheet filters allows the mounting close to the telescope focus where we



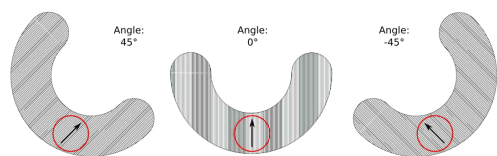
1 have some free space and the filter diameter and mechanical mounting can be small due to the
2 small beam diameter. However, it should be considered that the direction of the polarising
3 structure of a sheet filter is not necessarily constant over the whole sheet, which is usually not
4 specified by the manufacturers and should be inquired before the purchase.

5 $\lambda/4$ plates and circular polariser made of sheet films have similar constraints. Furthermore, the
6 $\Delta 90^\circ$ -calibration doesn't work with a $\lambda/4$ plate, because the $\pm 45^\circ$ errors don't compensate (Eqs.
7 (154), (164)), but in exchange we can determine with it the amount of circular polarisation
8 (Eqs. (158) and (168), and S.14). In contrast to that, the ideal circular polariser calibration
9 does not depend on the rotation error ε and the input light polarisation at all and doesn't need a
10 $\Delta 90^\circ$ -calibration, but inherent errors of a real circular polariser, which usually are not
11 sufficiently specified by manufacturers, would be difficult to assess, and the resulting error
12 equations are complex.

13 While all optical calibrators exhibit wavelength dependency and have the disadvantage of
14 possible inhomogeneities over the surface and other optical errors as inaccurate phase shift or
15 cross-talk, the only possible error source of the mechanical rotation calibrator (Sect. 7) is the
16 accuracy of the rotation itself. Although more bulky, it is the most reliable calibrator if used
17 with a cleaned analyser and accurate $\Delta 90^\circ$ rotation (Eq. (105)). It is independent of
18 wavelength, has no internal uncertainties, and is insensitive to temporal changes and
19 degradation.



20 Figure 4: Simple holder for sheet filters (linear polariser or $\lambda/4$ plate) with accurate
21 positioning for the $\Delta 90^\circ$ -calibration.



1 Figure 5: Linearly polarising sheet filter cutout for use in a rotation mount. The optical axis of
2 the filtered light beam is in the centre of the red circle. Reproduced with permission from
3 Kölbl (2010).

4 **14 Acknowledgments**

5 The financial support for EARLINET in the ACTRIS Research Infrastructure Project by the
6 European Union's Horizon 2020 research and innovation programme under grant agreement
7 n. 654169 and previously under grant agreement n. 262254 in the 7th Framework Programme
8 (FP7/2007-2013) is gratefully acknowledged.



1 **References**

- 2 Alvarez, J. M., Vaughan, M. A., Hostetler, C. A., Hunt, W. H. and Winker, D. M.: Calibration
3 Technique for Polarization-Sensitive Lidars, *J. Atmos. Oceanic Technol.*, 23, 683-699, 2006.
- 4 Anderson, R.: Polarization and atmospheric backscatter coefficient measurements, *Appl. Opt.*,
5 28, 865-874, 1989.
- 6 Ansmann, A. and Müller, D.: Lidar and Atmospheric Aerosol Particles, in: *Lidar*, 102, ,
7 Weitkamp, C. (Ed.), Springer New York, , 105-141, 2005.
- 8 Ansmann, A., Tesche, M., Seifert, P., Groß, S., Freudenthaler, V., Apituley, A., Wilson, K. M.,
9 Serikov, I., Linné, H., Heinold, B., Hiebsch, A., Schnell, F., Schmidt, J., Mattis, I., Wandinger,
10 U. and Wiegner, M.: Ash and fine-mode particle mass profiles from EARLINET-AERONET
11 observations over central Europe after the eruptions of the Eyjafjallajökull volcano in 2010, *J.*
12 *Geophys. Res.*, 116, 2011.
- 13 Azzam, R. M. A.: Ellipsometry in: *Handbook of Optics, Volume I (3rd Edition)*, Chapter 16,
14 McGraw-Hill, , 2009.
- 15 Behrendt, A. and Nakamura, T.: Calculation of the calibration constant of polarization lidar
16 and its dependency on atmospheric temperature, *Opt. Express*, 10, 805-817, 2002.
- 17 Belegante, L., Bravo-Aranda, J. A., Freudenthaler, V., Nicolae, D., Nemuc, A., Alados-
18 Arboledas, L., Amodeo, A., Pappalardo, G., D'Amico, G., Engelmann, R., Baars, H.,
19 Wandinger, U., Papayannis, A., Kokkalis, P. and Pereira, S. N.: Experimental assessment of
20 the lidar polarizing sensitivity, *Atmospheric Measurement Techniques Discussions*, 2016, 1-
21 44, 2016.
- 22 Bennett, J. M.: Polarization in: *Handbook of Optics, Volume I (3rd Edition)*, Chapter 12,
23 McGraw-Hill, , 2009a.
- 24 Bennett, J. M.: Polarizers in: *Handbook of Optics, Volume I (3rd Edition)*, Chapter 13,
25 McGraw-Hill, , 2009b.
- 26 Beyerle, G.: Untersuchungen stratosphärischer Aerosole vulkanischen Ursprungs und polarer
27 stratosphärischer Wolken mit einem Mehrwellen-Lidar auf Spitzbergen (79°N, 12°E),
28 *Berichte zur Polarforschung (Reports on Polar Research)*, 138, 1994.



- 1 Biele, J., Beyerle, G. and Baumgarten, G.: Polarization Lidar: Correction of instrumental
2 effects, *Opt. Express*, 7, 427-435, 2000.
- 3 Böckmann, C. and Osterloh, L.: Runge-Kutta type regularization method for inversion of
4 spheroidal particle distribution from limited optical data, *Inverse Problems in Science and*
5 *Engineering*, 22, 150-165, 2014.
- 6 Borovoi, A., Konoshonkin, A. and Kustova, N.: Backscatter ratios for arbitrary oriented
7 hexagonal ice crystals of cirrus clouds, *Opt. Lett.*, 39, 5788-5791, 2014.
- 8 Boucher, O., Randall, D., Artaxo, P., Bretherton, C., Feingold, G., Forster, P., Kerminen, V.-
9 M., Kondo, Y., Liao, H., Lohmann, U., Rasch, P., Satheesh, S., Sherwood, S., Stevens, B. and
10 Zhang, X.: 7 in: *Clouds and Aerosols*, Cambridge University Press, Cambridge, United
11 Kingdom and New York, NY, USA, 571–658 2013.
- 12 Bravo-Aranda, J. A., Belegante, L., Freudenthaler, V., Alados-Arboledas, A., Nicolae, D.,
13 Granados-Muñoz, M. J., Guerrero-Rascado, J. L., Amodeo, A., D'Amico, G., Engelmann, R.,
14 Pappalardo, G., Kokkalis, P., Mamouri, R., Papayannis, A., Navas-Guzmán, F., Olmo, F. J.,
15 Wandinger, U. and Haeffelin, M.: Assessment of lidar depolarization uncertainty by means of
16 a polarimetric lidar simulator, *Atmospheric Measurement Techniques Discussions*, 2016, 1-
17 35, 2016.
- 18 Bravo-Aranda, J. A., Navas-Guzmán, F., Guerrero-Rascado, J. L., Pérez-Ramírez, D.,
19 Granados-Muñoz, M. J. and Alados-Arboledas, L.: Analysis of lidar depolarization calibration
20 procedure and application to the atmospheric aerosol characterization, *International Journal of*
21 *Remote Sensing*, 34, 3543-3560, 2013.
- 22 Breckinridge, J. B., Lam, W. S. T. and Chipman, R. A.: Polarization Aberrations in
23 Astronomical Telescopes: The Point Spread Function, *Publications of the Astronomical*
24 *Society of the Pacific*, 127, pp. 445-468, 2015.
- 25 Burton, S. P., Hair, J. W., Kahnert, M., Ferrare, R. A., Hostetler, C. A., Cook, A. L., Harper, D.
26 B., Berkoff, T. A., Seaman, S. T., Collins, J. E., Fenn, M. A. and Rogers, R. R.: Observations
27 of the spectral dependence of particle depolarization ratio of aerosols using NASA Langley
28 airborne High Spectral Resolution Lidar, *Atmospheric Chemistry and Physics Discussions*,
29 15, 24751-24803, 2015.



- 1 Burton, S. P., Vaughan, M. A., Ferrare, R. A. and Hostetler, C. A.: Separating mixtures of
2 aerosol types in airborne High Spectral Resolution Lidar data, Atmos. Meas. Tech., 7, 419-
3 436, 2014.
- 4 Cairo, F., Donfrancesco, G. D., Adriani, A., Pulvirenti, L. and Fierli, F.: Comparison of
5 Various Linear Depolarization Parameters Measured by Lidar, Appl. Opt., 38, 4425-4432,
6 1999.
- 7 Cao, X., Roy, G. and Bernier, R.: Lidar polarization discrimination of bioaerosols, in: , 7672,
8 Chenault, D. B. and Goldstein, D. H. (Ed.), :76720P+, 2010.
- 9 Chipman, R. A.: Polarimetry in: Handbook of Optics, Volume I (3rd Edition), Chap. 15,
10 McGraw-Hill, , 2009a.
- 11 Chipman, R. A.: Mueller matrices in: Handbook of Optics, Volume I (3rd Edition), Chap. 14,
12 McGraw-Hill, , 2009b.
- 13 Clark, N. and Breckinridge, J. B.: Polarization compensation of Fresnel aberrations in
14 telescopes, in: , 8146, (Ed.), :814600-814600-13, 2011.
- 15 Clarke, D.: Stellar Polarimetry, Wiley-VCH Verlag GmbH & Co. KGaA, , 2009.
- 16 David, G., Miffre, A., Thomas, B. and Rairoux, P.: Sensitive and accurate dual-wavelength
17 UV-VIS polarization detector for optical remote sensing of tropospheric aerosols, Appl. Phys.
18 B: Lasers Opt., 108, 197-216, 2012.
- 19 David, G., Thomas, B., Coillet, E., Miffre, A. and Rairoux, P.: Polarization-resolved exact
20 light backscattering by an ensemble of particles in air, Opt. Express, 21, 18624-18639, 2013.
- 21 Del Guasta, M., Vallar, E., Riviere, O., Castagnoli, F., Venturi, V. and Morandi, M.: Use of
22 polarimetric lidar for the study of oriented ice plates in clouds, Appl. Opt., 45, 4878+, 2006.
- 23 Di, H., Hua, D., Yan, L., Hou, X. and Wei, X.: Polarization analysis and corrections of
24 different telescopes in polarization lidar, Appl. Opt., 54, 389-397, 2015.
- 25 Eloranta, E.: in: High Spectral Resolution Lidar, Springer New York, , 143-163 2005.
- 26 Eloranta, E. W. and Piironen, P.: Depolarization measurements with the High Spectral
27 Resolution Lidar, Seventeenth International Laser Radar Conference, Sendai, Japan, , 1994.
- 28 Engelmann, R., Kanitz, T., Baars, H., Heese, B., Althausen, D., Skupin, A., Wandinger, U.,
29 Komppula, M., Stachlewska, I. S., Amiridis, V., Marinou, E., Mattis, I., Linné, H. and



- 1 Ansmann, A.: EARLINET Raman Lidar PollyXT: the neXT generation, Atmospheric
- 2 Measurement Techniques Discussions, 8, 7737-7780, 2015.
- 3 Esselborn, M., Wirth, M., Fix, A., Tesche, M. and Ehret, G.: Airborne high spectral resolution
- 4 lidar for measuring aerosol extinction and backscatter coefficients, Appl. Opt., 47, 346-358,
- 5 2008.
- 6 Flynn, C. J., Mendoza, A., Zheng, Y. and Mathur, S.: Novel polarization-sensitive micropulse
- 7 lidar measurement technique, Opt. Express, 15, 2785-2790, 2007.
- 8 Freudenthaler, V., Esselborn, M., Wiegner, M., Heese, B., Tesche, M., Ansmann, A., Müller,
- 9 D., Althausen, D., Wirth, M., Fix, A., Ehret, G., Knippertz, P., Toledano, C., Gasteiger, J.,
- 10 Garhammer, M. and Seefeldner, M.: Depolarization ratio profiling at several wavelengths in
- 11 pure Saharan dust during SAMUM 2006, Tellus B, 61, 165-179, 2009.
- 12 Freudenthaler, V., Seefeldner, M., Gro S. and Wandinger, U.: Accuracy of linear depolarisation
- 13 ratios in clear air ranges measured with POLIS-6 at 355 and 532 nm, in: 27th International
- 14 Laser Radar Conference, , (Ed.), , 2015.
- 15 Gasteiger, J. and Freudenthaler, V.: Benefit of depolarization ratio at $\lambda = 1064$ nm for the
- 16 retrieval of the aerosol microphysics from lidar measurements, Atmos. Meas. Tech., 7, 3773-
- 17 3781, 2014.
- 18 Gasteiger, J., Wiegner, M., Groß, S., Freudenthaler, V., Toledano, C., Tesche, M. and Kandler,
- 19 K.: Modelling lidar-relevant optical properties of complex mineral dust aerosols, Tellus B, 63,
- 20 725-741, 2011.
- 21 Geier, M. and Arienti, M.: Detection of preferential particle orientation in the atmosphere:
- 22 Development of an alternative polarization lidar system , Journal of Quantitative
- 23 Spectroscopy and Radiative Transfer , 149, 16 - 32, 2014.
- 24 Gimmetstad, G. G.: Reexamination of depolarization in lidar measurements, Appl. Opt., 47,
- 25 3795-3802, 2008.
- 26 Goldstein, D.: Polarized Light, Marcel Dekker, , 2003.
- 27 Groß, S., Freudenthaler, V., Wirth, M. and Weinzierl, B.: Towards an aerosol classification
- 28 scheme for future EarthCARE lidar observations and implications for research needs, Atmos.
- 29 Sci. Lett., , n/a-n/a, 2014.



- 1 Hair, J. W., Hostetler, C. A., Cook, A. L., Harper, D. B., Ferrare, R. A., Mack, T. L., Welch,
- 2 W., Izquierdo, L. R. and Hovis, F. E.: Airborne High Spectral Resolution Lidar for profiling
- 3 aerosol optical properties, *Appl. Opt.*, 47, 6734-6752, 2008.
- 4 Hauge, P., Muller, R. and Smith, C.: Conventions and formulas for using the Mueller-Stokes
- 5 calculus in ellipsometry, *Surf. Sci.*, 96, 81-107, 1980.
- 6 Hayman, M.: *Optical Theory for the Advancement of Polarization Lidar*, , , 2011.
- 7 Hayman, M., Spuler, S., Morley, B. and VanAndel, J.: Polarization lidar operation for
- 8 measuring backscatter phase matrices of oriented scatterers, *Opt. Express*, 20, 29553-29567,
- 9 2012.
- 10 Hayman, M. and Thayer, J. P.: Explicit description of polarization coupling in lidar
- 11 applications, *Opt. Lett.*, 34, 611-613, 2009.
- 12 Hayman, M. and Thayer, J. P.: General description of polarization in lidar using Stokes
- 13 vectors and polar decomposition of Mueller matrices, *J. Opt. Soc. Am. A*, 29, 400-409, 2012.
- 14 Houston, J. D. and Carswell, A. I.: Four-component polarization measurement of lidar
- 15 atmospheric scattering, *Appl. Opt.*, 17, 614-620, 1978.
- 16 van de Hulst, H. C.: *Light scattering by small particles*, Dover Publications, New York, 1981.
- 17 Hunt, W. H., Winker, D. M., Vaughan, M. A., Powell, K. A., Lucker, P. L. and Weimer, C.:
- 18 CALIPSO Lidar Description and Performance Assessment, *J. Atmos. Oceanic Technol.*, 26,
- 19 1214-1228, 2009.
- 20 Kahnert, M., Nousiainen, T. and Lindqvist, H.: Review: Model particles in atmospheric optics
- 21 , *JQSRT*, 146, 41 - 58, 2014.
- 22 Kaul, B. V., Kuznetsov, A. L. and Polovtseva, E. R.: Measurements of backscattering phase
- 23 matrices of crystalline clouds with a polarization lidar, *Atmospheric and Oceanic Optics*, 5,
- 24 381-383, 1992.
- 25 Kaul, B. V., Samokhvalov, I. V. and Volkov, S. N.: Investigating Particle Orientation in Cirrus
- 26 Clouds by Measuring Backscattering Phase Matrices with Lidar, *Appl. Opt.*, 43, 6620-6628,
- 27 2004.
- 28 Kölbl, C.: Depolarization of lidar signals in the arctic atmosphere; Calibration and
- 29 optimization of the ALOMAR Troposphere Lidar, , , 2010.



- 1 Liu, Z., McGill, M., Hu, Y., Hostetler, C., Vaughan, M. and Winker, D.: Validating Lidar
- 2 Depolarization Calibration Using Solar Radiation Scattered by Ice Clouds, IEEE Geosci.
- 3 Remote Sens. Lett., 1, 157-161, 2004.
- 4 Lu, S.-Y. and Chipman, R. A.: Interpretation of Mueller matrices based on polar
- 5 decomposition, J. Opt. Soc. Am. A, 13, 1106-1113, 1996.
- 6 Mattis, I., Tesche, M., Grein, M., Freudenthaler, V. and Müller, D.: Systematic error of lidar
- 7 profiles caused by a polarization-dependent receiver transmission: quantification and error
- 8 correction scheme, Appl. Opt., 48, 2742-2751, 2009.
- 9 McGill, M., Hlavka, D., Hart, W., Scott, V. S., Spinhirne, J. and Schmid, B.: Cloud Physics
- 10 Lidar: instrument description and initial measurement results, Appl. Opt., 41, 3725-3734,
- 11 2002.
- 12 Mishchenko, M., Travis, L. and Lacis, A.: Scattering, absorption, and emission of light by
- 13 small particles, Cambridge University Press, , 2002.
- 14 Mishchenko, M. I. and Hovenier, J. W.: Depolarization of light backscattered by randomly
- 15 oriented nonspherical particles, Opt. Lett., 20, 1356-1358, 1995.
- 16 Müller, D., Hostetler, C. A., Ferrare, R. A., Burton, S. P., Chemyakin, E., Kolgotin, A., Hair, J.
- 17 W., Cook, A. L., Harper, D. B., Rogers, R. R., Hare, R. W., Cleckner, C. S., Obland, M. D.,
- 18 Tomlinson, J., Berg, L. K. and Schmid, B.: Airborne Multiwavelength High Spectral
- 19 Resolution Lidar (HSRL-2) observations during TCAP 2012: vertical profiles of optical and
- 20 microphysical properties of a smoke/urban haze plume over the northeastern coast of the US,
- 21 Atmospheric Measurement Techniques, 7, 3487-3496, 2014.
- 22 Müller, D., Wandinger, U. and Ansmann, A.: Microphysical Particle Parameters from
- 23 Extinction and Backscatter Lidar Data by Inversion with Regularization: Theory, Appl. Opt.,
- 24 38, 2346-2357, 1999.
- 25 Muller, R.: Definitions and conventions in ellipsometry, Surf. Sci., 16, 14-33, 1969.
- 26 Nee, S.-M. F.: Errors of Mueller matrix measurements with a partially polarized light source,
- 27 Appl. Opt., 45, 6497-6506, 2006.
- 28 Nemuc, A., Vasilescu, J., Talianu, C., Belegante, L. and Nicolae, D.: Assessment of aerosol's
- 29 mass concentrations from measured linear particle depolarization ratio (vertically resolved)
- 30 and simulations, Atmospheric Measurement Techniques, 6, 3243-3255, 2013.



- 1 Nisantzi, A., Mamouri, R. E., Ansmann, A. and Hadjimitsis, D.: Injection of mineral dust into
2 the free troposphere during fire events observed with polarization lidar at Limassol, Cyprus,
3 Atmospheric Chemistry and Physics, 14, 12155-12165, 2014.
- 4 Nousiainen, T., Kahnert, M. and Lindqvist, H.: Can particle shape information be retrieved
5 from light-scattering observations using spheroidal model particles?, JQSRT, 112, 2213 -
6 2225, 2011.
- 7 Pérez-Ramírez, D., Whiteman, D. N., Veselovskii, I., Kolgotin, A., Korenskiy, M. and Alados-
8 Arboledas, L.: Effects of systematic and random errors on the retrieval of particle
9 microphysical properties from multiwavelength lidar measurements using inversion with
10 regularization, Atmos. Meas. Tech., 6, 3039-3054, 2013.
- 11 Pal, S. R. and Carswell, A. I.: Polarization Properties of Lidar Backscattering from Clouds,
12 Appl. Opt., 12, 1530-1535, 1973.
- 13 Pezzaniti, L. J. and Chipman, R. A.: Angular dependence of polarizing beam-splitter cubes,
14 Appl. Opt., 33, 1916-1929, 1994.
- 15 Platt, C. M. R.: Lidar Observation of a Mixed-Phase Altostratus Cloud, J. Appl. Meteor., 16,
16 339-345, 1977.
- 17 Reichardt, J., Baumgart, R. and McGee, T. J.: Three-Signal Method for Accurate
18 Measurements of Depolarization Ratio with Lidar, Appl. Opt., 42, 4909-4913, 2003.
- 19 Roy, G., Cao, X. and Bernier, R.: On the information content of linear and circular
20 depolarization signatures of bioaerosols, in: , 8018, (Ed.), :801807-801807-8, 2011.
- 21 Sassen, K.: in: Polarization in lidar, in Lidar: Range-Resolved Optical Remote Sensing of the
22 Atmosphere, Springer, , 19-42 2005.
- 23 Sassen, K.: The Polarization Lidar Technique for Cloud Research: A Review and Current
24 Assessment, Bull. Amer. Meteor. Soc., 72, 1848-1866, 1991.
- 25 Sassen, K. and Benson, S.: A Midlatitude Cirrus Cloud Climatology from the Facility for
26 Atmospheric Remote Sensing. Part II: Microphysical Properties Derived from Lidar
27 Depolarization, J. Atmos. Sci., 58, 2103-2112, 2001.
- 28 Schotland, R. M., Sassen, K. and Stone, R.: Observations by Lidar of Linear Depolarization
29 Ratios for Hydrometeors, J. Appl. Meteor., 10, 1011-1017, 1971.



- 1 Seldomridge, N. L., Shaw, J. A. and Repasky, K. S.: Dual-polarization lidar using a liquid
- 2 crystal variable retarder, *Opt. Eng.*, 45, 106202+, 2006.
- 3 Shimizu, A., Sugimoto, N., Matsui, I., Arao, K., Uno, I., Murayama, T., Kagawa, N., Aoki, K.,
- 4 Uchiyama, A. and Yamazaki, A.: Continuous observations of Asian dust and other aerosols by
- 5 polarization lidars in China and Japan during ACE-Asia, *Journal of Geophysical Research:*
- 6 *Atmospheres*, 109, n/a-n/a, 2004.
- 7 Skumanich, A., Lites, B. W., Pillet, V. M. and Seagraves, P.: The Calibration of the Advanced
- 8 Stokes Polarimeter, *The Astrophysical Journal Supplement Series*, , 357+, 1997.
- 9 Snels, M., Cairo, F., Colao, F. and Di Donfrancesco, G.: Calibration method for depolarization
- 10 lidar measurements, *Int. J. Remote Sens.*, 30, 5725-5736, 2009.
- 11 Socas-Navarro, H., Elmore, D., Asensio Ramos, A. and Harrington, D. M.: Characterization
- 12 of telescope polarization properties across the visible and near-infrared spectrum, *A&A*, 531,
- 13 A2, 2011.
- 14 Spinhirne, J. D., Hansen, M. Z. and Caudill, L. O.: Cloud top remote sensing by airborne
- 15 lidar, *Appl. Opt.*, 21, 1564-1571, 1982.
- 16 Steinborn, E. and Ruedenberg, K.: Rotation and Translation of Regular and Irregular Solid
- 17 Spherical Harmonics, in: , 7, , Löwdin, P.-O. (Ed.), *Academic Press*, , 1 - 81, 1973.
- 18 Sugimoto, N. and Lee, C. H.: Characteristics of dust aerosols inferred from lidar
- 19 depolarization measurements at two wavelengths, *Appl. Opt.*, 45, 7468-7474, 2006.
- 20 Sugimoto, N., Matsui, I., Shimizu, A., Uno, I., Asai, K., Endoh, T. and Nakajima, T.:
- 21 Observation of dust and anthropogenic aerosol plumes in the Northwest Pacific with a two-
- 22 wavelength polarization lidar on board the research vessel Mirai, *Geophys. Res. Lett.*, 29,
- 23 1901+, 2002.
- 24 Veselovskii, I., Whiteman, D. N., Korenskiy, M., Kolgotin, A., Dubovik, O., Perez-Ramirez,
- 25 D. and Suvorina, A.: Retrieval of spatio-temporal distributions of particle parameters from
- 26 multiwavelength lidar measurements using the linear estimation technique and comparison
- 27 with AERONET, *Atmos. Meas. Tech.*, 6, 2671-2682, 2013.
- 28 Volkov, S. N., Samokhvalov, I. V., Cheong, H. D. and Kim, D.: Investigation of East Asian
- 29 clouds with polarization light detection and ranging, *Appl. Opt.*, 54, 3095-3105, 2015.



- 1 Winker, D. M., Vaughan, M. A., Omar, A., Hu, Y., Powell, K. A., Liu, Z., Hunt, W. H. and
- 2 Young, S. A.: Overview of the CALIPSO Mission and CALIOP Data Processing Algorithms,
- 3 J. Atmos. Oceanic Technol., 26, 2310-2323, 2009.
- 4 : Handbook of Optics, Volume I - Geometrical and Physical Optics, Polarized Light,
- 5 Components and Instruments (3rd Edition), Bass, M. (Ed.). McGraw Hill Professional, ,
- 6 2009.



1 15 Appendix

2 App. A Acronyms and shortcuts

| | | |
|----|----------------------------------|---|
| 3 | a | polarisation parameter of the atmospheric volume; see Eq. 9 |
| 4 | a_L | polarisation parameter of the light beam leaving the laser |
| 5 | a' | $a' = aa_L$, combined laser-atmosphere polarisation parameter |
| 6 | α | Rotation of the plane of horizontal-linear polarisation of the laser around the z-axis (laser rotation) |
| 7 | | |
| 8 | β | Rotation of the emitter optics around the z-axis |
| 9 | γ | Rotation of the receiver optics around the z-axis |
| 10 | $c_{2\varepsilon}$ | $\cos(2\varepsilon)$ |
| 11 | δ | (volume) linear depolarisation ratio of the atmospheric scattering volume; see Eq. 12 |
| 12 | | |
| 13 | δ^* | calibrated signal ratio including cross talk and alignment errors |
| 14 | D | diattenuation parameter. See |
| 15 | ε | error angle of the $\Delta 90$ -calibration setup |
| 16 | $\eta_{T,R}$ | electronic amplification of individual transmitted/reflected channels |
| 17 | η | $\eta = \eta_R T_R / \eta_T T_T$ calibration factor including only the electronic amplification and the optical diattenuation of the polarising beam-splitter |
| 18 | | |
| 19 | η^* | gain ratio i.e. the measured, apparent calibration factor η^* of the polarisation channels, i.e. the calibration factor η including the cross talk from optics before the polarising beam-splitter and from system alignment errors |
| 20 | | |
| 21 | | |
| 22 | $\eta_{\Delta 90}^*$ | $\Delta 90$ -gain ratio $\eta_{\Delta 90}^* \equiv \sqrt{\eta^*(+45^\circ + \varepsilon)\eta^*(-45^\circ + \varepsilon)}$; measured, apparent calibration factor retrieved with the $\Delta 90$ -calibration method |
| 23 | | |
| 24 | I | Power/flux of the light beam [watt/lumen] (colloquially: intensity) |
| 25 | \mathbf{I} | Stokes vector of the light beam |
| 26 | LDR | linear depolarisation ratio = δ |
| 27 | \mathbf{F} | Müller matrix of the atmospheric scattering volume in backscattering direction |
| 28 | F_{ij} | Element ij of \mathbf{F} |
| 29 | $\mathbf{M}_S, \mathbf{M}_{T,R}$ | Müller matrix of the polarising beam-splitter S , e.g. a polarising beam-splitter cube, in the transmission T and reflection R path. |
| 30 | | |
| 31 | PBS | polarising beam-splitter |
| 32 | $s_{2\varepsilon}$ | $\sin(2\varepsilon)$ |
| 33 | T_S | Transmission of matrix \mathbf{M}_S for unpolarised light (alias average transmission) |
| 34 | T^p, T^s, R^p, R^s | Intensity transmission and reflection coefficients of the polarising beam-splitter for parallel p and perpendicular s linearly polarised light with respect to the plane of incidence. |
| 35 | | |
| 36 | | |
| 37 | Z_o | $Z_o = \sqrt{1 - D_o^2}$ |
| 38 | W_o | $W_o = 1 - Z_o c_o = 1 - c_o \sqrt{1 - D_o^2}$ |
| 39 | c_o | $\cos(\Delta_o)$ |
| 40 | Δ | differential phase shift of the p and s polarised light $\varphi^p - \varphi^s$ |
| 41 | φ^p, φ^s | phase of the p and s polarised light |
| 42 | ψ | Rotation of the calibrator around the z-axis |
| 43 | ϕ | Rotation around z-axis |
| 44 | $\langle \mid$ | First row vector of a matrix; bra-vector. |



- 1 $| \rangle$ Stokes vector; always a column vector; ket-vector.
- 2 Setup parameters:
- 3 h binary operator to select either manual rotation ($h = +1$) or rotation by means
 4 of a $\lambda/2$ plate ($h = -1$).
- 5 x, z binary operators to select angles of $+45^\circ$ ($x, z = +1$) or -45° ($x, z = -1$)
- 6 y binary operator to select angles of $+0^\circ$ ($y = +1$) or $+90^\circ$ ($y = -1$)

7 App. B The <bra|ket> notation

8 Superscript T means the transposition of a row vector to a column vector and vice versa, while
 9 the $|\text{ket}\rangle$ and $\langle\text{bra}|$ vector symbols always stand for a column vector and row vector,
 10 respectively. That means:

$$11 \begin{pmatrix} a \\ b \\ c \\ d \end{pmatrix} = (a \ b \ c \ d)^T = |a \ b \ c \ d\rangle = \begin{pmatrix} a \\ b \\ c \\ d \end{pmatrix} \quad (\text{B.1})$$

12 are forms of column vectors, and

$$13 (a \ b \ c \ d) = \begin{pmatrix} a \\ b \\ c \\ d \end{pmatrix}^T = \langle a \ b \ c \ d| = \begin{pmatrix} a \\ b \\ c \\ d \end{pmatrix} \quad (\text{B.2})$$

14 are forms of row vectors.

15 App. C The calibration equation

16 The general equation for the calibration signals Eq. (81) can be written similar to Kaul et al.
 17 (2004) using general expressions for the analyser row vector $\langle\mathbf{A}_s|$ (see App. D) and for the
 18 input Stokes vector $|\mathbf{I}_{in}\rangle$ (see App. E) as in Eq. (C.1), irrespective of the actual position of the
 19 calibrator.

$$20 \frac{I_s}{\eta_s} = \langle\mathbf{A}_s| \mathbf{C}(x45^\circ + \varepsilon) |\mathbf{I}_{in}\rangle = I_{in} \begin{pmatrix} A_s^1 \\ A_s^2 \\ A_s^3 \\ A_s^4 \end{pmatrix} \mathbf{C}(x45^\circ + \varepsilon) \begin{pmatrix} i_{in} \\ q_{in} \\ u_{in} \\ v_{in} \end{pmatrix} \quad (\text{C.1})$$

21 For certain setups the fully expanded equations are very complex. But sometimes slighty
 22 expanded versions are sufficient to achieve significant insights. Demerging the $(\pm 45^\circ + \varepsilon)$



- 1 rotation from the calibrator, as in Eq. (C.2), or just the ε – rotations, as in Eq. (C.3), and
- 2 applying the appropriate parts to the analyser and to the input Stokes vector can help to show
- 3 general relations. For this purpose we define the rotated analyser vector $\langle \mathbf{A}_{S,\varepsilon} |$ and the rotated
- 4 input Stokes vector $|I_{in,\varepsilon}\rangle$ as shown in Eq. (C.3).

$$\begin{aligned}
 I_S &= \eta_S \langle \mathbf{A}_S | \mathbf{C}(x45^\circ + \varepsilon) | I_{in} \rangle = \\
 &= \eta_S \langle \mathbf{A}_S | \mathbf{R}(x45^\circ + \varepsilon) \mathbf{C}(0) \mathbf{R}(-x45^\circ - \varepsilon) | I_{in} \rangle \Rightarrow \\
 \frac{I_S}{\eta_S I_{in}} &= \left\langle \begin{array}{c} A_S^1 \\ A_S^2 \\ A_S^3 \\ A_S^4 \end{array} \left| \begin{array}{cccc} 1 & 0 & 0 & 0 \\ 0 & -xS_{2\varepsilon} & xC_{2\varepsilon} & 0 \\ 0 & xC_{2\varepsilon} & -xS_{2\varepsilon} & 0 \\ 0 & 0 & 0 & 1 \end{array} \right. \mathbf{C}(0) \left. \begin{array}{c} 1 & 0 & 0 & 0 \\ 0 & -xS_{2\varepsilon} & xC_{2\varepsilon} & 0 \\ 0 & -xC_{2\varepsilon} & -xS_{2\varepsilon} & 0 \\ 0 & 0 & 0 & 1 \end{array} \right| \begin{array}{c} i_{in} \\ q_{in} \\ u_{in} \\ v_{in} \end{array} \right\rangle = \\
 &= \left\langle \begin{array}{c} A_S^1 \\ x(C_{2\varepsilon} A_S^3 - S_{2\varepsilon} A_S^2) \\ -x(C_{2\varepsilon} A_S^2 + S_{2\varepsilon} A_S^3) \\ A_S^4 \end{array} \left| \mathbf{C}(0) \right. \begin{array}{c} i_{in} \\ x(C_{2\varepsilon} u_{in} - S_{2\varepsilon} q_{in}) \\ -x(C_{2\varepsilon} q_{in} + S_{2\varepsilon} u_{in}) \\ v_{in} \end{array} \right\rangle = \left\langle \begin{array}{c} A_S^1 \\ xA_{S,\varepsilon}^3 \\ -xA_{S,\varepsilon}^2 \\ A_S^4 \end{array} \left| \mathbf{C}(0) \right. \begin{array}{c} i_{in} \\ x u_{in,\varepsilon} \\ -x q_{in,\varepsilon} \\ v_{in} \end{array} \right\rangle
 \end{aligned} \tag{C.2}$$

$$\begin{aligned}
 I_S &= \eta_S \langle \mathbf{A}_S | \mathbf{C}(x45^\circ + \varepsilon) | I_{in} \rangle = \\
 &= \eta_S \langle \mathbf{A}_S | \mathbf{R}(+\varepsilon) \mathbf{C}(x45^\circ) \mathbf{R}(-\varepsilon) | I_{in} \rangle = \eta_S \langle \mathbf{A}_{S,\varepsilon} | \mathbf{C}(x45^\circ) | I_{in,\varepsilon} \rangle \Rightarrow \\
 \frac{I_S}{\eta_S I_{in}} &= \left\langle \begin{array}{c} A_S^1 \\ A_S^2 \\ A_S^3 \\ A_S^4 \end{array} \left| \begin{array}{cccc} 1 & 0 & 0 & 0 \\ 0 & C_{2\varepsilon} & -S_{2\varepsilon} & 0 \\ 0 & S_{2\varepsilon} & C_{2\varepsilon} & 0 \\ 0 & 0 & 0 & 1 \end{array} \right. \mathbf{C}(x45^\circ) \left. \begin{array}{c} 1 & 0 & 0 & 0 \\ 0 & C_{2\varepsilon} & S_{2\varepsilon} & 0 \\ 0 & -S_{2\varepsilon} & C_{2\varepsilon} & 0 \\ 0 & 0 & 0 & 1 \end{array} \right| \begin{array}{c} i_{in} \\ q_{in} \\ u_{in} \\ v_{in} \end{array} \right\rangle = \\
 &= \left\langle \begin{array}{c} A_S^1 \\ C_{2\varepsilon} A_S^2 + S_{2\varepsilon} A_S^3 \\ C_{2\varepsilon} A_S^3 - S_{2\varepsilon} A_S^2 \\ A_S^4 \end{array} \left| \mathbf{C}(x45^\circ) \right. \begin{array}{c} i_{in} \\ C_{2\varepsilon} q_{in} + S_{2\varepsilon} u_{in} \\ C_{2\varepsilon} u_{in} - S_{2\varepsilon} q_{in} \\ v_{in} \end{array} \right\rangle \equiv \left\langle \begin{array}{c} A_S^1 \\ A_{S,\varepsilon}^2 \\ A_{S,\varepsilon}^3 \\ A_S^4 \end{array} \left| \mathbf{C}(x45^\circ) \right. \begin{array}{c} i_{in} \\ q_{in,\varepsilon} \\ u_{in,\varepsilon} \\ v_{in} \end{array} \right\rangle
 \end{aligned} \tag{C.3}$$

7 Note the exchange of places of $A_{S,\varepsilon}^2$ and $A_{S,\varepsilon}^3$ and of $q_{in,\varepsilon}$ and $u_{in,\varepsilon}$ between Eqs. (C.2) and (C.3).

8 **App. C.1 Calibration with a rotator**

- 9 From Eqs. (C.1), (C.3), and (S.10.15.2) we get the general calibration signals Eq. (C.4) with
- 10 analyser vectors $\langle \mathbf{A} |$ from App. D and input Stokes vectors $|I_{in}\rangle$ from App. E.



$$\begin{aligned}
 \frac{I_S}{\eta_S I_{in}} &= \frac{\langle \mathbf{A}_S | \mathbf{M}_{rot}(x45^\circ + \varepsilon, h) | \mathbf{I}_{in} \rangle}{I_{in}} = \\
 &= \left\langle \begin{matrix} A_S^1 \\ A_S^2 \\ A_S^3 \\ A_S^4 \end{matrix} \left| \begin{pmatrix} 1 & 0 & 0 & 0 \\ 0 & -x s_{2\varepsilon} & -x h c_{2\varepsilon} & 0 \\ 0 & x c_{2\varepsilon} & -x h s_{2\varepsilon} & 0 \\ 0 & 0 & 0 & h \end{pmatrix} \right| \begin{matrix} i_{in} \\ q_{in} \\ u_{in} \\ v_{in} \end{matrix} \right\rangle = \\
 &= A_S^1 i_{in} + A_S^4 h v_{in} - x \left[(s_{2\varepsilon} A_S^2 - c_{2\varepsilon} A_S^3) q_{in} + (c_{2\varepsilon} A_S^2 + s_{2\varepsilon} A_S^3) h u_{in} \right] = \\
 &= A_S^1 i_{in} + A_S^4 h v_{in} + x \left[A_S^3 q_{in} - A_S^2 h u_{in} \right]
 \end{aligned} \tag{C.4}$$

2 App. C.2 Calibration with a linear polariser

3 From Eq. (C.3) and (S.10.7.1) we get the general calibration signals Eq. (C.5) with analyser
 4 vectors $\langle \mathbf{A} |$ from App. D and input Stokes $|\mathbf{I}_{in}\rangle$ vectors from App. E. With an ideal linear
 5 polariser Eq. (C.5) reduces to Eq. (C.6).

$$\begin{aligned}
 I_S &= \eta_S \langle \mathbf{A}_S | \mathbf{M}_P(x45^\circ + \varepsilon) | \mathbf{I}_{in} \rangle = \eta_S \langle \mathbf{A}_S | \mathbf{R}(+\varepsilon) \mathbf{M}_P(x45^\circ) \mathbf{R}(-\varepsilon) | \mathbf{I}_{in} \rangle \Rightarrow \\
 \frac{I_S}{\eta_S T_P I_{in}} &= \left\langle \begin{matrix} A_{S,\varepsilon}^1 \\ A_{S,\varepsilon}^2 \\ A_{S,\varepsilon}^3 \\ A_{S,\varepsilon}^4 \end{matrix} \left| \begin{pmatrix} 1 & 0 & x D_P & 0 \\ 0 & Z_P c_P & 0 & -x Z_P s_P \\ x D_P & 0 & 1 & 0 \\ 0 & x Z_P s_P & 0 & Z_P c_P \end{pmatrix} \right| \begin{matrix} i_{in} \\ q_{in,\varepsilon} \\ u_{in,\varepsilon} \\ v_{in} \end{matrix} \right\rangle = \\
 &= \left\{ \begin{aligned} &A_S^1 i_{in} + A_{S,\varepsilon}^3 u_{in,\varepsilon} + Z_P c_P (A_{S,\varepsilon}^2 q_{in,\varepsilon} + A_S^4 v_{in}) + \\ &+ x \left[D_P (A_S^1 u_{in,\varepsilon} + A_{S,\varepsilon}^3 i_{in}) - Z_P s_P (A_{S,\varepsilon}^2 v_{in} - A_S^4 q_{in,\varepsilon}) \right] \end{aligned} \right\}
 \end{aligned} \tag{C.5}$$

$$\begin{aligned}
 D_P = 1, Z_P = 0 &\Rightarrow \\
 \frac{I_S}{\eta_S T_P I_{in}} &= A_S^1 i_{in} + A_{S,\varepsilon}^3 u_{in,\varepsilon} + x (A_S^1 u_{in,\varepsilon} + A_{S,\varepsilon}^3 i_{in}) = (A_S^1 + x A_{S,\varepsilon}^3) (i_{in} + x u_{in,\varepsilon})
 \end{aligned} \tag{C.6}$$

8 App. C.3 Calibration with a $\lambda/4$ plate (QWP)

9 From Eq. (C.2) and Eq.(S.10.11.1) for the $\lambda/4$ -plate with retardation error ω as in Eq. (C.7) we
 10 get the general calibration signals Eq. (C.8) with an analyser vectors $\langle \mathbf{A} |$ from App. D and
 11 input Stokes vectors $|\mathbf{I}_{in}\rangle$ from App. E.

$$A_{QW} = 90^\circ + \omega \Rightarrow c_{QW} = -s_\omega, s_{QW} = c_\omega \tag{C.7}$$



$$\begin{aligned}
 \frac{I_S}{\eta_S T_{QW} I_{in}} &= \frac{\langle \mathbf{A}_S | \mathbf{M}_{QW}(x45^\circ + \varepsilon, \omega) | \mathbf{I}_{in} \rangle}{T_{QW} I_{in}} = \\
 &= \frac{\langle \mathbf{A}_S | \mathbf{R}(x45^\circ + \varepsilon) \mathbf{M}_{QW}(0, \omega) \mathbf{R}(-x45^\circ - \varepsilon) | \mathbf{I}_{in} \rangle}{T_{QW} I_{in}} = \\
 1 \quad &= \left\langle \begin{array}{c} A_S^1 \\ xA_{S,\varepsilon}^3 \\ -xA_{S,\varepsilon}^2 \\ A_S^4 \end{array} \left| \begin{array}{cccc} 1 & 0 & 0 & 0 \\ 0 & 1 & 0 & 0 \\ 0 & 0 & -s_\omega & c_\omega \\ 0 & 0 & c_\omega & -s_\omega \end{array} \right| \begin{array}{c} i_{in} \\ x u_{in,\varepsilon} \\ -x q_{in,\varepsilon} \\ v_{in} \end{array} \right\rangle = \\
 &= A_S^1 i_{in} + A_{S,\varepsilon}^3 u_{in,\varepsilon} - s_\omega (A_{S,\varepsilon}^2 q_{in,\varepsilon} + A_S^4 v_{in}) - x c_\omega (A_S^4 q_{in,\varepsilon} + A_{S,\varepsilon}^2 v_{in})
 \end{aligned} \tag{C.8}$$

$$\begin{aligned}
 \omega = 0 \Rightarrow \\
 2 \quad \frac{I_S}{\eta_S T_{QW} I_{in}} &= \frac{\langle \mathbf{A}_S | \mathbf{M}_{QW}(x45^\circ + \varepsilon, 0) | \mathbf{I}_{in} \rangle}{T_{QW} I_{in}} = A_S^1 i_{in} + A_{S,\varepsilon}^3 u_{in,\varepsilon} - x (A_S^4 q_{in,\varepsilon} + A_{S,\varepsilon}^2 v_{in}) = \\
 &= A_S^1 i_{in} - (s_{2\varepsilon} A_S^2 - c_{2\varepsilon} A_S^3) (s_{2\varepsilon} q_{in} - c_{2\varepsilon} u_{in}) - x [A_S^4 (c_{2\varepsilon} q_{in} + s_{2\varepsilon} u_{in}) + (c_{2\varepsilon} A_S^2 + s_{2\varepsilon} A_S^3) v_{in}]
 \end{aligned} \tag{C.9}$$

3 App. C.4 Calibration with a circular polariser (CP)

4 From Eq. (C.2) for a circular polariser composed of a linear polariser and a $\lambda/4$ -plate with
 5 retardation error ω as in Eq. (C.7) we get the general calibration signals Eq. (C.10) with
 6 analyser vectors $\langle \mathbf{A} |$ from App. D and input Stokes vectors $|\mathbf{I}_{in}\rangle$ from App. E. Note that $z =$
 7 ± 1 discerns between a right and left circular polariser, and $x = \pm 1$ between the $\pm 45^\circ$
 8 orientations of the whole circular polariser. With an ideal linear polariser this quite complex
 9 equation reduces to Eq. (C.11), with an ideal QWP without retardation error to Eq. (C.12), and
 10 to Eq. (C.13) with both constraints, i.e. for an ideal circular polariser. Since only the terms
 11 with an x in Eqs. (C.11) to (C.13) are compensated by means of the $\Delta 90$ -calibration, neither
 12 of the two constraints alone is sufficient to reduce the uncertainty.



$$\begin{aligned}
 \frac{I_S}{\eta_S T_{CP} I_{in}} &= \frac{\langle \mathbf{A}_S | \mathbf{M}_{CP}(z, x45^\circ + \varepsilon) | \mathbf{I}_{in} \rangle}{T_{CP} I_{in}} = \\
 &= \frac{\langle \mathbf{A}_S \mathbf{R}(x45^\circ + \varepsilon) | \mathbf{M}_{QW}(z45^\circ, \omega) \mathbf{M}_P | \mathbf{R}(-x45^\circ - \varepsilon) \mathbf{I}_{in} \rangle}{T_{QW} T_P I_{in}} = \\
 1 \quad &= \left\langle \begin{matrix} A_S^1 \\ xA_{S,\varepsilon}^3 \\ -xA_{S,\varepsilon}^2 \\ A_S^4 \end{matrix} \begin{matrix} \begin{pmatrix} 1 & 0 & 0 & 0 \\ 0 & -s_\omega & 0 & -zc_\omega \\ 0 & 0 & 1 & 0 \\ 0 & zc_\omega & 0 & -s_\omega \end{pmatrix} \begin{pmatrix} 1 & D_P & 0 & 0 \\ D_P & 1 & 0 & 0 \\ 0 & 0 & Z_P c_P & Z_P s_P \\ 0 & 0 & -Z_P s_P & Z_P c_P \end{pmatrix} \begin{matrix} i_{in} \\ xu_{in,\varepsilon} \\ -xq_{in,\varepsilon} \\ v_{in} \end{matrix} \end{matrix} \right\rangle = \quad (C.10) \\
 &= \left\{ \begin{matrix} (A_S^1 + A_S^4 zc_\omega D_P) i_{in} + (A_S^2 Z_P c_P - zA_{S,\varepsilon}^3 c_\omega Z_P s_P) q_{in,\varepsilon} - A_{S,\varepsilon}^3 s_\omega u_{in,\varepsilon} - A_S^4 s_\omega Z_P c_P v_{in} + \\ + x \left[\begin{matrix} -A_{S,\varepsilon}^3 s_\omega D_P i_{in} - A_S^4 s_\omega Z_P s_P q_{in,\varepsilon} + \\ (A_S^1 D_P + A_S^4 zc_\omega) u_{in,\varepsilon} - (A_{S,\varepsilon}^2 s_P + A_{S,\varepsilon}^3 zc_\omega c_P) Z_P v_{in} \end{matrix} \right] \end{matrix} \right\}
 \end{aligned}$$

2 From Eq.(C.10) we get with different conditions:

$$\begin{aligned}
 D_P = 1, Z_P = 0 &\Rightarrow \\
 3 \quad \frac{I_S}{\eta_S T_{CP} I_{in}} &= (A_S^1 + zc_\omega A_S^4 - s_\omega xA_{S,\varepsilon}^3) (i_{in} + xu_{in,\varepsilon}) \quad (C.11)
 \end{aligned}$$

$$\begin{aligned}
 \omega = 0 &\Rightarrow \\
 4 \quad \frac{I_S}{\eta_S T_{CP} I_{in}} &= \left\{ \begin{matrix} (A_S^1 + A_S^4 zD_P) i_{in} + (A_{S,\varepsilon}^2 Z_P c_P - zA_{S,\varepsilon}^3 Z_P s_P) q_{in,\varepsilon} \\ + x \left[(A_S^1 D_P + zA_S^4) u_{in,\varepsilon} - (A_{S,\varepsilon}^2 s_P + zA_{S,\varepsilon}^3 c_P) Z_P v_{in} \right] \end{matrix} \right\} \quad (C.12)
 \end{aligned}$$

$$\begin{aligned}
 \omega = 0, D_P = 1, Z_P = 0 &\Rightarrow \\
 5 \quad \frac{I_S}{\eta_S T_{CP} I_{in}} &= (A_S^1 + zA_S^4) (i_{in} - xu_{in,\varepsilon}) \quad (C.13)
 \end{aligned}$$

6 App. D The analyser row vector $\langle \mathbf{A}_S |$

7 The general formulation for the Stokes vector of a standard lidar signal \mathbf{I}_S at the detector in the
 8 reflected channel, \mathbf{I}_R , and transmitted channel, \mathbf{I}_T , is

$$9 \quad \mathbf{I}_S = \eta_S \mathbf{M}_S \mathbf{R}_y \mathbf{M}_O(\gamma) \mathbf{F}(a) \mathbf{M}_E(\beta) \mathbf{I}_L \quad (D.1)$$

10 Only the first Stokes parameter is directly measured, and therefore we can reduce the
 11 complexity of the full matrix equations to an inner product between the analyser row vector
 12 $\langle \mathbf{A}_S |$ and the input Stokes column vector \mathbf{I}_{in} similar to Kaul et al. (1992); Volkov et al. (2015)

$$13 \quad I_S = \langle \mathbf{A}_S | \mathbf{I}_{in} \rangle \quad (D.2)$$

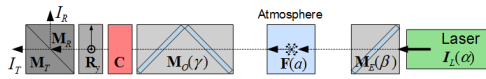


- 1 In case of a calibration measurement, we place a calibrator with matrix \mathbf{C} between the input
 2 Stokes vector and the analyser vector

$$3 \quad I_S = \langle \mathbf{A}_S | \mathbf{C} | \mathbf{I}_{in} \rangle \quad (D.3)$$

- 4 As calibrators we use a mechanical rotator, a rotation of the plane of polarisation by means of
 5 a $\lambda/2$ plate, a linear polariser, a $\lambda/4$ plate, and a circular polariser. We can place the calibrator
 6 anywhere in the optical setup, with different results. In the following we develop the general
 7 expressions of the analyser vector in App. D and of the input Stokes vector in App. E for the
 8 different setups.

9 **App. D.1 $\langle \mathbf{A}_S |$ with \mathbf{C} before the polarising beam-splitter**



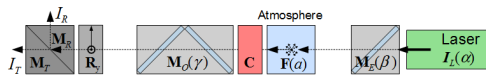
$$10 \quad I_S = \eta_S \mathbf{M}_S \mathbf{R}_y \mathbf{C} \mathbf{M}_O \mathbf{F} I_E \Rightarrow \mathbf{A}_S = \mathbf{M}_S \mathbf{R}_y \quad (D.4)$$

- 11 The analyser part consists of a polarising beam-splitter \mathbf{M}_S and an optional 90° rotation of the
 12 detector setup \mathbf{R}_y (see Eq.(47))

$$\begin{aligned} \frac{\langle \mathbf{A}_S |}{T_S} &= \frac{\langle \mathbf{M}_S \mathbf{R}_y |}{T_S} = \\ &= \left\langle \begin{pmatrix} 1 & D_S & 0 & 0 \\ D_S & 1 & 0 & 0 \\ 0 & 0 & Z_S c_S & Z_S s_S \\ 0 & 0 & -Z_S s_S & Z_S c_S \end{pmatrix} \begin{pmatrix} 1 & 0 & 0 & 0 \\ 0 & y & 0 & 0 \\ 0 & 0 & y & 0 \\ 0 & 0 & 0 & 1 \end{pmatrix} \right\rangle = \left\langle \begin{pmatrix} 1 & y D_S & 0 & 0 \\ D_S & y & 0 & 0 \\ 0 & 0 & y Z_S c_S & Z_S s_S \\ 0 & 0 & -y Z_S s_S & Z_S c_S \end{pmatrix} \right\rangle = \left\langle \begin{pmatrix} 1 \\ y D_S \\ 0 \\ 0 \end{pmatrix} \right\rangle \end{aligned}$$

$$13 \quad (D.5)$$

14 **App. D.2 $\langle \mathbf{A}_S |$ with \mathbf{C} before the receiving optics**



$$15 \quad I_S = \eta_S \mathbf{M}_S \mathbf{R}_y \mathbf{M}_O \mathbf{C} \mathbf{F} I_E \Rightarrow \mathbf{A}_S = \mathbf{M}_S \mathbf{R}_y \mathbf{M}_O \quad (D.6)$$

- 16 Using Eq. D.5 we get



$$\begin{aligned}
 & \frac{\langle \mathbf{A}_S(y, \gamma) \rangle}{T_O T_S} = \frac{\langle \mathbf{M}_S \mathbf{R}_y | \mathbf{M}_O(\gamma) \rangle}{T_O T_S} = \\
 1 \quad & = \left\langle y D_S \begin{pmatrix} 1 & c_{2\gamma} D_O & s_{2\gamma} D_O & 0 \\ c_{2\gamma} D_O & 1 - s_{2\gamma}^2 W_O & s_{2\gamma} c_{2\gamma} W_O & -s_{2\gamma} Z_O S_O \\ 0 & s_{2\gamma} D_O & s_{2\gamma} c_{2\gamma} W_O & 1 - c_{2\gamma}^2 W_O \\ 0 & 0 & s_{2\gamma} Z_O S_O & -c_{2\gamma} Z_O S_O \\ & & & Z_O c_O \end{pmatrix} \right\rangle = \left\langle \begin{pmatrix} 1 + y c_{2\gamma} D_O D_S \\ c_{2\gamma} D_O + y D_S (1 - s_{2\gamma}^2 W_O) \\ s_{2\gamma} (D_O + y c_{2\gamma} D_S W_O) \\ -y s_{2\gamma} D_S Z_O S_O \end{pmatrix} \right\rangle \quad (D.7)
 \end{aligned}$$

2 Simplifications: A rotation γ of a retarding diattenuator \mathbf{M}_O between the calibrator and the
 3 polarising beam-splitter \mathbf{M}_S complicates the equations considerably. In case \mathbf{M}_O is not rotated
 4 ($\gamma = 0$), the matrices \mathbf{M}_S , the optional 90° rotation \mathbf{R}_y , and \mathbf{M}_O and can be combined to a new
 5 polarising beam-splitter module \mathbf{M}_{SyO} according to S.10.10, and all equations developed for
 6 the Sect. 7.1 case can be applied in Sect. 7.2. For $\gamma = 0^\circ$ Eq. (D.7) becomes

$$\begin{aligned}
 & \gamma = 0^\circ \Rightarrow \\
 7 \quad & \langle \mathbf{A}_S | (y, 0^\circ) \rangle = \langle \mathbf{M}_S \mathbf{R}_y | \mathbf{M}_O(0^\circ) \rangle = T_O T_S \langle 1 + y D_S D_O \quad D_O + y D_S \quad 0 \quad 0 \rangle = \\
 & = \langle \mathbf{M}_{SyO}(0^\circ) \rangle = T_{SyO} \langle 1 \quad D_{SyO} \quad 0 \quad 0 \rangle \quad (D.8)
 \end{aligned}$$

$$8 \quad \text{with } T_{SyO} = T_O T_S (1 + y D_S D_O) \text{ and } D_{SyO} = \frac{D_O + y D_S}{1 + y D_S D_O} \quad (D.9)$$

9 With a cleaned analyser we get from Eq. (D.9)

$$\begin{aligned}
 & D_R = -1, D_T = +1 \Rightarrow \\
 10 \quad & D_{SyO} = y D_S, \quad D_{RyO} = -y, \quad D_{TyO} = +y \\
 & T_{RyO} = T_O T_R (1 - y D_O), \quad T_{TyO} = T_O T_T (1 + y D_O) \quad (D.10)
 \end{aligned}$$

11 and explicitly with Eqs. (S.10.10.11) and (S.10.10.14)

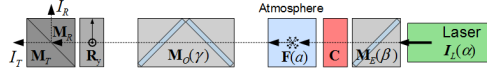
$$\begin{aligned}
 & D_R = -1, D_T = +1, y = +1 \Rightarrow \\
 & T_{R+O} = T_O T_R (1 - D_O) = 0.5 T_R^S k_1 T_O^S, \quad D_{R+O} = -1 \\
 & T_{T+O} = T_O T_T (1 + D_O) = 0.5 T_T^P k_1 T_O^P, \quad D_{T+O} = +1 \\
 12 \quad & D_R = -1, D_T = +1, y = -1 \Rightarrow \\
 & T_{R-O} = T_O T_R (1 + D_O) = 0.5 T_R^S k_1 T_O^P, \quad D_{R-O} = +1 \\
 & T_{T-O} = T_O T_T (1 - D_O) = 0.5 T_T^P k_1 T_O^S, \quad D_{T-O} = -1 \quad (D.11)
 \end{aligned}$$

13 See also S.10.10 and S.6 .

14 Only few special cases with rotated \mathbf{M}_O ($\gamma \neq 0$) (see Eq. (S.5.1.4)) are discussed additionally.



1 **App. D.3** $\langle \mathbf{A}_S |$ with **C** behind the emitter optics



2 $\mathbf{I}_S = \eta_S \mathbf{M}_S \mathbf{R}_y \mathbf{M}_O \mathbf{F} \mathbf{C} \mathbf{I}_E \Rightarrow \mathbf{A}_S = \mathbf{M}_S \mathbf{R}_y \mathbf{M}_O \mathbf{F} \mathbf{C}$ and $\mathbf{I}_{in} = \mathbf{I}_E$ (D.12)

3 The additional effect of the atmospheric depolarisation, $\mathbf{F}(a)$, on the analyser Eq. (D.7) is

4
$$\frac{\langle \mathbf{A}_S |}{T_O T_S F_{11}} = \frac{\langle \mathbf{M}_S \mathbf{R}_y \mathbf{M}_O(\gamma) | \mathbf{F}(a)}{T_O T_S F_{11}} = \left\langle \begin{array}{c} 1 + y c_{2\gamma} D_S D_O \\ c_{2\gamma} D_O + y D_S (1 - s_{2\gamma}^2 W_O) \\ s_{2\gamma} (D_O + y c_{2\gamma} D_S W_O) \\ -y s_{2\gamma} D_S Z_O S_O \end{array} \right| \left(\begin{array}{cccc} 1 & 0 & 0 & 0 \\ 0 & a & 0 & 0 \\ 0 & 0 & -a & 0 \\ 0 & 0 & 0 & 1 - 2a \end{array} \right) = \left\langle \begin{array}{c} 1 + y c_{2\gamma} D_S D_O \\ a [c_{2\gamma} D_O + y D_S (1 - s_{2\gamma}^2 W_O)] \\ -a s_{2\gamma} (D_O + y c_{2\gamma} D_S W_O) \\ -(1 - 2a) y s_{2\gamma} D_S Z_O S_O \end{array} \right|$$
 (D.13)

5 Without receiver optics rotation \mathbf{M}_O ($\gamma = 0^\circ$) we get with Eq. (D.8) ff.

6 $\langle \mathbf{A}_S | = \langle \mathbf{M}_{SyO}(0^\circ) | \mathbf{F}(a) = T_{SyO} \langle 1 \ a D_{SyO} \ 0 \ 0 |$ (D.14)

7 **App. E** The input Stokes vector \mathbf{I}_{in}

8 The formulation for the most general input Stokes vector \mathbf{I}_{in} into the analyser part \mathbf{A}_S is

9 $\mathbf{I}_{in}(\gamma, a, \beta) = \mathbf{M}_O(\gamma) \mathbf{F}(a) \mathbf{M}_E(\beta) \mathbf{I}_L$ (E.1)

10 and assuming a rotated, partly linear polarised laser with polarisation parameter a_L

11 $\mathbf{I}_{in}(\gamma, a, \beta, \alpha, a_L) = \mathbf{M}_O(\gamma) \mathbf{F}(a) \mathbf{M}_E(\beta) \mathbf{I}_L(\alpha, a_L)$ (E.2)

12 In the ideal case the laser has no depolarisation ($a_L = 1$) and is horizontal linearly polarised
 13 (see Eq. (E.6)), and the optical elements are not rotated, which results in Eq.(E.3):

14 $a_L = 1, i_L = q_L = 1, u_L = v_L = 0, \alpha = \beta = \gamma = 0 \Rightarrow$
 $\mathbf{I}_{in}(0, 0, 0, 0, 1) = T_O F_{11} T_E I_L (1 + D_E) | 1 + a D_O \ D_O + a \ 0 \ 0 \rangle$ (E.3)

15 **App. E.1** Laser \mathbf{I}_L

16 We start with the Stokes vector for the laser beam with arbitrary state of polarisation and
 17 additionally rotated by angle α around the optical axis (see Eq. S.5.1.1)



$$1 \quad \mathbf{I}_L(\alpha) = I_L \begin{pmatrix} i_{L,\alpha} \\ q_{L,\alpha} \\ u_{L,\alpha} \\ v_{L,\alpha} \end{pmatrix} = \begin{pmatrix} 1 & 0 & 0 & 0 \\ 0 & c_{2\alpha} & -s_{2\alpha} & 0 \\ 0 & s_{2\alpha} & c_{2\alpha} & 0 \\ 0 & 0 & 0 & 1 \end{pmatrix} I_L \begin{pmatrix} i_L \\ q_L \\ u_L \\ v_L \end{pmatrix} = I_L \begin{pmatrix} i_L \\ c_{2\alpha}q_L - s_{2\alpha}u_L \\ s_{2\alpha}q_L + c_{2\alpha}u_L \\ v_L \end{pmatrix} \quad (\text{E.4})$$

2 The total, linear, and circular degree of polarisation (DOP, DLP, and DCP, respectively) don't
 3 change with such a rotation.

4 • We get for a rotated, horizontal-linear polarised laser

$$5 \quad \mathbf{I}_L(\alpha) = I_L |1 \quad c_{2\alpha} \quad s_{2\alpha} \quad 0\rangle \quad (\text{E.5})$$

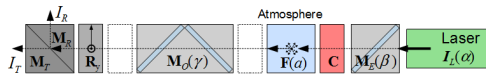
6 • for a horizontal-linear polarised laser

$$7 \quad \mathbf{I}_L(0) = I_L |1 \quad 1 \quad 0 \quad 0\rangle \quad (\text{E.6})$$

8 • and for a rotated, linearly polarised laser with polarisation parameter a_L with $\delta_L = (1-a_L)/$
 9 $(1+a_L)$

$$10 \quad \mathbf{I}_L(\alpha, a_L) = \begin{pmatrix} 1 & 0 & 0 & 0 \\ 0 & c_{2\alpha} & -s_{2\alpha} & 0 \\ 0 & s_{2\alpha} & c_{2\alpha} & 0 \\ 0 & 0 & 0 & 1 \end{pmatrix} I_L \begin{pmatrix} 1 \\ a_L \\ 0 \\ 0 \end{pmatrix} = I_L \begin{pmatrix} 1 \\ c_{2\alpha}a_L \\ s_{2\alpha}a_L \\ 0 \end{pmatrix} \quad (\text{E.7})$$

11 App. E.2 I_{in} with C behind the emitter optics



$$12 \quad \frac{\mathbf{I}_{in}(\beta, \alpha)}{T_E I_L} = \frac{\mathbf{I}_E(\beta, \alpha)}{T_E I_L} = \frac{\mathbf{M}_E(\beta) \mathbf{I}_L(\alpha)}{T_E I_L} = \quad (\text{E.8})$$

$$= |i_{in} \quad q_{in} \quad u_{in} \quad v_{in}\rangle = |i_E \quad q_E \quad u_E \quad v_E\rangle = \frac{\mathbf{M}_E(\beta)}{T_E} |i_L \quad q_L \quad u_L \quad v_L\rangle$$

13 Eq. (E.8) with input I_L from a rotated, linearly polarised laser Eq. (E.4) and with rotated
 14 emitter optics Eq. (S.10.4.1) results in Eq. (E.9).



$$\begin{aligned}
 \frac{\mathbf{I}_{in}(\beta, \alpha)}{T_E I_L} &= \frac{\mathbf{I}_E(\beta, \alpha)}{T_E I_L} = \frac{\mathbf{M}_E(\beta) | \mathbf{I}_L(\alpha) \rangle}{T_E I_L} = | i_E \quad q_E \quad u_E \quad v_E \rangle = \\
 &= \left(\begin{array}{cccc} 1 & c_{2\beta} D_E & s_{2\beta} D_E & 0 \\ c_{2\beta} D_E & 1 - s_{2\beta}^2 W_E & s_{2\beta} c_{2\beta} W_E & -s_{2\beta} Z_E S_E \\ s_{2\beta} D_E & s_{2\beta} c_{2\beta} W_E & 1 - c_{2\beta}^2 W_E & c_{2\beta} Z_E S_E \\ 0 & s_{2\beta} Z_E S_E & -c_{2\beta} Z_E S_E & Z_E c_E \end{array} \right) \left(\begin{array}{c} i_L \\ c_{2\alpha} q_L - s_{2\alpha} u_L \\ s_{2\alpha} q_L + c_{2\alpha} u_L \\ v_L \end{array} \right) = \\
 &= \left(\begin{array}{c} i_L + D_E (c_{2\alpha-2\beta} q_L - s_{2\alpha-2\beta} u_L) \\ c_{2\beta} D_E i_L + (c_{2\alpha} q_L - s_{2\alpha} u_L) + s_{2\beta} [W_E (s_{2\alpha-2\beta} q_L + c_{2\alpha-2\beta} u_L) - Z_E S_E v_L] \\ s_{2\beta} D_E i_L + (s_{2\alpha} q_L + c_{2\alpha} u_L) - c_{2\beta} [W_E (s_{2\alpha-2\beta} q_L + c_{2\alpha-2\beta} u_L) - Z_E S_E v_L] \\ -Z_E S_E (s_{2\alpha-2\beta} q_L + c_{2\alpha-2\beta} u_L) + Z_E c_E v_L \end{array} \right) \quad (E.9)
 \end{aligned}$$

- 2 • Special cases: Eq. (E.9) without rotation of the emitter optics with respect to the plane of
 3 polarisation of the laser

$$\begin{aligned}
 \alpha = \beta \Rightarrow \\
 \frac{\mathbf{I}_{in}(\alpha, \alpha)}{T_E I_L} &= \frac{\mathbf{I}_E(\alpha, \alpha)}{T_E I_L} = \left(\begin{array}{c} i_E \\ q_E \\ u_E \\ v_E \end{array} \right) = \left(\begin{array}{c} i_L + D_E q_L \\ c_{2\alpha} D_E i_L + (c_{2\alpha} q_L - s_{2\alpha} u_L) + s_{2\alpha} [W_E u_L - Z_E S_E v_L] \\ s_{2\alpha} D_E i_L + (s_{2\alpha} q_L + c_{2\alpha} u_L) - c_{2\alpha} [W_E u_L - Z_E S_E v_L] \\ -Z_E S_E u_L + Z_E c_E v_L \end{array} \right) = \\
 &= \left(\begin{array}{c} i_L + D_E q_L \\ c_{2\alpha} (D_E i_L + q_L) - s_{2\alpha} Z_E (c_E u_L + s_E v_L) \\ s_{2\alpha} (D_E i_L + q_L) + c_{2\alpha} Z_E (c_E u_L + s_E v_L) \\ -Z_E (s_E u_L - c_E v_L) \end{array} \right) \quad (E.10)
 \end{aligned}$$

- 5 • Eq. (E.9) without laser and emitter optics rotation

$$\begin{aligned}
 \alpha = \beta = 0 \Rightarrow \\
 \frac{\mathbf{I}_{in}(0, 0)}{T_E I_L} &= \frac{\mathbf{I}_E(0, 0)}{T_E I_L} = \frac{\mathbf{M}_E(0) | \mathbf{I}_L(0) \rangle}{T_E I_L} = \left(\begin{array}{c} i_E \\ q_E \\ u_E \\ v_E \end{array} \right) = \left(\begin{array}{c} i_L + D_E q_L \\ D_E i_L + q_L \\ Z_E (c_E u_L + s_E v_L) \\ Z_E (-s_E u_L + c_E v_L) \end{array} \right) \quad (E.11)
 \end{aligned}$$

- 7 • Eq. (E.9) with rotated, horizontal-linearly polarised laser with rotated emitter optics



$$\begin{aligned}
 & \mathbf{I}_L = I_L |1 \ 1 \ 0 \ 0\rangle \Rightarrow \\
 1 \quad & \frac{\mathbf{I}_{in}(\beta, \alpha)}{T_E I_L} = \frac{\mathbf{I}_E(\beta, \alpha)}{T_E I_L} = \frac{\mathbf{M}_E(\beta) | \mathbf{I}_L(\alpha) \rangle}{T_E I_L} = \begin{pmatrix} i_E \\ q_E \\ u_E \\ v_E \end{pmatrix} = \begin{pmatrix} 1 + D_E c_{2\alpha-2\beta} \\ c_{2\alpha} + c_{2\beta} D_E + s_{2\beta} W_E s_{2\alpha-2\beta} \\ s_{2\alpha} + s_{2\beta} D_E - c_{2\beta} W_E s_{2\alpha-2\beta} \\ -Z_E S_E s_{2\alpha-2\beta} \end{pmatrix} \quad (E.12)
 \end{aligned}$$

2 • Eq. (E.9) with rotated, linearly polarised laser without emitter optics rotation

$$\begin{aligned}
 & \alpha = \beta \wedge \mathbf{I}_L = I_L |1 \ 1 \ 0 \ 0\rangle \Rightarrow \\
 3 \quad & \frac{\mathbf{I}_{in}(\alpha, \alpha)}{T_E I_L} = |i_E \ q_E \ u_E \ v_E\rangle = (1 + D_E) |1 \ c_{2\alpha} \ s_{2\alpha} \ 0\rangle \quad (E.13)
 \end{aligned}$$

4 • Rotated, elliptically polarised light behind the emitter optics with.

$$5 \quad \mathbf{I}_{in} = \mathbf{I}_E = T_E I_L |i_E \ q_E \ u_E \ v_E\rangle = T_E I_L |1 \ b c_{2\alpha} \ b s_{2\alpha} \ v_E\rangle \quad (E.14)$$

6 with the degree of polarisation $DOP_E = 1$ and the degree of linear polarisation $DOLP_E = b$

$$7 \quad DOP_E = \sqrt{q_E^2 + u_E^2 + v_E^2} = \sqrt{b^2 + v_E^2} = 1 \Rightarrow v_E = \sqrt{1 - b^2} \quad (E.15)$$

$$8 \quad \mathbf{I}_{in} = \mathbf{I}_E = T_E I_L |i_E \ q_E \ u_E \ v_E\rangle = T_E I_L |1 \ b c_{2\alpha} \ b s_{2\alpha} \ \sqrt{1 - b^2}\rangle \quad (E.16)$$

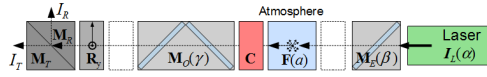
9 • Rotated, linearly polarised laser with linear polarisation parameter a_L with rotated emitter
 10 optics: Laser Stokes vector Eq.(E.7) and rotated diattenuator Eq.(S.10.4.1)

$$\begin{aligned}
 & \mathbf{I}_L = I_L |1 \ c_{2\alpha} a_L \ s_{2\alpha} a_L \ 0\rangle \Rightarrow \\
 & \frac{\mathbf{I}_{in}}{T_E I_L} = \frac{\mathbf{I}_E}{T_E I_L} = \frac{\mathbf{M}_E(\beta) | \mathbf{I}_L(\alpha, a_L) \rangle}{T_E I_L} = |i_E \ q_E \ u_E \ v_E\rangle = \\
 & = \begin{pmatrix} 1 & c_{2\beta} D_E & s_{2\beta} D_E & 0 \\ c_{2\beta} D_E & 1 - s_{2\beta}^2 W_E & s_{2\beta} c_{2\beta} W_E & -s_{2\beta} Z_E S_E \\ s_{2\beta} D_E & s_{2\beta} c_{2\beta} W_E & 1 - c_{2\beta}^2 W_E & c_{2\beta} Z_E S_E \\ 0 & s_{2\beta} Z_E S_E & -c_{2\beta} Z_E S_E & Z_E c_E \end{pmatrix} \begin{pmatrix} 1 \\ c_{2\alpha} a_L \\ s_{2\alpha} a_L \\ 0 \end{pmatrix} = \begin{pmatrix} 1 + a_L D_E c_{2\alpha-2\beta} \\ c_{2\beta} D_E + a_L (c_{2\alpha} + s_{2\beta} W_E s_{2\alpha-2\beta}) \\ s_{2\beta} D_E + a_L (s_{2\alpha} - c_{2\beta} W_E s_{2\alpha-2\beta}) \\ -a_L Z_E S_E s_{2\alpha-2\beta} \end{pmatrix} \quad (E.17)
 \end{aligned}$$

11



1 **App. E.3 I_{in} with C before the receiver optics**



2 General input Stokes I_{in} vector with atmospheric backscatter.

3
$$I_S = \eta_S M_S R_y M_O C F I_E \Rightarrow I_{in} = F I_E \quad (E.18)$$

4 With atmospheric depolarisation from Eq. (S.3.1) and an emitter beam I_E from App. E.2:

5
$$I_{in}(a) = |F(a)I_E\rangle = F_{11}T_E I_L |i_E \quad aq_E \quad -au_E \quad (1-2a)v_E\rangle \quad (E.19)$$

6 • Special cases: Eq. (E.19) becomes Eq. (E.20) with a rotated linearly polarised laser with

7 linear polarisation parameter a_L , with rotated emitter optics, and atmospheric backscatter, i.e.

8 Eq. (E.17). Note, that without laser depolarisation $a_L = 1$.

9
$$\frac{I_{in}(a, \beta, \alpha, a_L)}{F_{11}T_E I_L} = \frac{F(a) |M_E(\beta) I_L(\alpha, a_L)\rangle}{F_{11}T_E I_L} = \begin{matrix} \left\langle \begin{matrix} i_{in} \\ q_{in} \\ u_{in} \\ v_{in} \end{matrix} \right\rangle = \left\langle \begin{matrix} i_E \\ aq_E \\ -au_E \\ (1-2a)v_E \end{matrix} \right\rangle = \left\langle \begin{matrix} 1 + a_L D_E c_{2\alpha-2\beta} \\ a [c_{2\beta} D_E + a_L (c_{2\alpha} + s_{2\beta} W_E s_{2\alpha-2\beta})] \\ -a [s_{2\beta} D_E + a_L (s_{2\alpha} - c_{2\beta} W_E s_{2\alpha-2\beta})] \\ -(1-2a) a_L Z_E s_E s_{2\alpha-2\beta} \end{matrix} \right\rangle \end{matrix} \quad (E.20)$$

10 • Eq. (E.20) without rotation errors becomes Eq. (E.21), and additionally without laser
 11 depolarisation, i.e. $a_L = 1$, Eq. (E.22).

12
$$\alpha = \beta = 0 \Rightarrow \frac{I_{in}(a, 0, 0, a_L)}{F_{11}T_E I_L} = \frac{F(a) |M_E(0) I_L(0, a_L)\rangle}{F_{11}T_E I_L} = |1 + a_L D_E \quad aD_E + aa_L \quad 0 \quad 0\rangle \quad (E.21)$$

13
$$I_{in}(a, 0, 0, 0) = F_{11}T_E I_L (1 + D_E) |1 \quad a \quad 0 \quad 0\rangle \quad (E.22)$$

14 • Eq. (E.20) without emitter optics becomes Eq. (E.23).

15
$$[D_E = 0 \Rightarrow Z_E = 1, s_E = 0 \Rightarrow c_E = 1 \Rightarrow W_E = 0] \Rightarrow \frac{I_{in}(a, \alpha, a_L)}{F_{11}I_L} = \frac{F(a) |I_L(\alpha, a_L)\rangle}{F_{11}I_L} = |1 \quad aa_L c_{2\alpha} \quad -aa_L s_{2\alpha} \quad 0\rangle \quad (E.23)$$



1 Note it is impossible to combine $a' = aa_L$ if emitter optics \mathbf{M}_E with diattenuation parameter D_E
 2 $\neq 0$ or retardation (i.e. $Z_E \neq 0$ and $s_E \neq 0$) are between the laser and the atmosphere \mathbf{F} , even if
 3 there are no angular misalignments α and β in the emitter, which means that the atmospheric
 4 depolarisation cannot be retrieved without detailed knowledge of the emitter optics
 5 parameters and alignment errors.

6 • Eq. (E.20) without emitter optics \mathbf{M}_E and without laser depolarisation becomes Eq. (E.24).

$$a_L = 1, [D_E = 0 \Rightarrow Z_E = 1, s_E = 0 \Rightarrow c_E = 1 \Rightarrow W_E = 0] \Rightarrow$$

$$7 \frac{I_{in}(a, \alpha)}{I_{in}} = \frac{\mathbf{F}(a) |I_L(\alpha)\rangle}{F_{11} I_L} = |1 \quad ac_{2\alpha} \quad -as_{2\alpha} \quad 0\rangle \quad (E.24)$$

8 • Eq. (E.19) with I_E from Eq. (E.14), i.e. with rotated, elliptically polarised light behind the
 9 emitter optics

$$10 \frac{I_{in}(a, b, \alpha)}{I_{in}} = \frac{\mathbf{F}(a) I_E}{F_{11} T_E I_L} = |i_E \quad aq_E \quad -au_E \quad (1-2a)v_E\rangle =$$

$$= |1 \quad abc_{2\alpha} \quad -abs_{2\alpha} \quad (1-2a)\sqrt{1-b^2}\rangle \quad (E.25)$$

11 • Including the calibrator rotation $R(\varepsilon)$ in I_{in} in Eq. (E.19) with Eq. (S.10.15.1) gives Eq.
 12 (E.26), and with elliptically polarise laser of Eq. (E.16) we get Eq. (E.27), which results
 13 without emitter optics and horizontal-linear polarised laser light ($b = 1$) in Eq. (E.28).

$$14 \frac{I_{in, \varepsilon}(\varepsilon, h, a)}{I_{in}} = \frac{|\mathbf{R}(\varepsilon) \mathbf{M}_h \mathbf{F}(a) I_E\rangle}{T_{rot} F_{11} T_E I_L} =$$

$$= \left| \begin{array}{c} i_{in, \varepsilon} \\ q_{in, \varepsilon} \\ u_{in, \varepsilon} \\ v_{in, \varepsilon} \end{array} \right\rangle = \left(\begin{array}{cccc} 1 & 0 & 0 & 0 \\ 0 & c_{2\varepsilon} & -hs_{2\varepsilon} & 0 \\ 0 & s_{2\varepsilon} & hc_{2\varepsilon} & 0 \\ 0 & 0 & 0 & h \end{array} \right) \left| \begin{array}{c} i_E \\ aq_E \\ -au_E \\ (1-2a)v_E \end{array} \right\rangle = \left| \begin{array}{c} i_E \\ a(q_E c_{2\varepsilon} + hu_E s_{2\varepsilon}) \\ a(q_E s_{2\varepsilon} - hu_E c_{2\varepsilon}) \\ (1-2a)hv_E \end{array} \right\rangle \quad (E.26)$$

$$I_E = T_E I_L |i_E \quad q_E \quad u_E \quad v_E\rangle = T_E I_L |1 \quad bc_{2\alpha} \quad bs_{2\alpha} \quad \sqrt{1-b^2}\rangle \Rightarrow$$

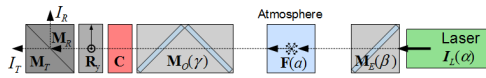
$$15 \frac{I_{in, \varepsilon}(\varepsilon, h, a, \alpha, b)}{I_{in}} = \frac{|\mathbf{R}(\varepsilon) \mathbf{M}_h \mathbf{F}(a) I_E(\alpha, b)\rangle}{T_{rot} F_{11} T_E I_L} =$$

$$= |i_{in, \varepsilon} \quad q_{in, \varepsilon} \quad u_{in, \varepsilon} \quad v_{in, \varepsilon}\rangle = |1 \quad abc_{2\varepsilon-h2\alpha} \quad abs_{2\varepsilon+h2\alpha} \quad (1-2a)h\sqrt{1-b^2}\rangle \quad (E.27)$$



$$\begin{aligned}
 \mathbf{M}_E &= \text{identity}, b = 1 \Rightarrow \\
 1 \quad \frac{\mathbf{I}_{in,\varepsilon}(\varepsilon, h, a, \alpha, b)}{I_{in}} &= \frac{|\mathbf{R}(\varepsilon)\mathbf{M}_R\mathbf{F}(a)\mathbf{I}_L(\alpha, b)\rangle}{T_{rot}F_{11}I_L} = \\
 &= |i_{in,\varepsilon} \quad q_{in,\varepsilon} \quad u_{in,\varepsilon} \quad v_{in,\varepsilon}\rangle = |1 \quad ac_{2\varepsilon-h2\alpha} \quad as_{2\varepsilon+h2\alpha} \quad 0\rangle
 \end{aligned} \tag{E.28}$$

2 App. E.4 I_{in} with C before the polarising beam-splitter



3 General input vector I_{in} with atmospheric backscatter and emitter and receiver optics.

$$4 \quad I_S = \eta_S \mathbf{M}_S \mathbf{R}_y \mathbf{C} \mathbf{M}_O \mathbf{F} \mathbf{M}_E I_L \Rightarrow I_{in} = \mathbf{M}_O \mathbf{F} I_E \tag{E.29}$$

5 The most complex case for the input Stokes vector I_{in} is, if the calibrator is placed before the
 6 polarising beam-splitter, because here we have to multiply several matrices. All other cases
 7 can be derived from this case by neglecting the appropriate parameters (see App. D). The
 8 emitted beam Stokes vector I_E from App. E.2 has to be multiplied with the atmospheric
 9 backscatter matrix \mathbf{F} (Eq. (S.3.1)) and the receiver optics matrix \mathbf{M}_O , the latter expressed as a
 10 rotated diattenuator (see Eq. (E.32)). In general the emitter optics and the laser polarisation I_L
 11 are rotated as in Eq. (E.30), which is not mentioned explicitly when needless.

$$12 \quad I_E(\beta, \alpha) = \mathbf{M}_E(\beta) |I_L(\alpha)\rangle = T_E I_L |i_E(\beta, \alpha) \quad q_E(\beta, \alpha) \quad u_E(\beta, \alpha) \quad v_E(\beta, \alpha)\rangle \tag{E.30}$$

$$\begin{aligned}
 13 \quad \frac{I_{in}(\gamma, a, \varepsilon)}{T_{in} I_L} &= \frac{\mathbf{M}_O(\gamma) |F(a)\mathbf{M}_E I_L\rangle}{T_O F_{11} T_E I_L} = \frac{\mathbf{M}_O(\gamma) |F(a)I_E\rangle}{T_O F_{11} T_E I_L} = |i_{in} \quad q_{in} \quad u_{in} \quad v_{in}\rangle = \\
 &= \left(\begin{array}{cccc} 1 & c_{2\gamma} D_O & s_{2\gamma} D_O & 0 \\ c_{2\gamma} D_O & 1 - s_{2\gamma}^2 W_O & s_{2\gamma} c_{2\gamma} W_O & -s_{2\gamma} Z_O S_O \\ s_{2\gamma} D_O & s_{2\gamma} c_{2\gamma} W_O & 1 - c_{2\gamma}^2 W_O & c_{2\gamma} Z_O S_O \\ 0 & s_{2\gamma} Z_O S_O & -c_{2\gamma} Z_O S_O & Z_O c_O \end{array} \right) \left(\begin{array}{c} i_E \\ a q_E \\ -a u_E \\ (1-2a)v_E \end{array} \right) = \\
 &= \left(\begin{array}{c} i_E + D_O a (c_{2\gamma} q_E - s_{2\gamma} u_E) \\ c_{2\gamma} D_O i_E + a q_E - s_{2\gamma} [W_O a (s_{2\gamma} q_E + c_{2\gamma} u_E) + Z_O S_O (1-2a)v_E] \\ s_{2\gamma} D_O i_E - a u_E + c_{2\gamma} [W_O a (s_{2\gamma} q_E + c_{2\gamma} u_E) + Z_O S_O (1-2a)v_E] \\ Z_O S_O a (s_{2\gamma} q_E + c_{2\gamma} u_E) + Z_O c_O (1-2a)v_E \end{array} \right)
 \end{aligned} \tag{E.31}$$

14 • Special cases: From Eq. (E.31) without receiver optics rotation γ we get Eq. (E.32).



$$\gamma = 0 \Rightarrow$$

$$1 \quad \frac{\mathbf{I}_{in}(0, a, \gamma)}{T_{in} I_L} = \frac{\mathbf{M}_O(0) | \mathbf{F}(a) \mathbf{M}_E \mathbf{I}_L \rangle}{T_O F_{11} T_E I_L} = | i_{in} \quad q_{in} \quad u_{in} \quad v_{in} \rangle = \left\langle \begin{array}{l} i_E + a D_O q_E \\ D_O i_E + a q_E \\ Z_O [-c_O a u_E + s_O (1-2a) v_E] \\ Z_O [s_O a u_E + c_O (1-2a) v_E] \end{array} \right\rangle \quad (\text{E.32})$$

- 2 • With linearly polarised laser \mathbf{I}_L with polarisation parameter a_L , with emitter optics \mathbf{M}_E ,
 3 atmosphere \mathbf{F} , and receiver optics \mathbf{M}_O , and with Eqs. (E.32) and (E.20) we get Eq. (E.33).

$$i_L = q_L = 1, u_L = v_L = 0 \Rightarrow$$

$$4 \quad \frac{\mathbf{I}_{in}(\gamma, a, \beta, \alpha, a_L)}{T_{in} I_L} = \frac{\mathbf{M}_O(\gamma) | \mathbf{F}(a) \mathbf{M}_E(\beta) \mathbf{I}_L(\alpha, a_L) \rangle}{T_O F_{11} T_E I_L} = \left\langle \begin{array}{l} 1 + a_L D_E c_{2\alpha-2\beta} \\ a [c_{2\beta} D_E + a_L (c_{2\alpha} + s_{2\beta} W_E s_{2\alpha-2\beta})] \\ -a [s_{2\beta} D_E + a_L (s_{2\alpha} - c_{2\beta} W_E s_{2\alpha-2\beta})] \\ -(1-2a) a_L Z_E s_E s_{2\alpha-2\beta} \end{array} \right\rangle \quad (\text{E.33})$$

- 5 • Eq. (E.33) with rotated, linearly polarised laser without laser depolarisation ($a_L = 1$) and
 6 rotated emitter optics (Eq. (E.20)) the input Stokes vector becomes explicitly

$$a_L = 1, i_L = q_L = 1, u_L = v_L = 0, \gamma = 0 \Rightarrow$$

$$7 \quad \frac{\mathbf{I}_{in}}{T_{in} I_L} = \frac{\mathbf{M}_O(0) | \mathbf{F}(a) \mathbf{M}_E(\beta) \mathbf{I}_L(\alpha) \rangle}{T_O F_{11} T_E I_L} = \left\langle \begin{array}{l} (1 + D_E c_{2\alpha-2\beta}) + a D_O (c_{2\alpha} + c_{2\beta} D_E + s_{2\beta} W_E s_{2\alpha-2\beta}) \\ D_O (1 + D_E c_{2\alpha-2\beta}) + a (c_{2\alpha} + c_{2\beta} D_E + s_{2\beta} W_E s_{2\alpha-2\beta}) \\ -Z_O \{ s_O Z_E s_E s_{2\alpha-2\beta} + a [c_O (s_{2\alpha} + s_{2\beta} D_E - c_{2\beta} W_E s_{2\alpha-2\beta}) - 2s_O Z_E s_E s_{2\alpha-2\beta}] \} \\ -Z_O \{ c_O Z_E s_E s_{2\alpha-2\beta} - a [s_O (s_{2\alpha} + s_{2\beta} D_E - c_{2\beta} W_E s_{2\alpha-2\beta}) + 2c_O Z_E s_E s_{2\alpha-2\beta}] \} \end{array} \right\rangle \quad (\text{E.34})$$

- 8 • Eq. (E.34) with laser polarisation and emitter optics aligned

$$a_L = 1, i_L = q_L = 1, u_L = v_L = 0, \gamma = 0, \beta = \alpha \Rightarrow$$

$$9 \quad \frac{\mathbf{I}_{in}}{T_{in} I_L} = \frac{\mathbf{M}_O(0) | \mathbf{F}(a) \mathbf{M}_E(\alpha) \mathbf{I}_L(\alpha) \rangle}{T_O F_{11} T_E I_L} = (1 + D_E) \left\langle \begin{array}{l} 1 + a D_O c_{2\alpha} \\ D_O + a c_{2\alpha} \\ -Z_O a c_O s_{2\alpha} \\ +Z_O a s_O s_{2\alpha} \end{array} \right\rangle \quad (\text{E.35})$$

- 10 • and without any optics and laser rotation



$$1 \quad a_L = 1, i_L = q_L = 1, u_L = v_L = 0, \alpha = \beta = \gamma = 0 \Rightarrow$$

$$1 \quad \frac{\mathbf{I}_{in}(0,0,0,0,1)}{T_{in}I_L} = \frac{\mathbf{M}_O(0) \mathbf{F}(a) \mathbf{M}_E(0) \mathbf{I}_L(0)}{T_O F_{11} T_E I_L} = (1 + D_E) |1 + a D_O \quad D_O + a \quad 0 \quad 0\rangle \quad (\text{E.36})$$

2 • Eq. (E.33) without emitter optics \mathbf{M}_E

$$D_E = 0, s_E = 0, W_E = 0, a' = a a_L \Rightarrow$$

$$3 \quad \frac{\mathbf{I}_{in}(\gamma, a, 0, \alpha, a_L)}{T_{in}I_L} = \frac{\mathbf{M}_O(\gamma) \mathbf{F}(a) \mathbf{I}_L(\alpha, a_L)}{T_O F_{11} I_L} = \left\langle \begin{array}{l} 1 + c_{2\gamma+2\alpha} a' D_O \\ c_{2\gamma} D_O + a' [c_{2\alpha} - s_{2\gamma} s_{2\gamma+2\alpha} W_O] \\ s_{2\gamma} D_O - a' [s_{2\alpha} - c_{2\gamma} s_{2\gamma+2\alpha} W_O] \\ s_{2\gamma+2\alpha} a' Z_O S_O \end{array} \right\rangle \quad (\text{E.37})$$

4 • No emitter optics \mathbf{M}_E and no receiver optics rotation

$$\text{with } \gamma = 0, T_E = 1, D_E = 0, s_E = 0, W_E = 0, a' = a a_L \Rightarrow$$

$$5 \quad \frac{\mathbf{I}_{in}(0, a, 0, \alpha, a_L)}{T_{in}I_L} = \frac{\mathbf{M}_O(0) \mathbf{F}(a) \mathbf{I}_L(\alpha, a_L)}{T_O F_{11} I_L} =$$

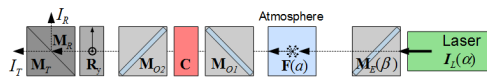
$$= |1 + c_{2\alpha} a' D_O \quad D_O + c_{2\alpha} a' \quad -s_{2\alpha} a' Z_O c_O \quad s_{2\alpha} a' Z_O s_O\rangle \quad (\text{E.38})$$

6 • The latter and no laser rotation

$$\text{with } \alpha = 0, \gamma = 0, T_E = 1, D_E = 0, s_E = 0, W_E = 0, a' = a a_L \Rightarrow$$

$$7 \quad \frac{\mathbf{I}_{in}(0, a, 0, 0, a_L)}{T_{in}I_L} = \frac{\mathbf{M}_O(0) \mathbf{F}(a) \mathbf{I}_L(0, a_L)}{T_O F_{11} I_L} = |1 + a' D_O \quad D_O + a' \quad 0 \quad 0\rangle \quad (\text{E.39})$$

8 App. E.5 \mathbf{I}_{in} with C amidst the receiving optics



9 In case there is polarising or/and retarding optics before (\mathbf{M}_{O1}) and after (\mathbf{M}_{O2}) the calibrator
 10 as in Eq. (E.40), the basic equations can be constructed by using the analyser matrix \mathbf{A}_S from
 11 App. D.2 and the input Stokes vectors \mathbf{I}_{in} from App. E.4.

$$12 \quad \mathbf{I}_S = \eta_S \mathbf{M}_S \mathbf{R}_y \mathbf{M}_{O2} \mathbf{C} \mathbf{M}_{O1} \mathbf{F} \mathbf{I}_E \Rightarrow \mathbf{A}_S = \mathbf{M}_S \mathbf{R}_y \mathbf{M}_{O2} \quad \text{and} \quad \mathbf{I}_{in} = \mathbf{M}_{O1} \mathbf{F} \mathbf{I}_E \quad (\text{E.40})$$